University of Padua

Industrial Engineering Department

Master's Degree course in Electrical Engineering

Master's Thesis

MONITORING AND OPERATION OF A SYNCHRONOUS GENERATOR ON SHORT CIRCUIT ON THE ROTOR OF A COMBINED CYCLE POWER PLANT

Supervisor: Prof. Arturo Lorenzoni
INDUSTRIAL ENGINEERING DEPARTMENT

Co-Supervisor: M. Giuseppe Zagami
MARCINELLE ENERGIE S.A.

Graduand: Riccardo Zen

Academic year 2012/2013

Abstract

The continuous research of most productive energy sources have built the electrical power system that we may see today.
The thermal generation, that exploits coal, oil, uranium and natural gas, represents the backbone of the world electrical power system. This is due to specific features such as: regulation to match shifts in demand or supply, turn on or off according to the trade market and may provide many technical services which help to keep the system stable and in balance.
They are the baseload power plants, but they provide the necessary flexible whenever variable renewables such as wind power and photovoltaic produce their output. Consequently, the thermal generation allows the great development of the renewable energy. An important feature of this type of generation is the environmental pollution.

It is of the utmost importance to reach a more sustainable and efficient power system, finding new ways to produce electricity, a more thorough demand forecast, about short and long terms, with a good power quality.

The last theme is very important to the main operations of industrial and service sectors, because they require many guarantees about the electrical service. Unfortunately, no machines or power plants may operate forever without problems but it is indispensable to improve the power generation quality, through a more extensive use of sensors and digital supervisory systems, so that it is possible to act at the right time if there are anomalous or dangerous situations. Long-term use and efficient operation of equipment in power plants demand diagnosis techniques to improve reliability and to reduce operating and maintenance costs, requested due to larger in size of power plants as well as inter-annual decrepitude due to aging. Nowadays power plants incorporate large quantities of devices that supervise all parts of the plant, particularly the synchronous generator, the most delicate one. This machine carries out the mechanical-to-electrical energy conversion, and through an evaluation of its parameters it is possible to ensure its good (or not) operation.
Nevertheless this conversion process is possible only if there is the excitation winding, located on the rotor. Consequently, to ensure a good operation of the machine, there must not be damages on the rotor winding (e.g. shorted turns); a method to supervise its operation will be proposed in this work with reference to a combined cycle power plant.

Acknowledgements

I would like to thank Professor Arturo Lorenzoni of University of Padua for the huge opportunity that he offered me and for all the help and the support furnished from the beginning of this project. His total helpfulness and his exceptional teacher capability have allowed me to complete this work.

Many thanks to my tutor M. Zagami Giuseppe of Enel spa, director of the Marcinelle C.C.G.T. power plant, for his technical competences and his support during the internship.

For helping me with the shaft voltage F.F.T. analysis and with technical papers, I would like to thank Mr. Paolo Tattini of ASP-GEM of Enel spa. The kindness, understanding and enthusiasm that he has showed me have been an inspiration.

A friendly thank goes to M. Ganino Thierry for his helpfulness during the plant inspection and for technical materials.

Special thanks go to the Marcinelle Energie s.a. and its entire staff; this experience was very important for my personal and professional growth. It has given me the opportunity to enrich my capabilities at the end of my academic career.

Not for last, I would like to thank a lot my family, for always being at my side and for always encouraging me to achieve my goals. I would like to express a sense of gratitude and love to my relatives, to Chiara and my friends. I never could do it without you.

Thank you.

Contents

Introduction

The electrical system, generation, transmission and load, is always changing since it's born.
Nowadays coal, oil, gas and uranium are the main energy sources although the volatility of their wholesale prices is very high. In the latest years the production fleet has been liable to alterations about the numbers, types and locations of the power plants.
This is mainly due to innovations and a more sustainable mind of the collectivity, to reach the depletion of the carbon dioxide emissions and the others G.H.G.s.
The first huge change was the switch in fuel used in power generator, e.g. from coal to natural gas and the improvement in efficiency of technologies used in energy conversion.
Nowadays the fuel-fired power plants are the most widespread in the electrical power generation sector.
About the security of supply if there is plant inefficiency, another power plant must operate in turn; this could be a thermoelectric or a hydroelectric plant, grounds to the locations and the hours in which the fault was happened. Consequently, the fault plant must be disconnected from the grid and thus a maintenance service is necessary, with disadvantages for the customers. That is why the monitoring systems have been more and more utilized in the power generation sector, from power plants output until the auxiliary systems supervision. Currently, the generator parameters must be supervised, particularly on the excitation winding (the core of the electro-mechanic conversion process), if it is possible with a real-time acquisition system.

The aim of this project is the monitoring of a round rotor synchronous generator in a C.C.G.T. power plant, through an innovative digital supervision system that utilizes a magnetic flux probe and a grounding device.
Substantially, the monitoring system uses a magnetic flux probe because, through an evaluation of the slots flux generated by the rotor winding (and other signals), it is possible to understand if there are shorted turns on the rotor winding. The next operations are very important about the service maintenance because only if there are not threats at the machine operation it is possible to resume the service.
In the chapter one there is a general outline of the Marcinelle Energie combined cycle gas turbine power plant (C.C.G.T.), with some features and typical configurations.
In the chapter two, in the specific instance about the power plant synchronous generator, with its technical specifications.
In the chapter three you will find a close description of the magnetic flux probe, deployed in the rotor winding supervision system with the insertion operation.
The chapter four is specific about the monitoring of the rotor winding state. After a quick introduction about causes and effects of shorted turns, it will describe the method and the detection procedures. The chapter five shows the results of the generator monitoring and their explanation. With the chapter six will be concluded this work with conclusions; although the rotor monitoring is provided for many generators there are important future developments in this sector. This is mainly due to avoid damage on the round rotor and consequently, to the power plant service, to foresee possible anomalous situations.

Table of acronyms

Name:	Acronym:
Combined Cycle Gas Turbine	C.C.G.T.
Steam Turbine	S.T.
Heat Recovery Steam Gen.	H.R.S.G.
Electromotive Force	e.m.f.
Fast Fourier Transform	F.F.T.
Magnetomotive Force	m.m.f.
Flux Density Zero Crossing	F.D.Z.C.
Silicon Controlled Rectifier	S.C.R.
Current Transformer	C.T.
Grounding device (“messa a terra”)	M.A.T.
Root Mean Square	R.M.S.
Medium Voltage	M.V.
Air Gap Monitoring System®	A.G.M.S.®

CHAPTER 1

"Marcinelle Energie" power plant

This project will make reference to the 420 MW *Marcinelle Energie s.a.* (Enel s.p.a.) C.C.G.T. power plant, located in *Marchienne au Pont* (*Charleroi,* Belgium) and in service since April 2012. Some brief introductions about the main parts of the power plant, emphasizing technical specifications of the machines. Even though they are the most deployed power plants in Europe, they are less known because their outline is so far from traditional fuel-fired power plants. Nevertheless they represent the most attractive range of power plants about the load modulation, as e.g. hydroelectric power plants.

1.1 The *Marcinelle* C.C.G.T. Power Plant

The great advantages of gas-fired power generation are a wide flexibility, the ability to set the price in competitive electricity markets, hedging financial risk for its operators and its lower CO2 profile. On the other hand, when they are used for baseload service it has comparatively high costs given by gas price assumptions. According to their easy power modulation, it is not required a continuous operation; this is mainly due to fuel wholesale price, much unsteady, and to electrical trade market conditions.
The fuel is furnished way by a natural gas pipeline and through filters it comes introduced inside the gas turbine. The near river (*La Sambre*) is utilized to supply the steam cooling system. Moreover there are demineralized water plants and several systems for the mud disposal. The plant configuration is single shaft.

Figure.1.1: *Marcinelle Energie s.a*. (Enel spa) Combined cycle power plant 420MW, *Marchienne au Pont*, Belgium.

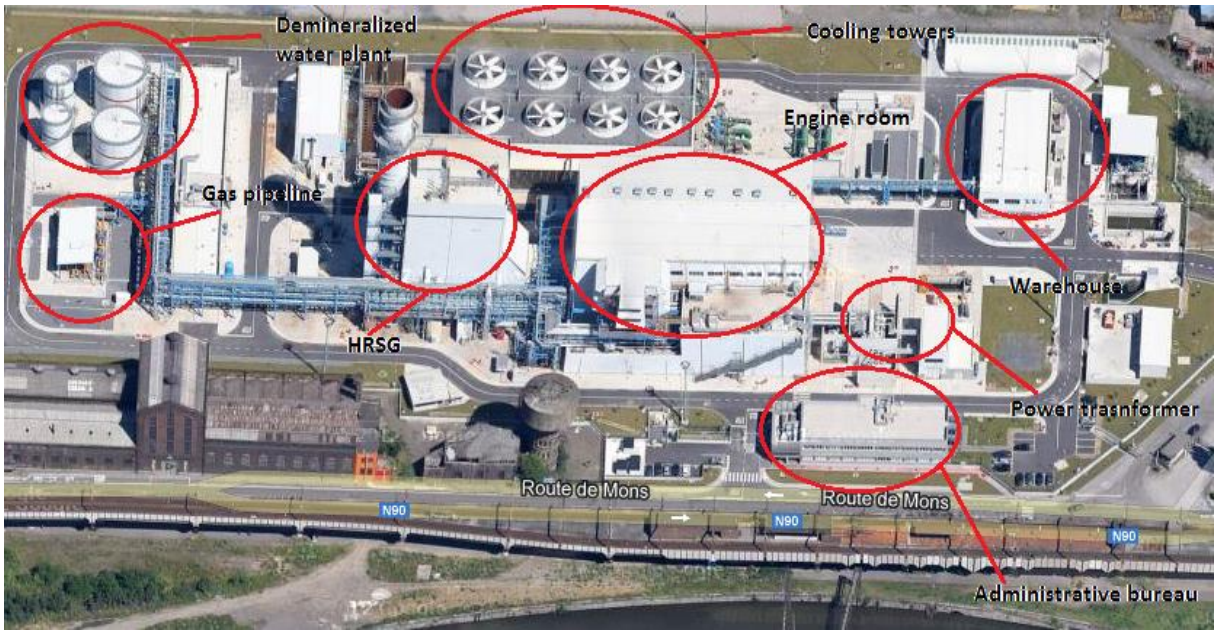

Figure.1.2: Power Island.

The main parts of power plant:

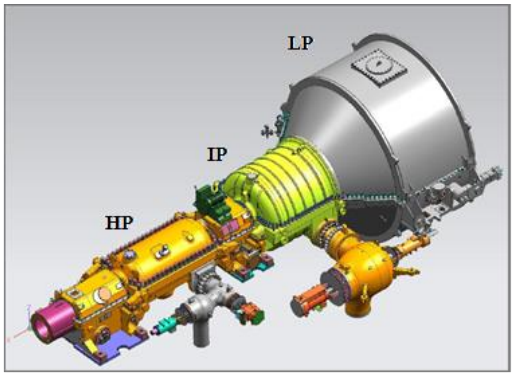

Figure.1.3: Ansaldo Energia steam turbines, 140 MW (H.P. and I.P. / L.P.).

Figure.1.4: Eight cooling towers, forced ventilation.

Figure.1.5: The condenser.

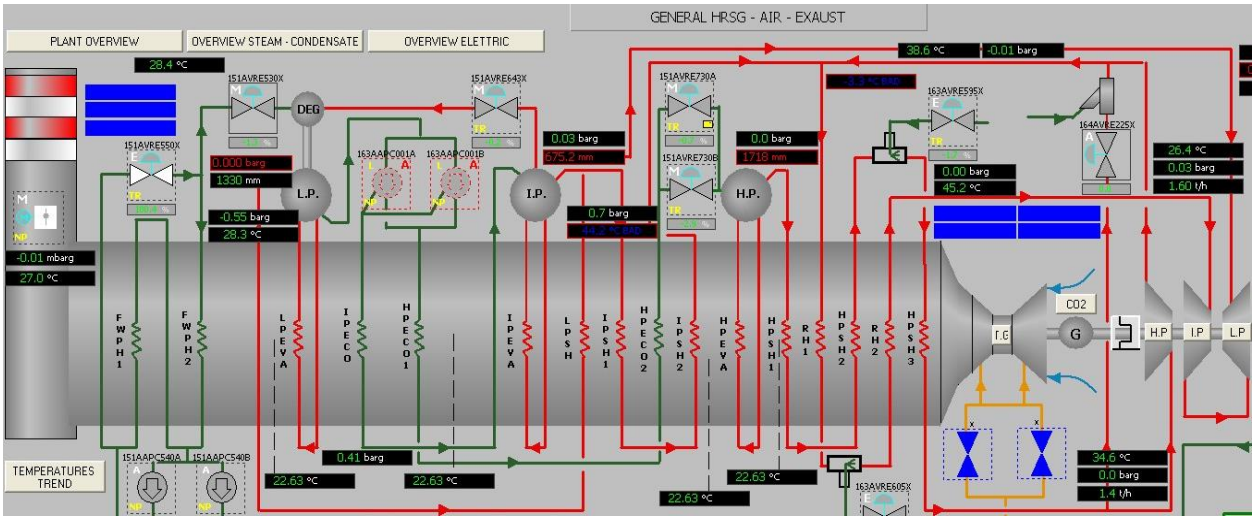

Figure.1.6: H.R.S.G., heat recovery steam generator, (G.V.R., *Gènèrateur vapeur rècup*)[1].

[1] Barbieri C., MARCINELLE_LG_2000 DESCRIZIONE GENERALE IMPIANTO.DOC, Enel University, Operations Learning center, 20/10/2009, p. 28.

PRODUCTIBILITÉ DE LA SECTION HP

Producibilità vapore	t/h	290,4
Pressione vapore usc. SH	Mpa	10,13
Temperatura vapore usc. SH	°C	540
Pressione corpo cilindrico	Mpa	10,56
Temperatura acqua uscita ECO AT[6]	°C	306
Temperatura acqua uscita ECO BT[6]	°C	217
Temperatura ingresso ECO (BT)	°C	173

PRODUCTIBILITÉ DE LA SECTION MP

Producibilità vapore	t/h	24,5
Pressione vapore usc. SH	MPa	2,80
Temperatura vapore usc. SH	°C	310
Pressione corpo cilindrico	MPa	2,89
Temperatura acqua uscita ECO	°C	217
Temperatura acqua ingresso ECO	°C	172

PRODUCTIBILITÉ DE LA SECTION RESURCHAUFFEUR

Portata VRF, a monte miscelazione con vapore surriscaldato MP	t/h	274,8
Temperatura VRF, a monte miscelazione con vapore surriscaldato MP	°C	366,5
Pressione vapore ingr. RH	MPa	2,80
Pressione vapore usc. RH	MPa	2,66
Portata vapore usc. RH	t/h	299,7
Temperatura vapore usc. RH	°C	540

PRODUCTIBILITÉ DE LA SECTION BP

Producibilità vapore	t/h	44
Pressione vapore usc. SH	MPa	0,76
Temperatura vapore usc. SH	°C	304
Pressione corpo cilindrico	MPa	0,82
Temperatura acqua uscita ECO[7]	°C	162
Temperatura condensato ingresso GVR	°C	30
Temperatura condensato ingresso ECO BP	°C	60 [8]

Figure.1.7: H.R.S.G. productive data, H.P., I.P., L.P., R.H. sections[2].

Step-up Power transformer (1T.P.):

Manufacturer: Tamini.
YNd11 (with neutral grounding reactor, Z = 5.3 Ω, 5150 A for 10 sec);
P_n= 490 MVA;
O.D.A.F. (oil direct, forced air);
V= 155±8*125% / 20kV;
V_{cc}% = 15;
I_1 = 14145 A;
V_1= 20kV;
V_2= 155kV[3].

Figure.1.8: Step-up transformer.

[2] Barbieri C., MARCINELLE_LG_1041 aspetti costruttivi GVR.doc, Enel University, Operations Learning center, 20/10/2009, p. 13.
[3] Look Barbieri C., MARCINELLE_LG_2000 DESCRIZIONE GENERALE IMPIANTO.DOC, Enel University, Operations Learning center, 20/10/2009, p. 35.

1.2 The gas turbine

1.2.1 The thermodynamic cycle:

This plant type represents a different range than traditional fossil fuel-fired cycles because the prime mover is a gas turbine. The rated power usually is smaller than the steam power plants; e.g. the output power range of General Electric is about 40MW – 340 MW (G.E. Heavy Duty Gas Turbine). A gas turbine uses a fine fuel as natural gas and thus it has high operating costs and low efficiency.

Its quick development is mainly due to low initial capital cost, great operation flexibility and less emissions (G.H.G.) than others fuel-fired plants; therefore a gas turbine power plant is employed in the main daily hours to satisfy the power peaks.
Thus the energy costs (€/MWh) are higher during this hours than during the night.
For these machines the thermodynamic cycle is that of *Brayton-Joule*.

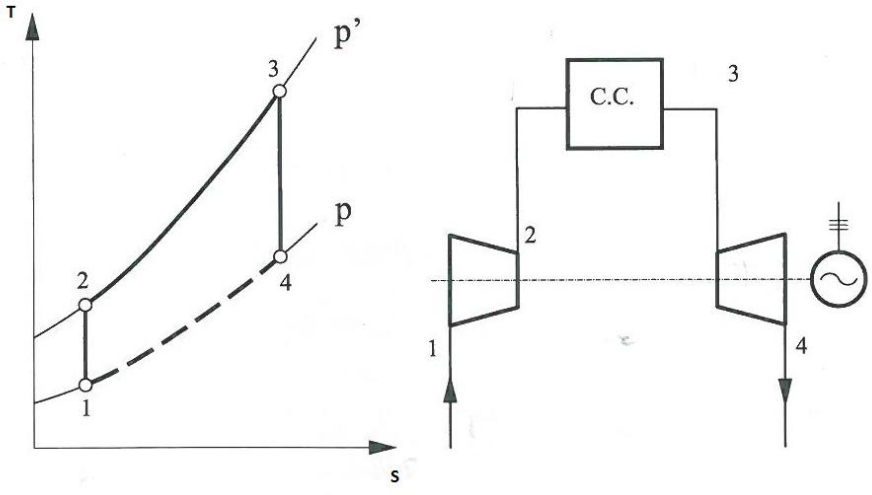

Figure.1.9: *Brayton-Joule* open cycle, gas turbine plant outline[4].

The chart in figure 1.9 displays the thermodynamic cycle and an outline of the engine. In the chart, the X axis represents the entropy S [kcal/(kg*K)], the Y axis represents the absolute temperature T [K].
The main plant parts are:

- Compressor (1→2 isentropic);
- Combustion chamber (2→3 isobar);
- Turbine (3→4 isentropic);
- Generator.

[4] Roberto Caldon, Impianti di produzione dell'energia elettrica, Università degli studi Padova, Libreria Progetto Padova, 2011, p. 151.

1.2.2 The compressor:

Substantially, this device must suck up air from the environment and compress it through 15 phases until to the achievement of the final pressure. Afterwards, the compressed air will enter in the combustion chamber. Usually, with reference to power generation, it is built with axial flux because this solution leads to lesser tightness problems than the centrifugal one. Furthermore, compressors with axial flux are fewer cumbersome than centrifugal ones.
The output ℓ and the compression factor ρ (per phase) are very different between axial and centrifugal compressors:

- Axial flux compressor: $\ell = 20 – 25$ kJ/kg, $\rho = 1.1 – 1.3$;

- Centrifugal flux compressor: $\ell = 150 - 200$ kJ/kg, $\rho = 4 – 6$.[5]

Thus it is necessary to use more than one phase to get the optimal pressure (between 10 and 20). The I.S.O. environment air conditions (International Standard Organization) are fixed at 15°C, 1013 mbar and 60% comparative humidity.[6]
The air bulk sucked up from the environment is very huge, about 2.000.000 m3/h (with reference to power generation applications).

1.2.3 The combustion chamber:

The air flow entering in the combustion chamber is already hot (≈ 400°C) because of frictions in the compressor. Subsequently, it must be mixed with natural gas, making the operative flow, through 24 burners. The combustion process happens with air surplus because this shrewdness allows keeping an acceptable temperature for the turbine materials.
The air surplus does not lead to a drop in combustion efficiency, which in steam plants where big air excesses involve big flows that take away heat from the boiler. Conversely, in gas turbines these greater fluid flows are entering in the turbine, making output. [7]
The combustion process happens through two ways:

- **Diffusion**: air and gas flows are mixed in the combustion chamber, the temperature of the flame is about 1800 – 2200 °C to burners out, but with the air flow in near zones the temperature comes down to 1400 – 1600 °C; [8]

- **Pre-mix**: air and gas flows must be mixed previously, as result the temperature has kept to 1400 – 1600 °C, uniform in the chamber.

[5] Look Anna Stoppato, Turbine a gas, note corso di Impianti Energetici, Università di Padova, A.A. 2010-2011, p. 12.
[6] Look LG_4790.1_2 Principe fonctionnemnt turbines à gaz_FR.doc – Rev 0, Enel University, Operations learning center, 20/10/2009, p. 4.
[7] To compare Anna Stoppato, Turbine a gas, note corso di Impianti Energetici, Università di Padova, A.A. 2010-2011, p. 14.
[8] Look Barbieri C., MARCINELLE_LG 4671.1_Aspetti costruttivi della turbine a gas SIEMENS V94.3A-FR.doc, Enel University, Operations Learning center, 20/10/2009, p. 61.

1.2.4 The turbine:

The operative flow expands between turbine blades and involves the rotation of the driving shaft. The entering flow (≈ 1300°C, 18 bar) goes through four shorts blades (movables, H.P.), and subsequently, through other four longs blades (fixed, L.P.). The output range is about 300 – 350 kJ/kg. [9]
As seen with the compressor, gas turbines may be at centrifugal or axial flux; the last type has been utilized at the *Marcinelle* power plant.
Other differences are represented by energy conversion ways:

- **Action**: the relative speeds at the turbine exhaust and at the entrance are the same (no difference of pressure);

- **Reaction**: the relative speed of the flow increases from the entrance to the exhaust (pressure decreases through the turbine). This process is the best in term of efficiency than action turbines but it requires more than one phase to gain the same final pressure.

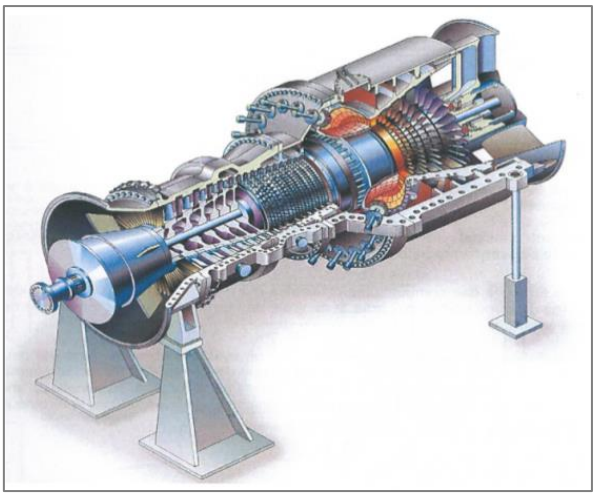

Figure.1.10: Ansaldo Energia gas turbine V94.3A[10].

1.2.5 The efficiency:

The chart in figure 1.9 may provide an evaluation of the cycle efficiency:

$$\eta = \frac{output}{input} = \frac{P_{turbine} - P_{compressor}}{Q_{input}} = \frac{(h_3 - h_4) - (h_2 - h_1)}{(h_3 - h_2)}$$

The numerator represents the plant output (turbine output minus compressor input).

[9] To compare Anna Stoppato, Turbine a gas, note corso di Impianti Energetici, Università di Padova, A.A. 2010-2011, p. 15.
[10] Barbieri C. "MARCINELLE_LG_2000 DESCRIZIONE GENERALE IMPIANTO.DOC", Enel University, Operations learning center, 20/102009, p. 16.

The gas turbine has only one driving shaft consequently, during the standard operation the turbine output must be higher than the compressor input; otherwise there is not mechanical output from the plant. The denominator represents the furnished heat to the system through the combustion process, it increases the energy system. All factors are expressed in terms of difference of enthalpy.
With reference to ideals transformations:

$$\eta = 1 - \frac{h_4 - h_1}{h_3 - h_2} = 1 - \frac{c_p * (T_4 - T_1)}{c_p * (T_3 - T_2)}$$

with $dh = c_p * dT$, h = enthalpy, T = absolute temperature, c_p = constant pressure heating.
With reference to an ideal gas that operates an isentropic transformation:

$$T * p^{\frac{1-k}{k}} = cost$$

where $k = \frac{c_p}{c_v}$, c_v = constant capacity heating.
If $\rho = \frac{P'}{P}$ is the compression factor:

$$\eta_{ideal} = 1 - \frac{1}{p^{\frac{1-k}{k}}}$$

as ideal efficiency.
It depends on from ρ and not from the maximum cycle temperature T3; this means that an ideal cycle is equal to that Carnot's between T_1 (environment) and T_2 (compressor output):

$$\eta = 1 - \frac{T_1}{T_2}$$

Thus the efficiency increases with ρ, the theoretical limit is the Carnot's efficiency for $\rho \rightarrow \infty$.
But it is impossible to get an infinite compression thus the real efficiency will be lower than the ideal one:

$$\eta_{real} = \eta_{ideal} * \eta_{compressor} * \eta_{turbine} * \eta_{c.c.}$$

With reference to this project, the gas turbine model is Ansaldo Energia V94.3A, with ρ = 16, k = 1.4, heat rate ≈ 9600 kJ/kWh.[11]

η_{ideal}= 0.45 $\eta_{compressor}$= 80 – 85%

$\eta_{combustion\ chamber}$= 0.97 $\eta_{turbine}$= 80 – 85%[12]

As a result the real efficiency is between 35% and 38%, lower than a steam cycle plant.

[11] Barbieri C., LG_4790.1_2 Principe fonctionnemnt turbines à gaz_FR.doc – Rev 0, Enel University, Operations learning center, 20/10/2009, p. 25.
[12] To compare Roberto Caldon, Impianti di produzione dell'energia elettrica, Università degli studi Padova, Libreria Progetto Padova, 2011, p. 152.

1.3 Introduction about the combined cycle power plants

1.3.1 Combined cycle gas turbine (C.C.G.T.):

These plants combine Rankine and Brayton-Joule cycles assets, because it is possible to introduce a high temperature heat (only possible in internal combustion systems) and release to the environment a low temperature heat (only possible in condensation systems).
Nevertheless their development is far recent because it was necessary to wait a technological maturation of the gas turbines.
In the figure 1.11 are stated the main devices of a C.C.G.T. power plant; first a gas turbine and last the steam cycle with a heat recovery steam generator (H.R.S.G.).
The exhausted smokes from the G.T. at ≈ 550°C are introduced inside a boiler (or more than one) with three counter-current heat exchangers, where they exchange their heat with a demineralized water circuit that becomes steam; subsequently, this flow expands inside of steam turbines.

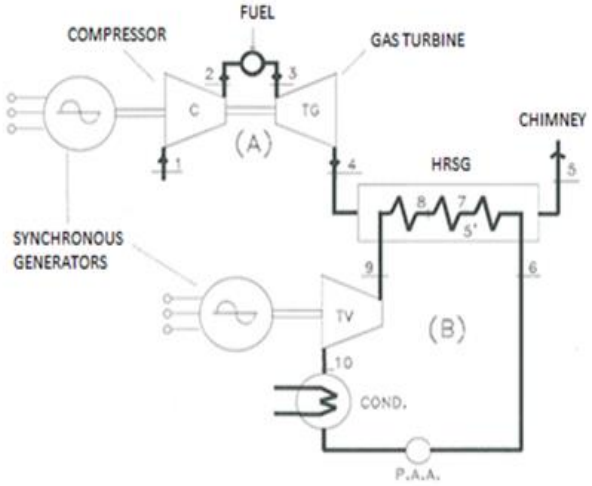

Figure.1.11: Combined cycle power plant[13].

Afterwards, the steam will condense to the liquid phase inside a condenser that utilizes sea water and / or cooling towers. The efficiency range is between 50% and 60%.

[13] Barbieri C., MARCINELLE_LG_2000 DESCRIZIONE GENERALE IMPIANTO.DOC, Enel University, Operations learning center, 20/10/2009, p. 10.

1.3.2 Possible thermodynamic configurations:

Combined cycle gas turbine power plants may belong to one of these classes:

1) **Unfired:**

The boiler is actually a heat exchanger that uses exhausted smokes from the G.T. to produce steam and to operate the turbines. The rated power of the steam cycle is lower than the gas turbine. Indeed this layout is typical of new plants, as the *Marcinelle* power plant.

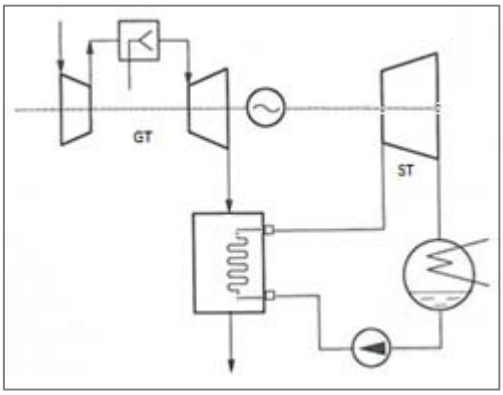

Figure.1.13: Unfired combined cycle power plant, with double shafts[14].

2) **Fully fired:**

The exhausted smokes enter inside a boiler where traditional fossil fuel combustion occurs. It is a conventional fossil fuel-fired plant but there is a gas turbine in addition. In this case it is possible to get a repowering of the plant.

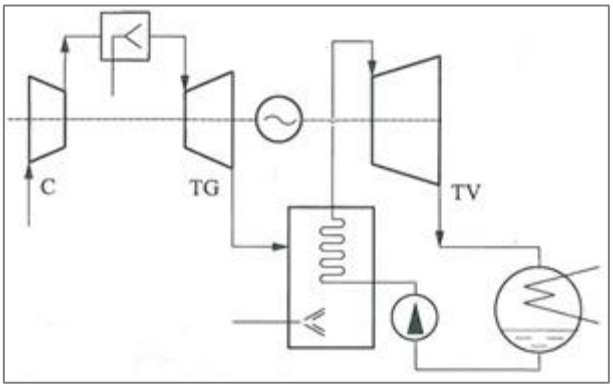

Figure 1.14: Fully fired combined cycle power plant, with two synchronous generators[15].

[14] Roberto Caldon, Impianti di produzione dell'energia elettrica, Università degli studi Padova, Libreria Progetto Padova, 2011, p. 154.

[15] Roberto Caldon, Impianti di produzione dell'energia elettrica, Università degli studi Padova, Libreria Progetto Padova, 2011, p. 155.

1.3.3 Possible connection configurations:

The conventional outlines are:

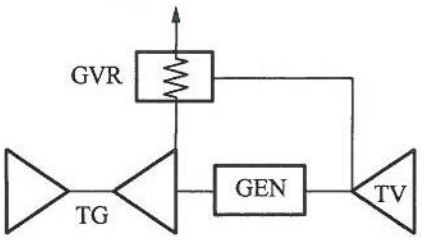

Figure.1.15: Single shaft[16].

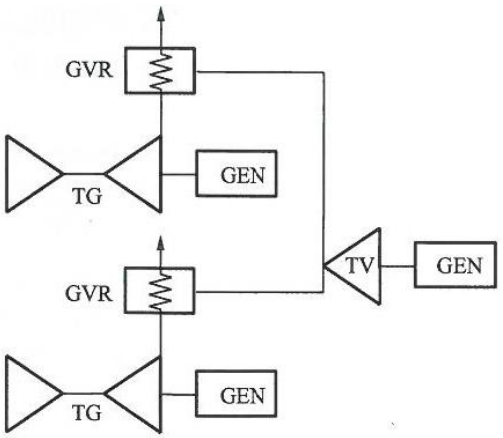

Figure.1.15: Multi shaft[17].

The first configuration deploys one high rated power generator and one driving shaft (conventional template); thus there is an economics saving and a better reliability than the second solution.
The second solution indeed shows more machines; nevertheless the power output modulation is less complex.

1.3.4 Features & Benefits:

Operational Flexibility:

- Technical minimum power output 190 MW (exhaust emissions);
- $\eta = 50.78\%$ at 190 MW;
- Starting times: hot shaft = 90 min, tepid shaft = 120 min, cold shaft=160 min;
- Equal to 13 MW/min while maintaining emissions guarantees.

[16] Roberto Caldon, Impianti di produzione dell'energia elettrica, Università degli studi Padova, Libreria Progetto Padova, 2011, p. 155.
[17] Roberto Caldon, Impianti di produzione dell'energia elettrica, Università degli studi Padova, Libreria Progetto Padova, 2011, p. 155.

1.4 Conclusions

At the end of this chapter some information about the most widespread thermodynamic cycle utilized nowadays has been acquired; it offers many advantages and an easy load control than other cycles. A C.C.G.T. power plant may be turned on and turned off in few hours and the plant efficiency is very high.
At first the layout of the plant could be very simple but a more careful examination leads to several discoveries. The facility includes other devices: a demineralized water plant, a hydrogen production system, gas filters, chemistry analysis, etc…
Also these parts of the plant are very important for its correct operation.
The synchronous generator will be discussed in the next chapter, because it requires a more accurate description.

CHAPTER 2

Technical specifications of the "Marcinelle" C.C.G.T. power plant synchronous generator

This chapter concerns the specifications of the synchronous generator installed in this power plant, beginning from the induced electromotive forces and the operation ranges; subsequently, it is provided for a description of the parallel maneuvering and the management of shaft vibrations. Their supervision requires a lot of sensors. These explanations will allow to state that this generator type is one of most deployed for these indispensable applications.

2.1 The electro-magnetic theory of a power plant generator

2.1.1 The electromotive force

The three-phase synchronous generator is the most utilized A.C. electrical machine for electrical power generation; "speed under steady state condition is proportional to the frequency of the current in its armature"[18]. They may have salient poles or a round rotor. The magnetic field created by the stator currents rotates at the same speed (synchronous speed) of that one created by the field current on the rotor. The conversion system is mainly due to an electromagnetic interaction between the inductor field and the armature conductors; a fixed part, called stator, is composed by three-phase A.C. conductors; a rotating part, called rotor, is connected to the turbines and it provides an excitation winding supplied by a direct current. All generators are provided with a damper winding designed to damp out rotor swings after sudden load changes.

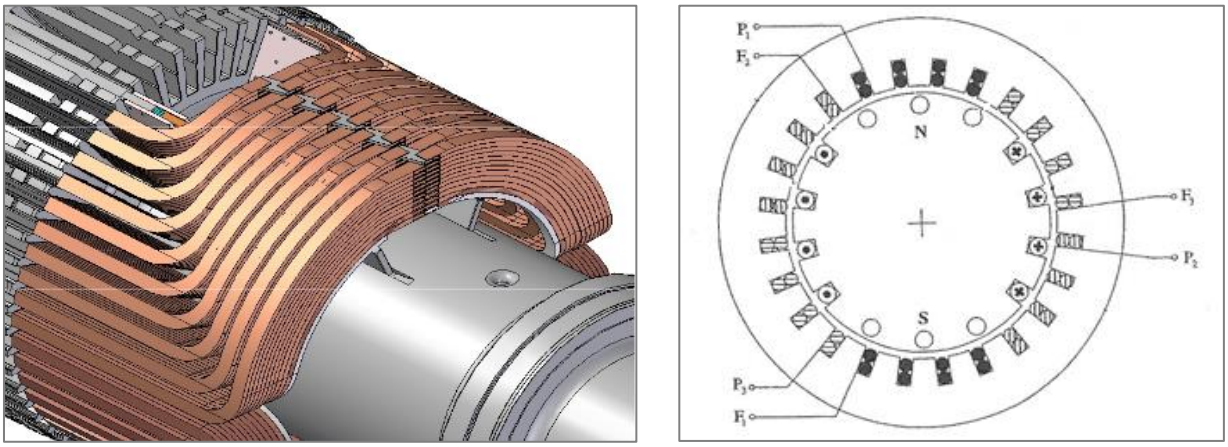

Figure.2.1: The excitation winding of a 2 poles round rotor synchronous generator and a cross-section[19].

[18] http://servicies.eng.uts.edu.au/cempe/subjects_JGZ/eet/eet_ch6.pdf, p. 1.
[19] Giovanni Martinelli, Macchine Elettriche rotanti, Capitolo II macchine sincrone, p. 79.

The instantaneous e.m.f. in each single conductor (no-load operation) is:

$$e(t) = \left(\vec{v} \times \vec{b}\right) \cdot \vec{L}$$

whose v = Ω*D/2 peripheral speed, Ω = angular speed [rad/s], D = internal stator diameter [m], b = magnetic induction [T] and L = conductor length [m].
In a synchronous generator the induced electromotive force on the stator during no-load operation may be expressed by (phase voltage):

$$E_0 = K_f * \emptyset * \omega = 2 * K_f * K_{i1} * N_i * f * \emptyset^{20} = K * \omega * I_{ecc}$$

whose K_f is the *Kapp*'s factor (or winding factor, 0.85 – 0.95[21]), K_{i1} is the *Kapp*'s factor with reference to the fundamental, $N_i = 2*p*n_i*q_i$ the number of stator turns, f the frequency [Hz], ϕ the linked magnetic flux [T] and ω the angular speed rotation. Consequently, E_0 is proportional to ϕ.
Frequency and speed are connected by:

$$n = \frac{120 * f}{p}$$

whose p as number of poles (e.g. p = 2), with reference to 50 Hz results n = 3000 rpm.

2.1.2 The magnetization curve

The link which connects the e.m.f. and the inductor flux due to the excitation current is clear in figure 2.2; it may be reached from a no-load test[22]:

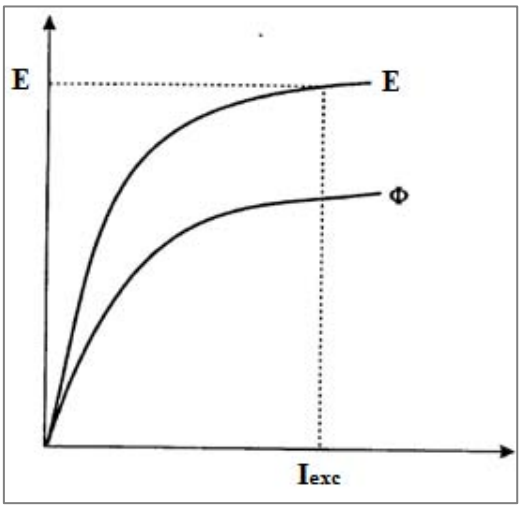

Figure.2.2: Open circuit curves, E = E (I_{exc}), ϕ = ϕ (I_{exc})[23].

[20] To compare Giovanni Martinelli, Macchine Elettriche rotanti, Capitolo II macchine sincrone, pp. 86 – 87.
[21] http://www.uotechnology.edu.iq/dep-eee/lectures/3rd/Electrical/Machines 2/II_SG.pdf
[22] http://www.uotechnology.edu.iq/dep-eee/lectures/3rd/Electrical/Machines 2/II_SG.pdf, pp. 15 – 16.
[23] Barbieri C., MARCINELLE_LG_1014 PRINCIPIO FUNZIONAMENTO ALTERNATORE.DOC, Enel University, Operations Learning center, 20/10/2009, p. 13.

In figure 2.2 the chart displays the trends of e.m.f. and air gap flux with reference to the excitation current. The trend always is not linear because of the saturation of the magnetic circuit; it occurs over a certain value of the excitation current.

2.2 Electrical circuit

The armature reaction is characterized by a voltage drop as $jX_i*\underline{I}$ (from no-load to on-load conditions). Substantially, it is possible to utilize only one term, the synchronous reactance $X_s = X_i + X_\sigma$. Then it is possible to state which:

$$\underline{Z_s} = R + jX_s$$

is the synchronous impedance (whose $X_s >> R$ in the real engine).

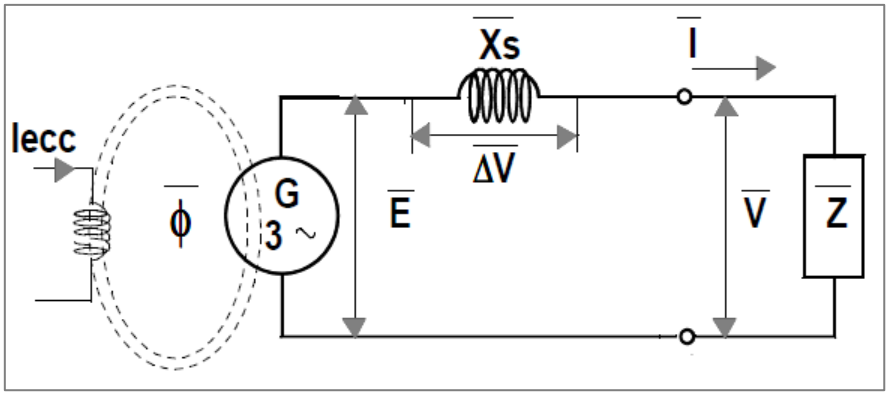

Figure.2.7: Single-phase electrical circuit[24].

2.3 The connection with the grid

2.3.1 The parallel maneuvering and the synchronous device

The electrical parallel between power plant and grid is possible if is ensured the equality in term of modulus, phase and frequency of the stator voltages. Thus to reach the synchronism three operations (and evaluations) must be carried out:

1. to equalize grid voltage and generator it is possible to act on the excitation current;
2. to equalize the frequency it is required to act on the turbines speed;
3. to equalize the voltage phases it is necessary a slip of the two systems with a little speed difference.

The synchronism manoeuvre before the electrical parallel leads to the generator switch closing; it happens through a synchronous device. [25]

[24] Barbieri C., MARCINELLE_LG_1014 PRINCIPIO FUNZIONAMENTO ALTERNATORE.DOC, Enel University, Operations Learning center, 20/10/2009, p. 33.
[25] To compare Barbieri C., MARCINELLE_LG_1014 PRINCIPIO FUNZIONAMENTO ALTERNATORE.DOC, Enel University, Operations Learning center, 20/10/2009, pp. 36-38.

This operation requires a human supervision yet, in a different way from others, because of the parameter volatility (to avoid irreparable damages to electrical devices).
The figure 2.8 displays the synchronism cubicle and indicators (beginning from left voltage, phase and frequency). Unfortunately, it is not possible to get the perfect synchronism between generator and grid; the comparison occurs keeping a range of uncertainty.

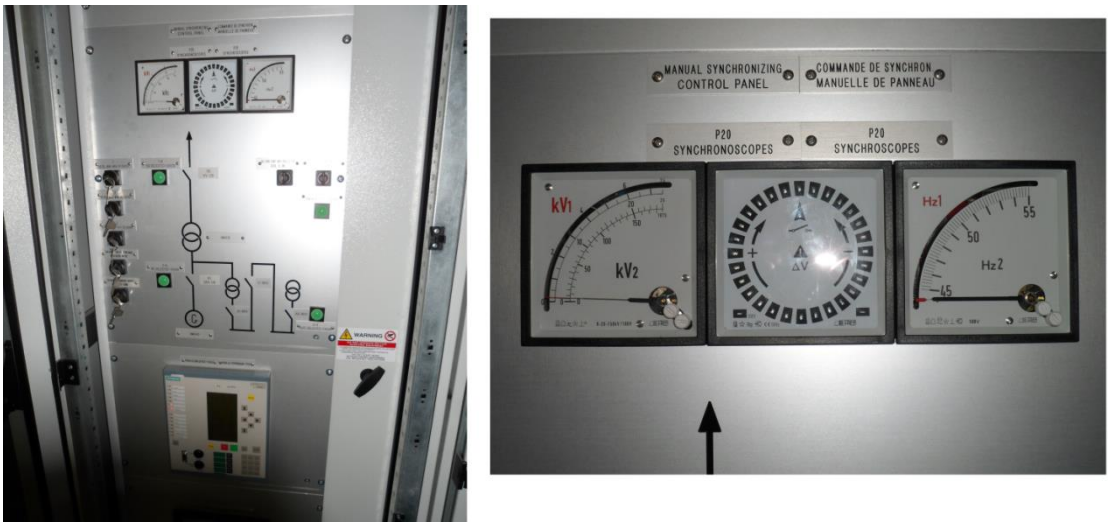

Figure.2.8: The synchronism cubicle.

2.3.2 The active power

As already seen, the electrical power generation is the main power plants task. But in an alternate (and sinusoidal) electrical system only the real power produces output inside electrical devices, in a different way from the reactive and the apparent powers.
As regards a three-phase circuit of a generator, the active power is expressible as:

$$P = \sqrt{3} * V * I * cos\varphi = \sqrt{3} * \frac{E * V}{X_s} * \sin\delta \ [W]^{26}$$

Whose

- V is the three-phase voltage (grid);
- E the internal e.m.f. of the engine, on load operation;
- I the armature current (average values);
- cosφ the power factor;
- X_s the synchronous reactance (X_d=X_q=X_s);
- δ the angle between $\underline{E}$ and $\underline{V}$. (__ is the complex vector symbol).

The last term is very important to understand how the machine operates; the active power is maximum when δ = 90°. Thus a torque change of the prime mover represents the way to change the active power P because δ changes.

[26] http://www.uotechnology.edu.iq/dep-eee/lectures/3rd/Electrical/Machines 2/II_SG.pdf

2.3.3 The reactive power

Otherwise from few years ago also the reactive power becomes very important in the electrical sector; the good operation of many devices depends by its availability (inductive or capacitive). The active power represents the real power utilized by the costumers whereas the reactive power is produced to balance the voltage inside the grid. Thus it could be regulated on the one hand to the other to avoid overloaded or voltage holes in the grid. Two cases are possible:

- **Over-excitation:** the excitation current is higher than that one which is necessary to a given load (thus the e.m.f. is higher than the grid voltage). The generator supplies the grid with reactive power as a synchronous condenser;

- **Under-excitation:** the excitation current is lower than that one which is necessary to a given load (thus the e.m.f. is lower than the grid voltage). The generator becomes an inductor.

Thus the reactive power may be regulated acting to the excitation current.
The large quantities of the A.C. electrical devices and the more and more extensive use of the power electronic (rectifiers, A.C./D.C., D.C./A.C. drivers) requires the absorption of inductive reactive power from the grid (Ω-L loads) due to their internal impedance Z.

$$Q = \sqrt{3} * V * I * sen\varphi = \sqrt{3} * \frac{E * V}{X_s} * \cos\delta - \frac{V^2}{X_s} \ [var]^{27}$$

2.3.4 The apparent power

The apparent power is an "unreal" power; it is used to define the rated power of the electrical devices like motors / generators, transformers, power electronic devices, etc…

$$S = \sqrt{3} * V * I \ [VA] \qquad \text{or} \qquad S = \sqrt[2]{P^2 + Q^2} \ [VA]$$

It is the vector sum of the active power and the reactive one.

2.3.5 The capability curves

They represent the generator capability to supply power loads; on the X semi-axis there is the active power, on the Y semi-axis the reactive one (over-excitation for positives Y, under-excitation for negatives Y).
Each curve belongs to a single operation state (voltage, frequency, cooling fluid condition).
From the chart in figure 2.9 it is possible to show the curve trend: the highest limit is thermal (with reference to the X axis), the lowest Y-limit is the rated rotor current and the highest Y-limit is the machine stability.

[27] http://www.uotechnology.edu.iq/dep-eee/lectures/3rd/Electrical/Machines 2/II_SG.pdf

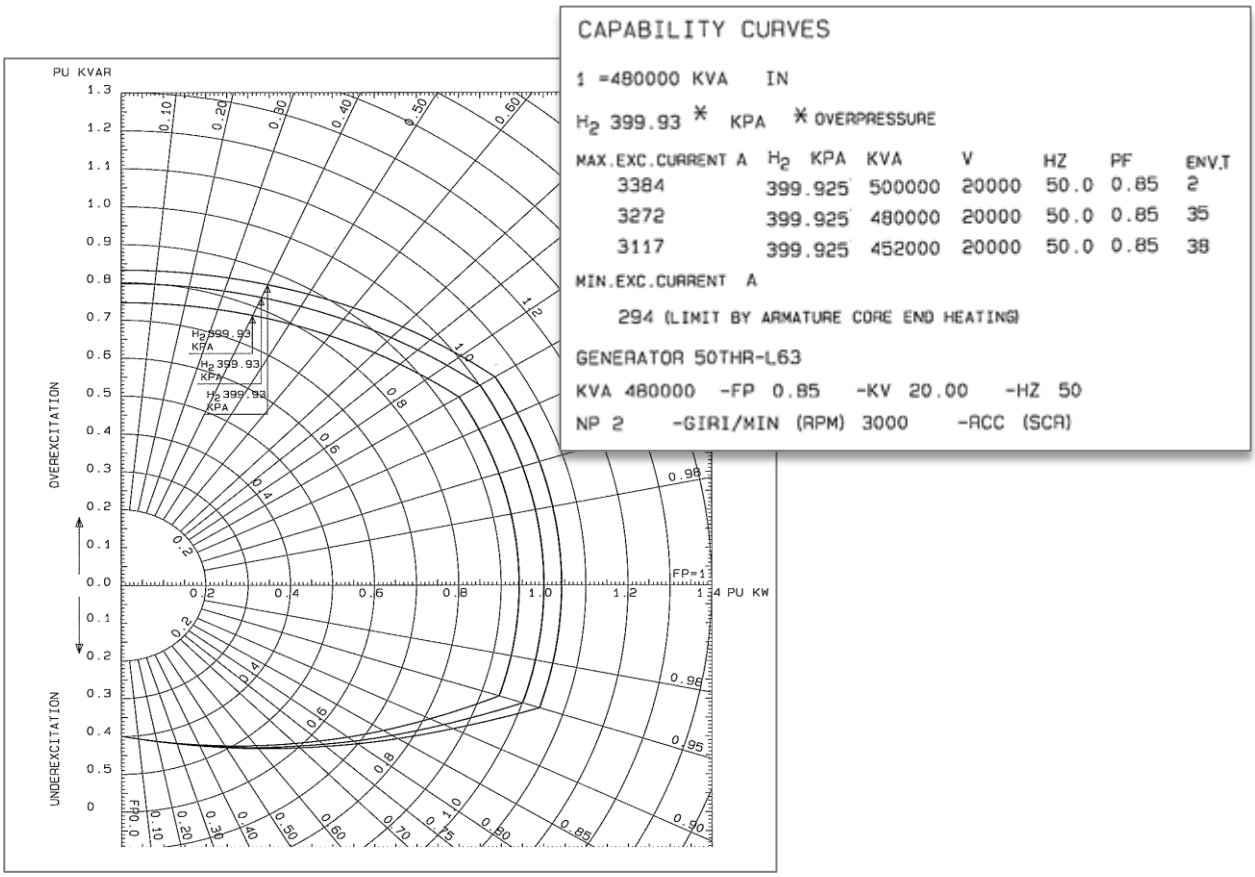

Figure.2.9: Capability curves at nominal operation of the 50THR – L63 generator.[28]

On the diagram are stated several circles with origin as centre: they represent the different apparent power values. The internal area instead represents possible operation points.

2.4 Technical specifications

The generator is a round rotor machine; the rotor has a solid iron frame, the stator core is fabricated from low-loss silicon alloy magnetic steel laminations. During the operation the speed of the inductor magnetic field is the same to the rotor one, tied to the grid frequency and to the number of poles (synchronism speed).

- Type: 50THR – L63;
- Year: 2009;
- Manufacturer: Ansaldo Energia spa;
- Series number: 0435AT;
- Rotation direction viewed from prime mover: clockwise;
- Rated power: 480 MVA;
- Rated voltage: 20 kV;

[28] M. Scagliotti, GENERATOR PERFORMANCE CURVES, Marcinelle CCGT power plant, 10/10/2008, p. 5.

- Rated current: 13856 A;
- Power factor lagging: 0.85;
- Rated frequency: 50 Hz;
- Voltage variation range: +/- 7.5 %;
- Frequency variation range: +3/-5 %;
- Combined variation voltage/frequency p.u. 1.075;
- Excitation system (rated load): 490 V, 3272 A;
- Rated speed/ Overspeed (test for 2 minutes) - 3000/3600 rpm;
- Phase number/ Phase connection: 3 / Star;
- Weight: Stator - 2765 kN, Rotor – 610 kN, Frontal covers – 550 kN, End shields – 225 kN, Coolers empty – 40 kN, Terminals – 30 kN, Slip ring housing – 30 kN, Generator total weight - 4250 kN;
- Absolute Hydrogen pressure: 500 kPa;
- Hydrogen cold Temperature: 40°C;
- Stator winding temperature: 102°C;
- Rotor winding temperature: 120°C;
- Number of bars per phase: 48;
- Inertia moment: 8500 kg*m^2. [29]

Figure.2.10: *Marcinelle* power plant synchronous generator, longitudinal section.

2.5 The vibrations

The magnetic interaction between stator and rotor may lead to vibrations on the support frame; this phenomenon may represent a likely threat because it is necessary to use elastics supports between the rotor and the static structure. Furthermore it is of the utmost importance to avoid that the vibrations find a way to switch from the stator winding to the external casing.
This phenomenon is mainly due to an eccentricity of the rotating masses (generator and turbines), the centre of gravity of these masses and the rotational centre do not exactly coincide.

[29] Barbieri C., MARCINELLE_LG_2005_CARATTERISTICHE COSTRUTTIVE E AUSILIARI ALTERNATORE.DOC, Enel University, Operations Learning center, 20/10/2009, p. 9.

The engine is positioned at height of over two meters from earth; necessary consequence is the use of a steel bearing construction. Consequently, it is indispensable to ensure the non-equality between the resonance frequency of the bearing structure and that of the rotating machines. This prevents the resonance phenomenon that involves "oscillations", and thus to dangerous effects. The rotating masses frequency is f and the resonance bearing construction frequency is f_0.

Therefore two possible ways are available:

- Hypocritical construction if $f_0 < 1700$;
- Hypercritical construction if $f_0 \geq 3600$.[30]

These are two safety limits to avoid the resonance of the construction.
But there is a seeming issue: if the bearing structure is hypocritical, during the machines start the resonance frequency must be crossed to arrive to 3000 rpm; but if the transitory is quick this does not lead to problems. The eccentricity of the rotating masses creates centrifugal forces and vibrations inside the machines and in the bearing structure (where the frequency is proportional to the rotation speed, 3000 rpm):

$$F_c = m * \omega^2 * e$$

whose F_c is the centrifugal force [N], m the mass [kg], ω the electrical angular speed [rad/s] and "e" represents the eccentricity [mm]. It is a good rule that $e \leq 0.05$ mm for 3000 rpm.
Consequently, the centrifugal force involves a bending of the driving shaft and therefore an "arrow" y displayed in figure 2.11:

$$y = \frac{F_c * l^3}{48 * E * J}$$ [31]

whose E= material resilience modulus, J = inertia moment of the rotor cross section, l = the rotor length.

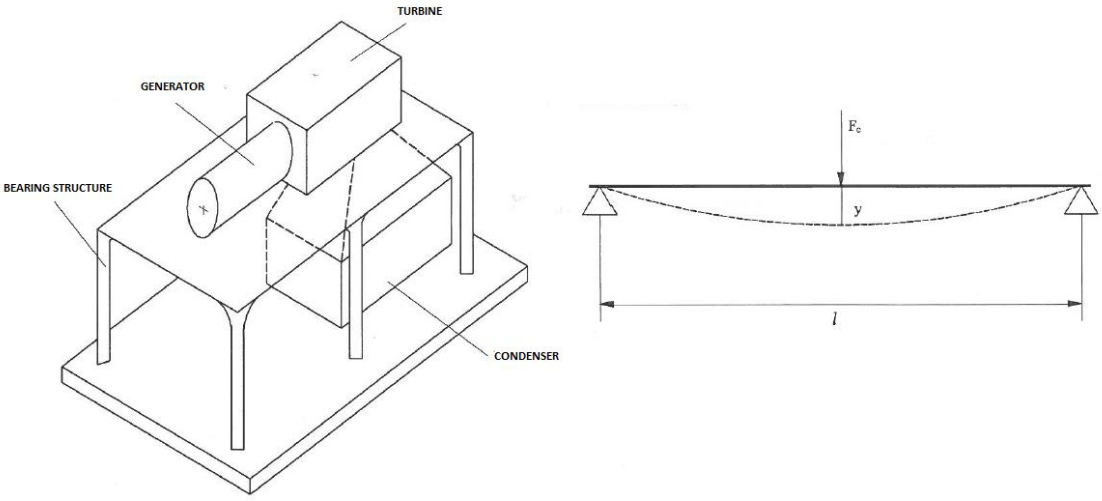

Figure.2.11: Vibrations of the generator-turbines system;[32]

[30]Look Roberto Caldon, Impianti di produzione dell'energia elettrica, Università degli studi Padova, Libreria Progetto Padova, 2011, p. 149.
[31] To compare Roberto Caldon, Impianti di produzione dell'energia elettrica, Università degli studi Padova, Libreria Progetto Padova, 2011, p. 150.
[32] Roberto Caldon, Impianti di produzione dell'energia elettrica, Università degli studi Padova, Libreria Progetto Padova, 2011, pp. 149 - 150.

Afterwards this "arrow" increases the centrifugal force effect:

$$F_c = m * \omega^2 * (e + y)$$

thus, it is possible to get y, the result is as follow:

$$y = \frac{\omega^2 * e}{\frac{1}{\alpha * m} - \omega^2}$$

with $\alpha = \frac{l^3}{48*E*J}$.

When $\omega \rightarrow \omega_0 = \sqrt{\frac{1}{\alpha * m}}$ (resonance angular speed), the "arrow" tends to the infinite thus the oscillations are amplified until the collapse of the facility. To prevent these situations currently there are many vibrations sensors on the driving shaft (particularly, between the generator and the turbines); their signals are very important for the good operation of the power plant and they foresee possible anomalies.

2.6 Excitation system

2.6.1 Possible configurations

The direct current could be supply through a rotating excitation system or a static one:

- **First case**: the excitation system is connected to the generator by the same driving shaft; in this machine the armature is the rotor and the inductor is the stator. The rotor is provided for rotating diodes; they must straighten the current, generating a direct current. Subsequently, this current will supply power to the rotor winding of the generator.

- **Second case**: the direct current is supplied by a rectifier bridge (S.C.R.) supplied by a three-phase system; through rings and brushes happens the supply of the rotor winding. This is the excitation system type deployed in the *Marcinelle* power plant. "Slip rings are metal rings that encircle the rotor shaft but are insulated from it. Each of the two slip rings on the shaft is connected to one end of the D.C. rotor winding and a number of brushes ride on each slip ring. The rings are made of non-magnetic steel (18Mn18Cr). This ensures that the same DC voltage is applied to the field windings regardless of the angular position or speed of the rotor."[33]

[33] The McGraw-Hill Companies, Power generation handbook, Digital Engineering Library, cap. 31, p. 1.

2.6.2 Electrical circuit

The auxiliary services bars supply power the static excitation system through a transformer M.V. / L.V. . The connection of windings is clear in figure 2.12.

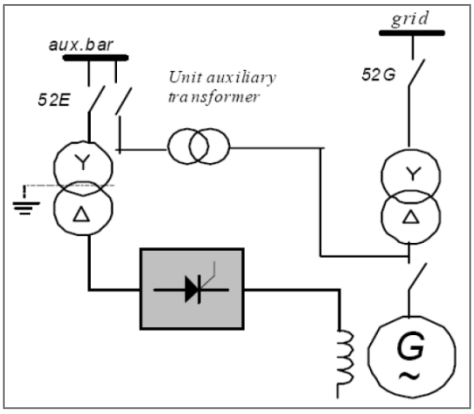

Figure.2.12: Excitation system single-line diagram and the excitation transformer.[34]

Figure.2.13: The excitation system (collector and the rings), focus of a brush.

The transformer 1T.E. supplies power the excitation system (6 kV, rated power 4,1 MVA, Yd11).

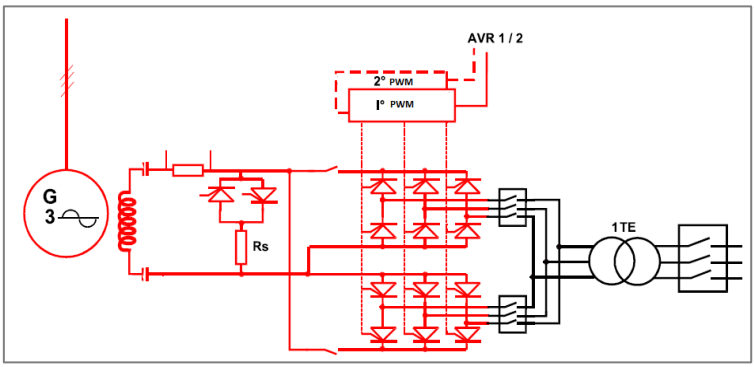

Figure.2.14: Typical excitation system outline.[35]

[34] Barbieri C., MARCINELLE_LG_2005_CARATTERISTICHE COSTRUTTIVE E AUSILIARI ALTERNATORE.DOC, Enel University, Operations Learning center, 20/10/2009, p. 63.

[35] Barbieri C., MARCINELLE_LG_4790_ECCITAZIONE E AVVIATORE STATICO.DOC, Enel University, Operations Learning center, 20/10/2009, p. 11.

The excitation system provides for the deployment of two rectifier bridges, powered by one transformer (one in operation, another in standby). Each S.C.R. provides for the use of a temperature sensor (the switch out of the S.C.R. is applied when the temperature rises up over 70 °C). Furthermore there are RC filters on the A.C. and D.C. sides. R_s represents a resistance that damps down the excitation, together to electronic switches (two S.C.R. in antiparallel).

2.6.3 Regulator

The excitation parameters are controlled by the voltage regulator to maintain a certain value of the excitation voltage. The parameter setting was selected by an operator; the energy supply comes by a three-phase line (A.C. 220 V) and batteries (D.C. 110 V).

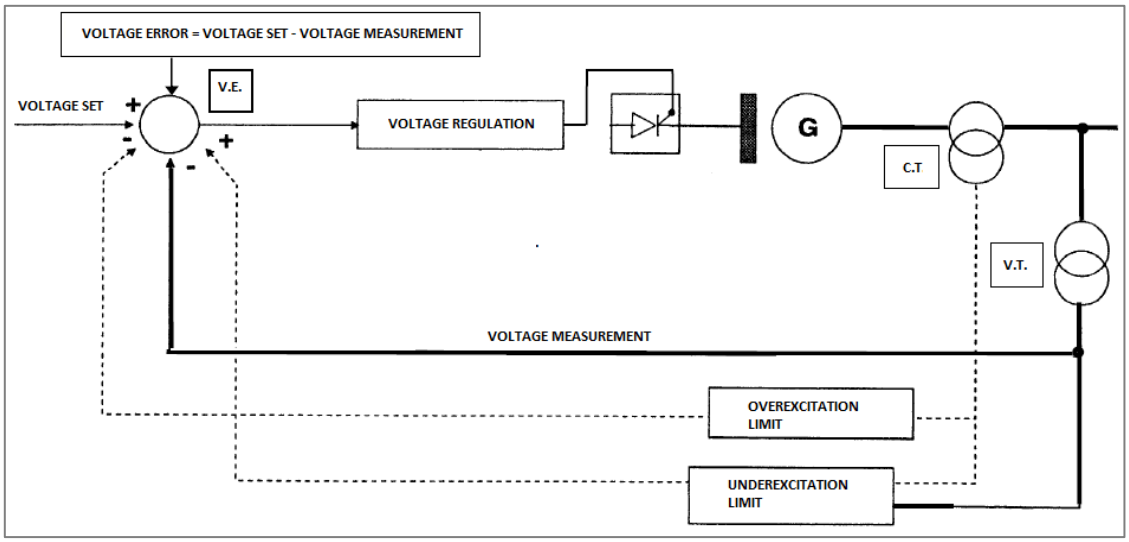

Figure.2.15: Voltage regulator.[36]

2.7 Conclusions

This chapter represents the beginning point to understand the behaviour of the generator at various operation stages. The machine control is far complex because the grid conditions are always changing. But a C.C.G.T. power plant has got a wider flexibility than the traditional baseload plants; consequently, the machine does not always operate at nominal conditions. This could be a problem about the gas turbine and the generator, designed for the continual operation. With this chapter the opening part is concluded; now the knowledge is enough to carry on with the main share of this project; subsequent to a quick introduction about the magnetic flux probe, the chapter will allow to understand how it is possible to know when a short circuit in the rotor occurs. Thus the correct operation of the generator depends on the conditions of the rotor winding.

[36] Barbieri C., MARCINELLE_LG_4790_ECCITAZIONE E AVVIATORE STATICO.DOC, Enel University, Operations Learning center, 20/10/2009, p. 13.

CHAPTER 3

The Magnetic flux probe

This chapter contains the part of materials deployed in this elaborate. This analysis needs to use a magnetic flux probe and a digital supervision system; about the flux probe, the insertion operation will be explained. Subsequently, an analysis of the data acquired will be provided.
A part of the data gathered in this project arises from the deployment of an unusual sensor, the magnetic flux probe or *Hall* effect sensor.
Its name is due to the first observer of the phenomenon, a physicist called *Edwin Hall*, in 1879.

3.1 Electrical and magnetic fields interaction

3.1.1 The Lorentz force

An electron which is moving through a region characterized by a direct magnetic field (empty space) is liable to a force:

$$\vec{F} = q * \vec{v} \times \vec{B}$$

with:

F = force which acts to the electron [N];
q = elementary charge of the electron = $-1.6*10^{-19}$ C;
v = electron speed [m/s];[37]
B = magnetic induction [T].

It is possible to expect that this force acts to the moving electron, leading to a deviation of the original path.
Nevertheless the electron charge is negative; consequently, the direction of the force vector is opposite of that found. The magnetic flux probe takes advantage of this phenomenon to get a magnetic field intensity measure.

[37] Electron speed: they can have got a wide range of speeds (the speed at which the electrons themselves move in the wire, so-called electron drift velocity); although the drift velocity in a wire is small, the thermal velocity of the electrons tends to be quite large, the order of 100,000 meters/sec. So they are buzzing about at random at high speeds, with a small superimposed drift velocity caused by the electric field. A current of 1 A corresponds to a transfer of 1 Coulomb of charge per second. An electron carries -1.6*10-19C (means 6.3*10^18 electrons/sec). Divide by the density of electrons in a copper wire (about 8.45*10^22 electrons/cm^3) and the cross section of the wire (e.g. 0.008 cm^2) and get 0.0093 cm/s.

3.2 The *Hall* effect sensor

3.2.1 Fundamental theory

The probe utilizes the interaction between an electrical current and a magnetic field to get a measure of the last one. Therefore the flux probe is a magnetic field meter.
As seen in the paragraph 3.1.1, the operation principle is based on the interaction between electrical charges and magnetic field; e.g. it may be considered a thin sheet (conductor or semiconductor such as gallium arsenide GaAs, indium antimonide InSb or indium arsenide InAs), liable to a direct voltage supplied power by a battery. Consequently, the sheet is crossed by a direct current. Subsequently, this sheet is leaded inside a region characterized by a magnetic field perpendicular to the sheet. According to the *Lorentz* law the electrons which cross the sheet are liable to a force (direction is opposite for the positive and negative charges). It involves inside the sheet an accumulation of negative charges on the one hand and positive ones on the other (to maintain the charges' neutrality). The figure 3.1 displays the accumulation process.

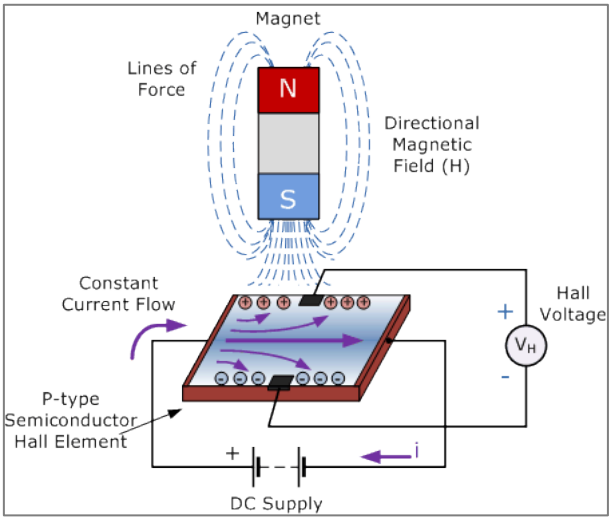

Figure.3.1: *Hall* effect.

The equality between electrical field and magnetic one may be reached through the equality between the forces:

$$q * E = q * v_d * B$$

where E is the electrical field and v_d the drift speed of the electron.

Consequently, a difference of potential arises, called Hall's voltage; this voltage may be gauged by a voltmeter and the result is proportional to the magnetic induction B and thus to the magnetic field H. The values of this voltage are very small: normally few microvolts for the small machines, but it could increase to hundreds of volts for the large ones. It is of the utmost importance the use of electronic boosters. If the semiconductor sheet is n-type doped, the moving charges are the electrons; conversely, if the semiconductor is p-type doped, the moving charges are the holes. If the probe operates inside the saturation zone, the growth of the output (Hall's voltage) does not follow the input (magnetic induction B) with linear trend. It is indispensable to work under this limit to gain an accurate estimate of the magnetic induction.

3.2.2 Real sensor

Indeed the real probe does not resemble to the probe displayed in figure 3.1, otherwise could not be possible to insert it inside the generator, the distance between the conductors is far small. The probe is a very thin printed circuit board sensor that is glued to a tooth of the stator (not the wedge) to measure the magnetic flux of each slot. Moreover the probe has to be fewer cumbersome as possible. Consequently, now it is possible to understand the frame of the real magnetic flux probe displayed in figure 3.2.

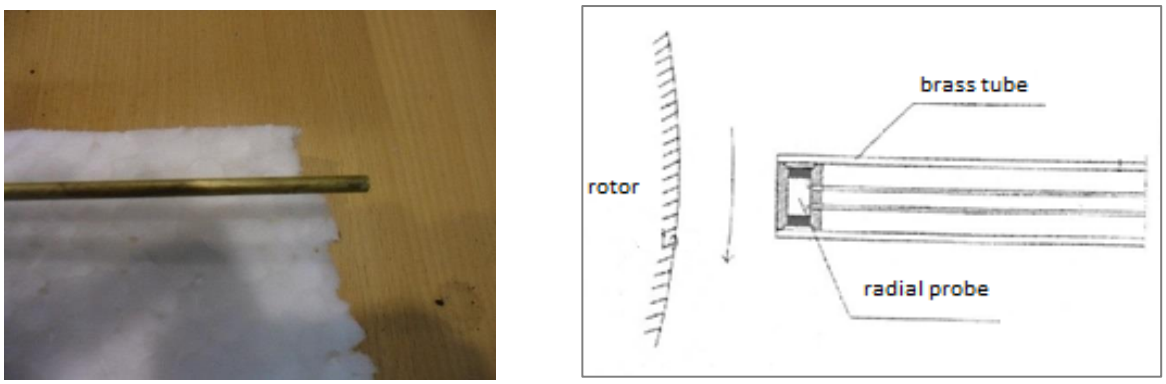

Figure.3.2: Sensitive element of the magnetic flux probe and its outline.

The part displayed in figure 3.2 shows the sensitive part, near the rotor.
The probe is a tube, inside it there are the sensitive device and the electrical terminals.
Figure 3.3 displays the opposite part of the probe, with the mechanical fixing.

Figure.3.3: External part of the flux probe.

3.2.3 Unipolar and bipolar sensors

There are two basic types of magnetic flux probe, Bipolar and Unipolar.
A bipolar sensor requires a positive magnetic field to operate (South Pole) and a negative field to release (North Pole) while unipolar sensor requires only a single magnetic south pole both to operate and to release because it moves in and out by the magnetic field. The probe utilized in this project is bipolar.

3.2.4 Specifications[38]

Magnetic flux probe technical specifications:

Mechanical data:

- Manufacturer: Ansaldo Energia;
- Weight: 2 kg;
- Length: 1900 mm;
- External framework: brass (no-magnetic);
- External diameter: 5 mm.

Electrical data:

- Resistance: 18 Ω;
- Inductance: 108 μH;
- Q factor: 0.5.

The test has been performed with a frequency = 1 kHz, with a multimeter Fluke 87, LCR meter HP 4262A. The Q factor is a no-dimensional index that compares the resonance frequency and the total wasted energy rate in an alternate sinusoidal circuit, deployed in electronic engineering.
The probe is a magnetic flux sensor (a Ω-L circuit), thus it has an operation range characterized by a resonance frequency and by a bandwidth. Consequently, if the input signal is included within the bandwidth then the output signal will be proportional to the input. Conversely, it could be distorted and then the output signal is not reliable. The sensitive sensor assesses the rotor slots flux of the rotor winding; it was carried out by Ansaldo Energia spa laboratories.
According to [13] here are reported the typical trends (X axis = time) of the ouptut signal of a flux probe:

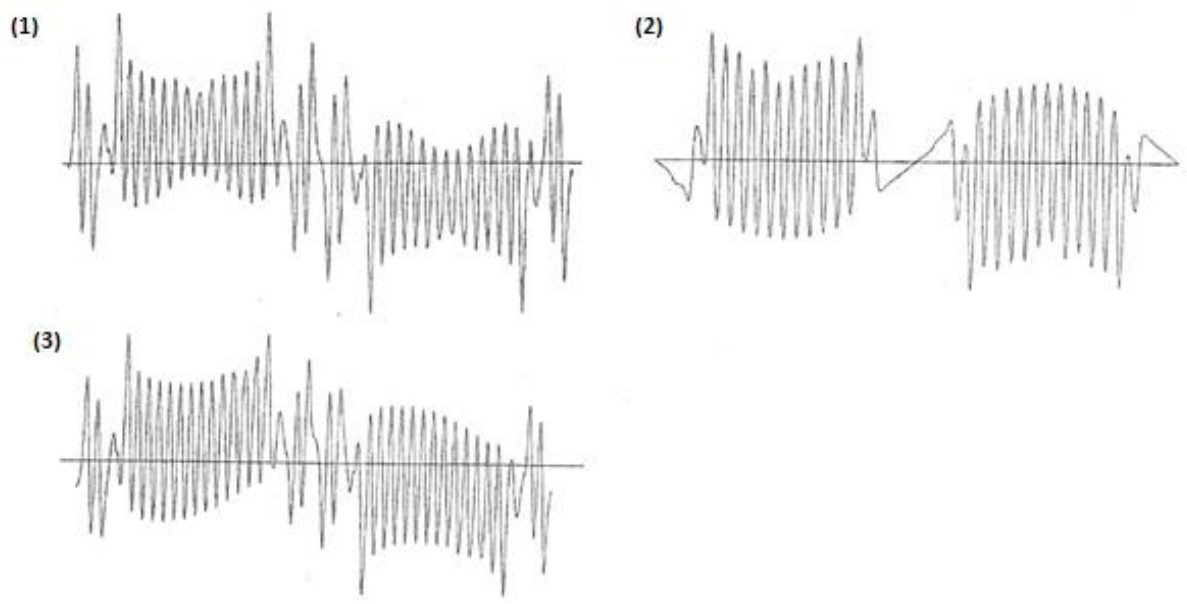

Figure.3.6: Typical flux probe output trends: no-load operation (1), short circuit operation (2), nominal operation (3).[39]

The peaks in figure 3.6 are equals to the change of the flux φ for each rotor coil.
The amplitude of these peaks is proportional to the m.m.f. of the rotor cave and thus to the numbers of turns (for each cave). Consequently, if there are shorted turns, the peak reduces its amplitude (proportional way with the number of turns with short circuit).

[38] To compare Ansaldo Energia, Sonda di flusso, certificato di taratura e collaudo, 13/9/2013, p. 1.
[39] P.Bruzzone, Sistema Cortrot, Sonda di flusso, manuale operativo, 11/07/2005, pp. 2 - 3.

Chapter four will describe the output signal management and a more thorough data analysis.
To get the insertion of the probe, the generator must be provided with:

- Probe attach flage;
- Adonlyment flange;
- Sferic valve;
- Rail threaded connection;
- Sleeve;
- Gum gasket;
- Pressure screw with locknut.

Furthermore the generator has to be disconnected from the grid, without hydrogen and with rotor stop.
It is possible to gain the probe insertion during the operation; nevertheless it is indispensable the deployment of an oscilloscope to acquire the correct waveform (as in figure 3.6).
Subsequently, it is necessary to carry on with these operations:

- Solder the flange;
- Lead the adjustment flange on that one soldered, between the two flanges serves a gum gasket;
- Test with a tube that has the same diameter of the real probe;
- Screw the sferic valve on the adjustement flange (in the middle a gum gasket);
- Screw the sleeve on the valve (in the middle a gum gasket);
- Screw the locknut on the pressure screw. To screw the pressure screw on the sleeve (in the middle a gasket);
- Seal the sferic valve.

3.3 The insertion inside the generator

3.3.1 H_2 to CO_2 change

During the operation, the cooling gas (hydrogen) is kept to a pressure about 3.8 bars, too dangerous for the insertion operation. Therefore a shrewdness involves the exchange with carbon dioxide (CO_2) kept to 0.9 bars.
It is of the utmost importance to perform a test with a false probe to ensure the feasibility of the operation.

3.3.2 The insertion

The operation of insertion involves that the probe must move closer to the rotor and subsequently, it must move away, the gap between the rotor and the probe must be 20 mm (depth reached is 1600 mm). The operation was performed by two Ansaldo Energia operators. At the end of the operation the generator was took back in hydrogen. The operation of insertion involves that the probe must move closer to the rotor and subsequently, it must move away, the gap between the rotor and the probe must be 20 mm (depth reached is 1600 mm).

The operation was performed by two Ansaldo Energia operators. At the end of the operation the generator was took back in hydrogen.

Figure.3.7: The insertion valve and the rail of the probe.

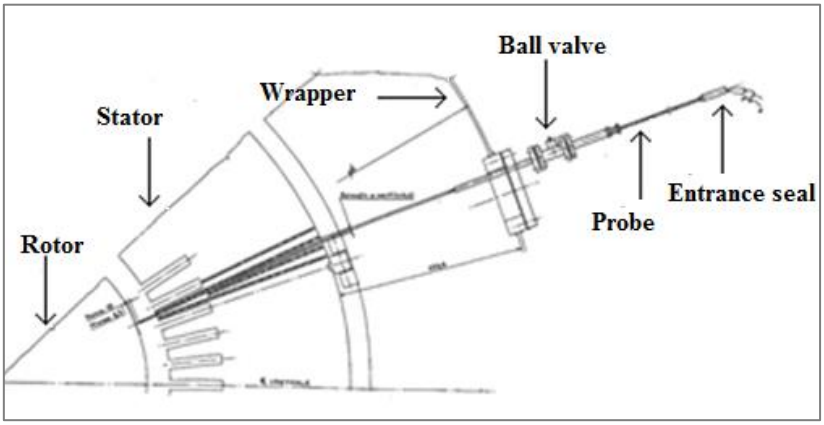

Figure.3.8: Cross section of the insertion operation.

Figure.3.9: The time of the insertion inside the generator and the external connection.

3.4 The external output management

3.4.1 Connections

The flux probe has been connected with the supervision system through a coaxial connector (characteristic of an oscilloscope, B.N.C. connector).

Figure.3.10: The external connection of the flux probe.

3.4.2 Supervision system ("MORAL")

The task of the rotor monitoring is the online supervision of the rotor winding, to detect possible shorted turns and to following their time domain evolution. This system allows the supervision of the insulation system and the rotor neutral grounding conditions. The main advantages of the real-time monitoring are:

- Automatic acquisition of the data, stored in servers;
- Measure of rotor slots flux, shaft voltage, shaft current, grounding voltage ($V_{M.A.T.}$);
- Warnings available (via relays and email);
- Real-time supervision of the rotor condition;
- Low cost.

The system has the task to analyse the rotor slots flux and the shaft voltage; it is indispensable utilize a magnetic flux probe and a RC filter (resistance and capacitor) on the rings. A current transformer (C.T.) is necessary for the shaft current and a crawling contact for the voltage drop. The software was created with National Instruments LabView. The computer server rack format is 19" 8U, 220 V A.C., connected with the L.A.N. network.

It is equipped with a terminal board for these signals:

1. Tachometric impulsive signal 1 x rpm +;
2. Tachometric impulsive signal 1 x rpm -;
3. Rings side filter;
4. Crawling contact of the grounding device;
5. Conductor of the grounding device;
6. C.T. shaft current +;
7. C.T. shaft current -;
8. Magnetic flux probe +;
9. Magnetic flux probe -;
10. Not connected;
11. No-energizing terminal (possible use about warning);
12. No-energizing terminal (possible use about warning).[40]

Figure.3.11: Supervision system cubicle.

The rings side filter is a FLT03/05 model, it has been carried out on an insulation support and it includes the crawling contact and the grounding device bolt. To minimizing the brush consumption the best installation point must be on the rotor head because of the lower peripheral speed. This filter drains the high frequency component of the shaft voltage due to static excitation system (a shaft voltage signal has been shunted from this filter).

Figure.3.12: FLT03/05 filter.[41]

[40] Look A. Ballerini, P. Tattini, A. Rossi, Nota tecnica, installazione del sistema di monitoraggio rotore alternatore "MORAL", Enel spa, 20/08/2010, p. 5.

[41] A. Ballerini, P. Tattini, A. Rossi, Nota tecnica, installazione del sistema di monitoraggio rotore alternatore "MORAL", Enel spa, 20/08/2010, p. 6.

The grounding device has the task to supervise the shaft voltage to detect possible grounding currents. The crawling contact of the grounding device must be insulated by the other contacts (of the shaft grounding device); the figure 3.13 displays the carrying out of the connection. The C.T. has the task to measure the shaft current, that crossing the grounding device. Its specifications are:

- Manufacturer: PANDOLFI spa ;
- 100 Ω, 10 V;
- Input 50 A output 0.1 A;
- Toroidal frame.

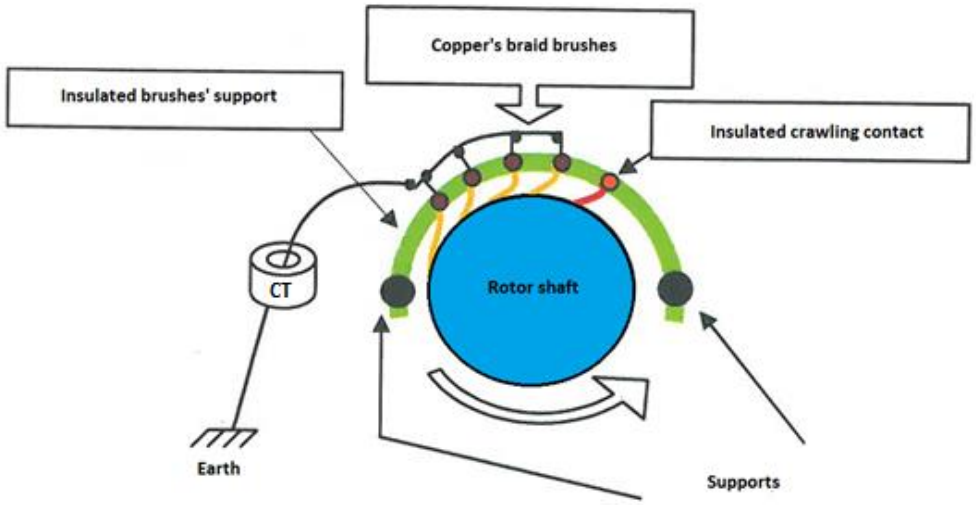

Figure.3.13: Crawling contact connection.[42]

In the chapter four it will be clear how to use these systems (about the shaft voltage analysis) and the many assets which will lead to the service maintenance.

Figure.3.14: The crawling contact and the shaft supervisory cubicle with shaft voltage and current meters.

[42] A. Ballerini, P. Tattini, A. Rossi, Nota tecnica, installazione del sistema di monitoraggio rotore alternatore "MORAL", Enel spa, 20/08/2010, p. 7.

3.5 Conclusions

These paragraphs had the task to justify the use of a magnetic flux probe for identifying possible shorted turns on the rotor. Nowadays it is a conventional choice mainly due to its small size and the real-time supervision of the rotor conditions.
This solution increases the power quality; a continuous and automated monitoring system offers several advantages:

- Reduced of site operations / maintenance staff;
- The data may be collected remotely by Windows based software from the user's pc at convenient generator load points. Consequently, this reduces the test time and costs.

CHAPTER 4

Monitoring of a rotor winding on short circuit

Subsequent to the parts that concern the Marcinelle power plant, the generator features and the excitation system, this chapter makes reference to the machine behaviour during an anomalous operation, in terms of shorted turns on the rotor winding. Obviously, this phenomenon must be avoided but it could happen for various reasons, do not foreseeable, a damage of the insulation among some turns of the excitation winding. The magnetic flux probe introduced in chapter three is sensitive to the time rate-of-change of the radial flux in the air gap. This probe measures the rotor slots fluxes produced by the excitation winding. With reference to the round rotor generator of the Marcinelle power plant, the probe acquires the flux signal for both poles. An analysis about the rotor slots fluxes and the shaft voltage F.F.T. will be performed.

4.1 Rotor winding shorted turns

4.1.1 The causes

The failed insulation between rotor turns may cause shorted turns; this may happen after a turn-to-turn movement of the rotor coils that may be due to the normal running speed. This relative movement may degrade the insulation layer and lead to a turn-to-turn contact. A short circuit between turns decreases the m.m.f. produced by a coil of the generator, thus born a magnetic distortion.

The failure mechanisms include coil foreshortening, end-strap elongation and inadequate end-turn blocking:

- **Coil foreshortening** involves a rotor turn copper decrease in length inside a rotor slot after a number of stop-start cycles. During operation the copper in the rotor tends to expand because of heating. Nevertheless this expansion is countered by frictional forces (due to centrifugal force) that develop when rotor is at speed; the blocking arrangements create a compressive force that tends to oppose this expansion. Thus the copper tends to compress inside the slot in the rotor body and, if these forces are excessive, this involves a deformation of the material in the body.

- **End-strap elongation** instead it results of an excessive friction between the end-straps and the retaining ring insulation. The top turns may move with the retaining ring if the friction coefficient becomes too great at running speed. Unfortunately, this process could repeat every start and stop cycle, and may involve elongation of the end turns (and it may lead to a contact between turns of near coils).

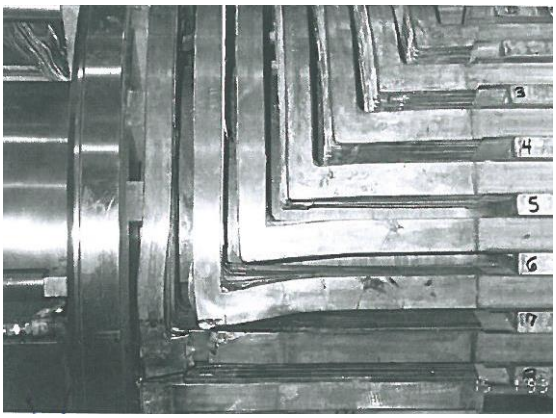

Figure.4.1: Elongated coil 6 contacts coil 7.[43]

- **End-turn blockings** are required to ensure a fixed position rotor winding end turns; obviously, the non-appropriate end-turn blocking may involve movements and shorted turns. The rotor frame provides coils distance supports.

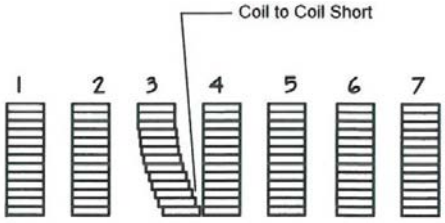

Figure.4.2: Coil short due to migrating end blocks.[44]

As already seen more times may happen that a turn (or more than one) could be on short circuit, but this phenomenon involves two cases:

1. The short circuit does not include the round rotor but only turns;
2. The short circuit includes the driving shaft because of a physical contact between turns and rotor iron (ground fault).

In the first case the excitation circuit stays insulated from the ground, the excitation impedance changes according to the number of turns with short circuit. In the second case the grounding device, through the crawling contacts, detects anomalous shaft current and voltage values to the ground. Moreover high currents cross bearings and supports.

With or without shorted turns, shaft voltages are induced inside the driving shaft; some causes of shaft voltages may be the magnetic configuration of the stator core, the insulation condition of the shaft, an anomalous design of the RC filter, a possible eccentricity of the rotor and at last shorted turns.
Therefore for detecting the anomaly it is possible to deploy a magnetic flux probe and/or to analyse the shaft voltage F.F.T. .

[43] Donald R. Albright, David J. Albright, Generator field winding shorted turns: observed conditions and causes, Generatortech, Inc, 2007, p. 4.
[44] Donald R. Albright, David J. Albright, Generator field winding shorted turns: observed conditions and causes, Generatortech, Inc, 2007, p. 5.

4.1.2 The effects

It is of the utmost importance to define the fault seriousness:

- **Insulation defect**: the defect does not absorb enough current to distort the rotor flux and thus there are not even harmonics in the shaft voltage F.F.T. ;

- **Shorted turns**: the short circuit absorbs enough current to distort the rotor winding flux, a magnetic unbalance occurs and even harmonics appear in the F.F.T. of the shaft voltage.

Moreover shorted turns could not be permanents: this involves that a fault may occur with reference to the winding temperature or to the generator speed.
If a turn or more than one is on short circuit the impedance of the rotor winding changes; then changes the rotor m.m.f. value. Thus to reach the same magnetic field it is necessary to increase the excitation current:

$$\underline{V} = \underline{Z} * \underline{I}$$

Through a transitory the impedance will change and consequently, will change the inductor magnetic flux.

This will lead to rotor vibrations, shaft voltage, rotor winding burnt-out, generator loss of excitation, generator components magnetization and so on and system security will be threatened.
If the short circuit triggers discharges on the iron rotor (and consequently, a ground short circuit) all the machines must be disconnected and stopped (also the gas turbine and the steam ones).
This involves damage to the synchronous generator but also a loss of profit for the operator.

When shorted turns occur, higher excitation current is required to supply power a specific load. This is mainly due to that the same amp-turns have to be generated by fewer active turns and this may involve a limit on the generator output.
The amp-turns relationship is:[45]

$$I_s = I_N * \frac{T_N}{T_s}$$

where I_S and T_S are the excitation current and the active turns with shorted turns, I_N and T_N are the same without shorted turns.

Nevertheless the Joule losses change such as $R*I^2$ at a specific load thus with $[T_N / T_S]^2$; this leads to an increase of the winding losses (the increase of the excitation current could not be appreciable if the number of shorted turns is not high, the R values range could change about few unit %). Others effects are the induction of voltages and currents in the driving shaft and thus a deterioration of the bearings conditions. Thus it is of the utmost important to supervise this phenomenon.

[45] Look Donald R. Albright, David J. Albright and James D. Albright, Generator field winding shorted turn detection technology, IRMC, May 1999, p. 2.

The shorted turns phenomenon leads to rotor vibrations because of the magnetic field changing and different rotor heating; "wide vibrations on bearings is one of the early indicators that a turn short has occurred."

Two types of vibrations:

- **Magnetic vibrations**: a shorted coil leads to a magnetic force distortion, only on four poles machines because the reduction of the magnetic field will affect both the North and the South poles equally; the effect depends by the defect location and an unbalance of radial magnetic field between rotor and stator could lead to vibrations.

- **Thermal vibrations**: they are produced by the change of Joule losses in the rotor winding but without uniformity; this difference may lead to vibrations in the rotor, caused by a bending (a part of the rotor operates cooler and another one operates at higher temperature). The thermal sensitivity of the rotor may be measured at different loads (this will be clear in paragraph 4.2). The thermal sensitivity is higher on the coils near the pole axis than the ones near the quadrature axis (because of the different size of the coils, different thermal inertia).

Thus possible shorted turns near the quadrature axis will have fewer effects about the thermal balance because of these coils are nearly 180° apart.
In brief the effects of shorted turns may be (connected between them, compared to nominal operation):

- Flux losses;
- Higher excitation current (with reference to the generator output);
- Higher Joule's losses (with reference to the generator output);
- Shaft vibrations (due to the m.m.f. unbalancing, higher during under-excitation operation than during over-excitation one);
- Higher rotor winding temperature;
- Deceasing of the reactive power (due to the magnetic field decrease);
- Shaft voltage waveform distortion and shaft currents.

4.2 Initial data

"Analysis of air-gap flux probe data can pinpoint the number and location (pole and coil) of shorted turns without having to take the generator offline. If the percentage of total turns shorted out is small, the generator may be able to run at rated load for years without further problems."[46]
With reference to the synchronous generator 50THR – L63 installed at the *Marcinelle* C.C.G.T. power plant the analysis begins with the following data, a nominal operation of the machine.
The beginning data in Table.4.1 were acquired on May 21th 2013 at 10.30 a.m., AVR1 regulator on:

General:		**Generator:**			
			L1	**L2**	**L3**
T_{amb} [°C]	10,4	**V stator [kV]**	19,3	19,4	19,3
n [rpm]	3000	**I stator [kA]**	11,1	11,2	11,1
f [Hz]	50	**P [MW]**	373,1		
GT-ST power [MW]	374	**Q [Mvar]**	3,4		
Exported power [MW]	370	**S [MVA]**	480		
Auxiliary power [MW]	5,6	**cosφ**	0,77729		
		T stator windings [°C]	44 - 56		
		T stator core [°C]	39 - 45		
Grid:					
Integrated absorbed Energy	**Integrated produced Energy**	**Resultive Integrated Energy**			
4201,56	937451,1	-933252,4	**[MWh]**		
875,88	17614,45	-16738,57	**[Mvarh]**	inductive	
37146,66	36205,37	941,6	**[Mvarh]**	capacitive	
Excitation system:					
V_{exc} [V]	275,7				
I_{exc} [A]	2205,7				
T_{exc} [°C]	37				

Table 4.1

[46] Donald R. Albright, David J. Albright and James D. Albright, Generator field winding shorted turn detection technology, IRMC, May 1999, p. 1.

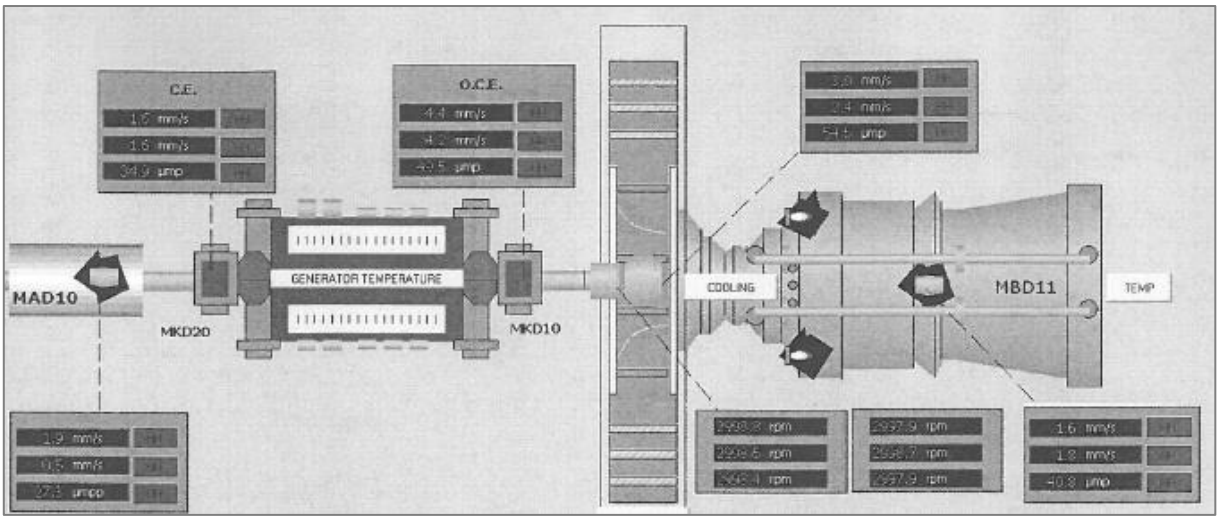

Figure.4.3: Turbine-generator bearings vibrations supervision.

Figure 4.3 displays the bearings vibrations supervision system; it ensures the good operation of the generator and the turbines. MKD20 and MKD10 are the link flanges (with vibrations sensors). The vibrations data were gathered on May 21th at 9.32 a.m., with the power plant at nominal operation:

VIBRATIONS DATA:		**MKD10**	**MKD20**
VIBRATIONS:	Absolute [mm/s]	4,3	1,6
	Relative [µmp]	49,5	34,9
TEMPERATURE:	[°C]	88,2	91,4
	[°C]	89	91,1
	[°C]	88,9	90,4

Table 4.2.

4.3 Assumptions

According to the data in paragraph 2.5:

- 2 poles synchronous generator, round rotor, 8 coils per pole;
- n = 3000 rpm constant during the monitoring (50 Hz power system);
- constant air gap between the round rotor and the flux probe = 20 mm;
- data acquisition every hour (magnetic flux probe, shaft voltage, shaft current, speed), except during the start time, characterized by a more busy schedule of data;
- RC filter on the exciter rings end.

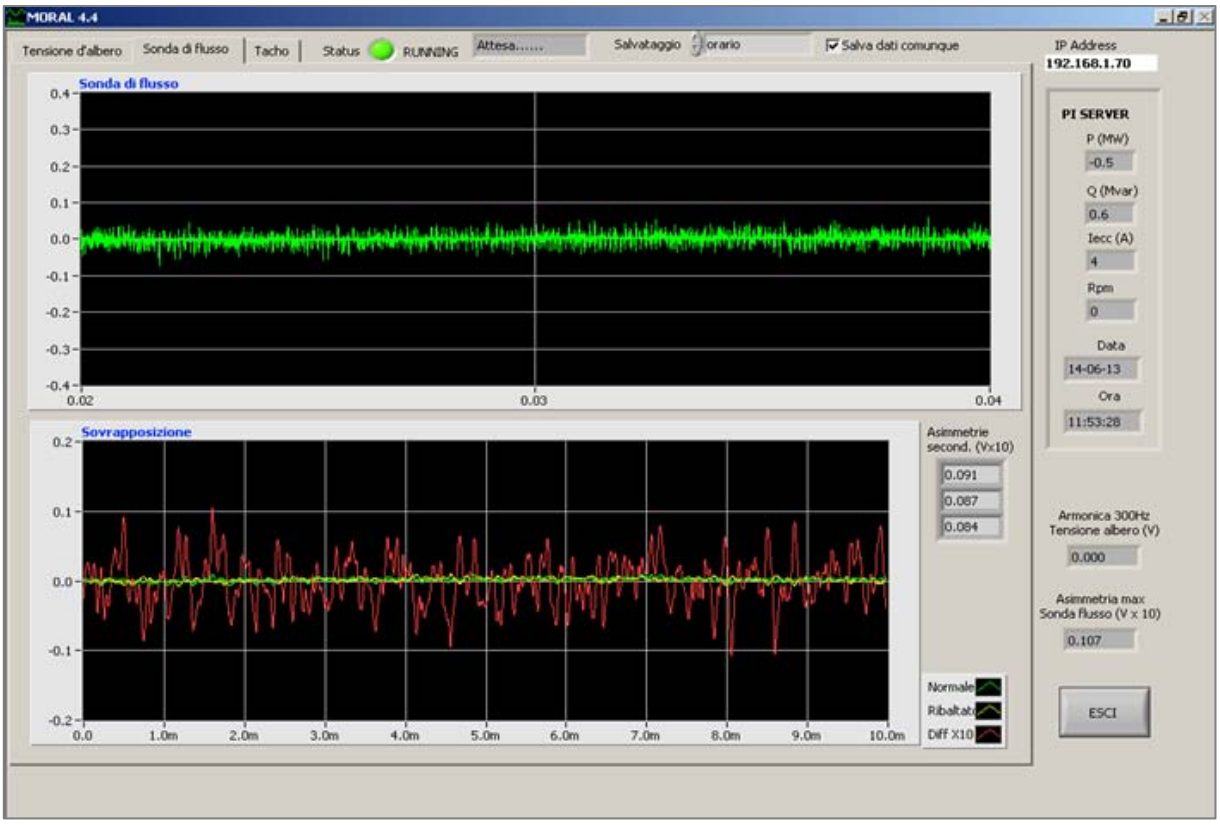
MORAL 4.4
Tensione d'albero
Sonda di flusso
Tacho
Status
RUNNING
Attesa.....
Salvataggio
orario
Salva dati comunque
IP Address
192.168.1.70
Sonda di flusso
Sovrapposizione
Asimmetrie second. (Vx10)
0.091
0.087
0.084
PI SERVER
P (MW)
-0.5
Q (Mvar)
0.6
Iecc (A)
4
Rpm
0
Data
14-06-13
Ora
11:53:28
Armonica 300Hz Tensione albero (V)
0.000
Asimmetria max Sonda flusso (V x 10)
0.107
Normale
Ribaltato
Diff X10
ESCI

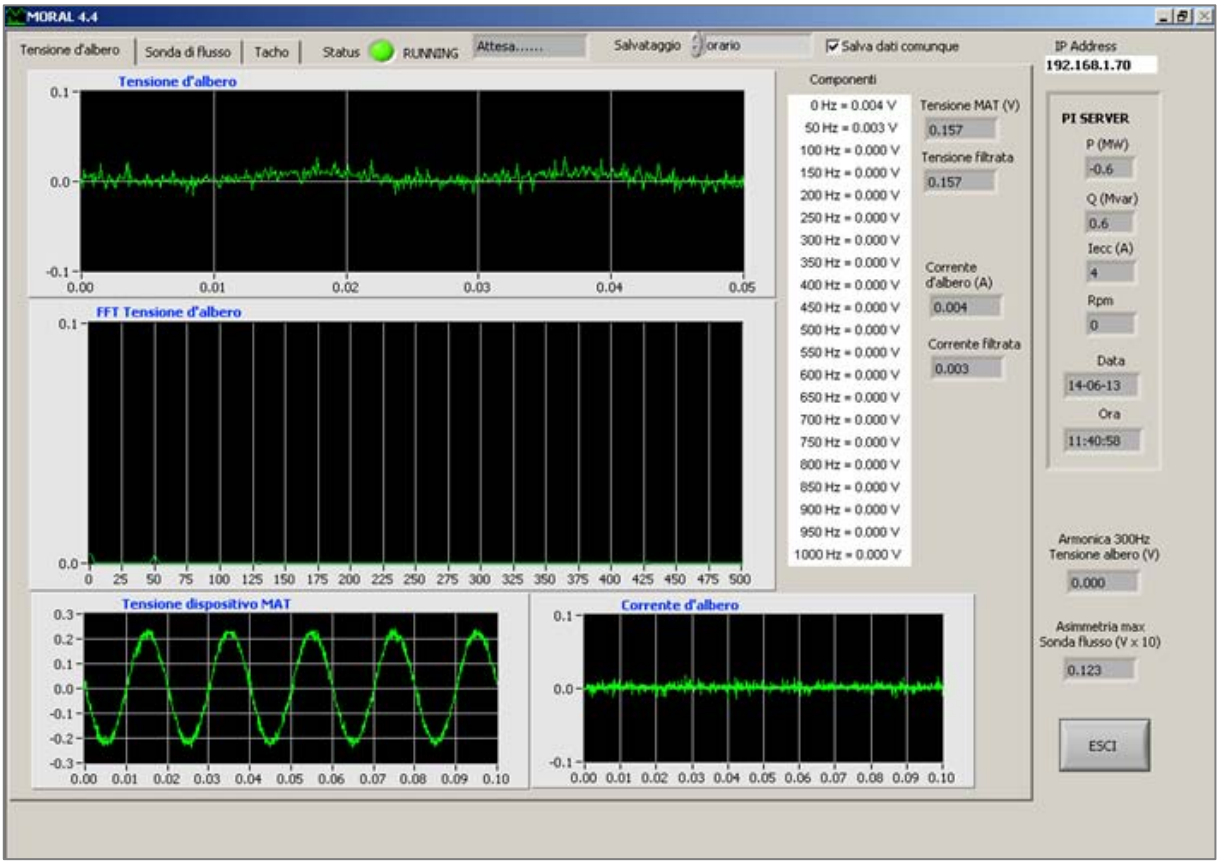
MORAL 4.4
Tensione d'albero
Sonda di flusso
Tacho
Status
RUNNING
Attesa.....
Salvataggio
orario
Salva dati comunque
IP Address
192.168.1.70
Tensione d'albero
FFT Tensione d'albero
Componenti
0 Hz = 0.004 V
50 Hz = 0.003 V
100 Hz = 0.000 V
150 Hz = 0.000 V
200 Hz = 0.000 V
250 Hz = 0.000 V
300 Hz = 0.000 V
350 Hz = 0.000 V
400 Hz = 0.000 V
450 Hz = 0.000 V
500 Hz = 0.000 V
550 Hz = 0.000 V
600 Hz = 0.000 V
650 Hz = 0.000 V
700 Hz = 0.000 V
750 Hz = 0.000 V
800 Hz = 0.000 V
850 Hz = 0.000 V
900 Hz = 0.000 V
950 Hz = 0.000 V
1000 Hz = 0.000 V
Tensione MAT (V)
0.157
Tensione filtrata
0.157
Corrente d'albero (A)
0.004
Corrente filtrata
0.003
Tensione dispositivo MAT
Corrente d'albero
PI SERVER
P (MW)
-0.6
Q (Mvar)
0.6
Iecc (A)
4
Rpm
0
Data
14-06-13
Ora
11:40:58
Armonica 300Hz Tensione albero (V)
0.000
Asimmetria max Sonda flusso (V x 10)
0.123
ESCI

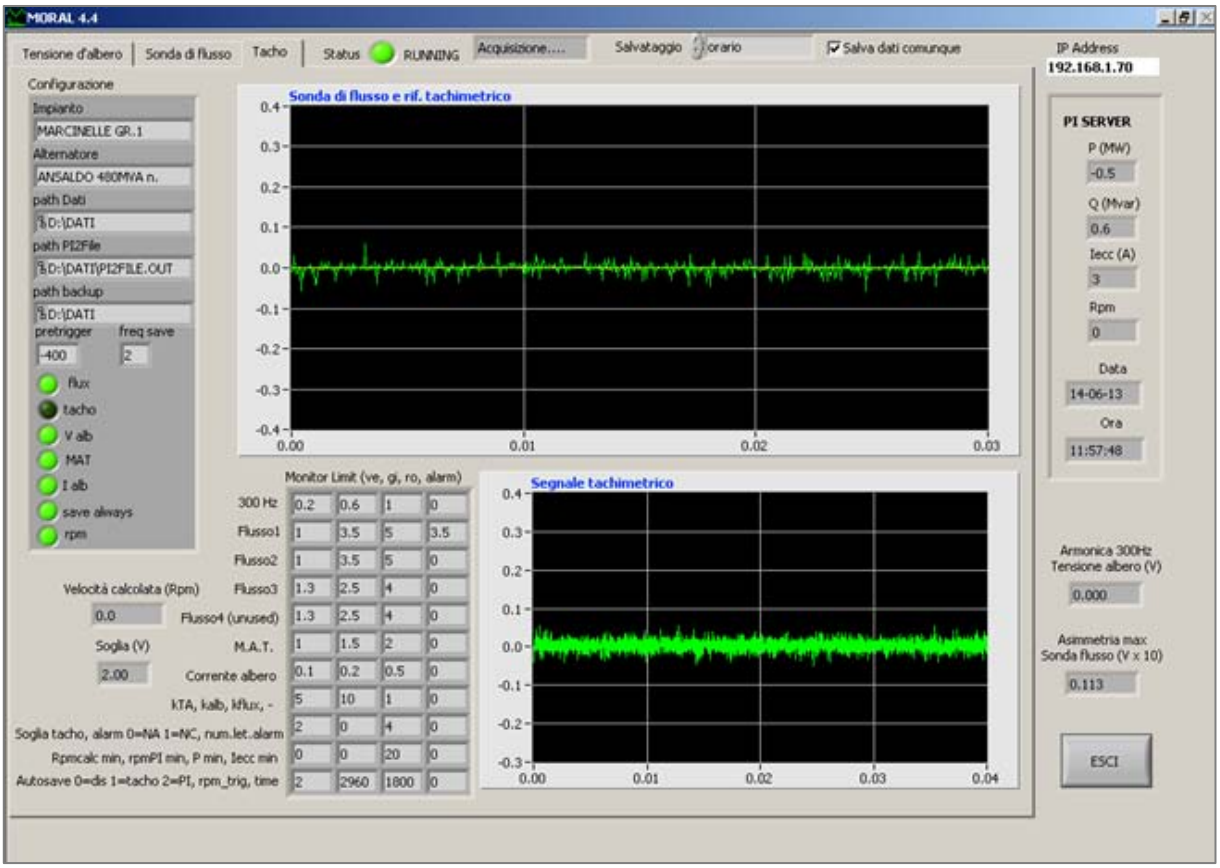

Figure.4.4: The supervision system screens with power plant off: flux probe data and superimposition, shaft voltage and current with F.F.T., flux probe data and speed comparison.

4.4 Methods

Several methods are available to supervise a synchronous generator. They may be collected in two classes: offline and online methods. This is mainly due to results evaluation, because with an offline method there is not any thermal effect (out of service). The combined use of offline and online methods may involve a high reliability of results.

- **Offline methods:**
  - Rotor dynamic impedance measure;
  - Time domain reflectometry (T.D.R.).
- **Online methods:**
  - Magnetic flux probe;
  - Shaft voltage F.F.T. .

4.4.1 The magnetic flux probe

This method foresees the rotor radial flux analysis for each rotor winding coil, to detect possible shorted turns. To show a result it is possible to use an oscilloscope or even better a digital system (developed in the paragraph 3.4.2) as it leads to a more reliable evaluation.
The results are given by a cartesian graph where on the X axis there is the time and on the Y axis there is the signal magnitude in Volts. The magnetic flux probe signal waveform displays a peak for each rotor slot. The magnitude of these peaks is related to the amp-turns in the slots.

The amp-turns are directly proportional to the active turns in the coil thus a coil with shorted turns will display a smaller peak than a coil without shorted turns.
Shorted turn calculations are performed by measuring the magnitude of each lead slot peak and then making a pole-to-pole comparison for each coil. Subsequently, a superposition between the two flux trends of the same pole will allow detecting possible defects.
To gain a full view of the rotor condition is needed to deploy a point called F.D.Z.C. (flux density curve zero-crossing) that is the point of intersection between the X axis (time) and the integral flux curve; this point must be aligned with the under-analysis coil slot peak in the flux probe waveform, otherwise it is not possible to get an accurate measure (if the coil under-analysis is far from the F.D.Z.C., the amplitude of possible shorted turns is dampened).
It is easy to intuit as the F.D.Z.C. varies with the load conditions of the generator. At 0 MW and 0 Mvar the F.D.Z.C. is located on the quadrature axis, when the load condition verges to the full load one the F.D.Z.C. will be near to the coil 1.[47]

"To calculate the shorted turns for a particular coil, the load point whose F.D.Z.C. most closely aligns with the lead slot of the desired coil is selected. Optimally, there would be a load point whose F.D.Z.C. aligns with the lead slot for each coil. Consequently, to achieve the maximum sensitivity to a shorted turn, the F.D.Z.C. position must be changed by the machine load changes.
For example, if 10% of the turns in a coil are shorted out, the pole's coil slot peak would be expected to decrease by approximately 10%."[48]
The chart in figure 4.5 displays an example of the flux measure (at 240 MW and 55 Mvar test generator).

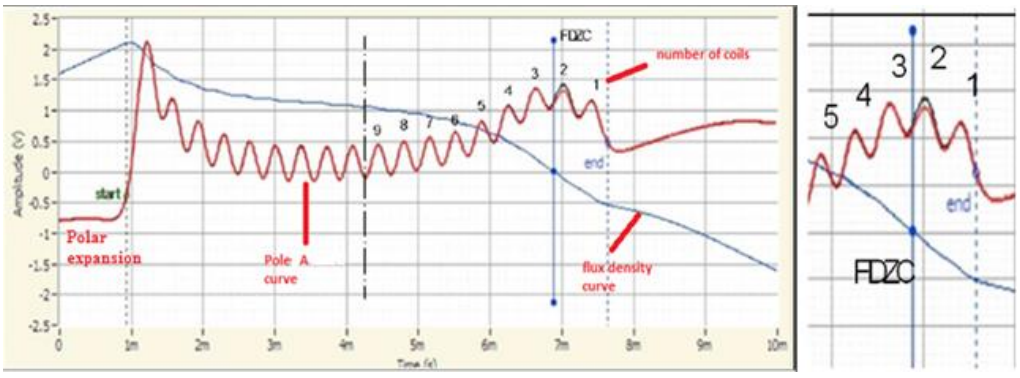

Figure.4.5: Example of flux measure and the F.D.Z.C. point.

[47] Look M. Manarini, Metodo per l'esecuzione della misura dei flussi disperse con generatore sotto carico, Enel spa, 18/01/2012, p. 4.
[48] Donald R. Albright, David J. Albright and James D. Albright, Flux probes provide on-line detection of generator shorted turns, Generatortech, Inc, 1999, p. 3. This is true if only the FDZC point is aligned with the under-analysis coil peak.

Nevertheless may occur that two or more coils of one pole become shorted together; this involves a total absence of signal for these coils. Nevertheless possible magnetic asymmetries could lead to a flux waveform distortion and thus to affect the measure reliability.

4.4.2 Shaft voltage F.F.T. analysis

A widespread problem to all electrical machines is the induction of shaft currents and voltages in the driving shaft. The phenomenon of motor shaft voltages producing circulating shaft currents was recognized since the 1920s. When a generator is operated under sinusoidal power, shaft voltages are caused by alternating flux linkages with the shaft. They appear i.e. between shaft ends, between shaft and external case and between shaft and bearings. "Shaft currents are a result of the shaft voltage being discharged through the bearings. Shaft voltages above 50 V peak to peak can occur from electrostatic charges developed on low-pressure turbine blades. Stator magnetic asymmetries, residual magnetization of the rotor or frame and high-frequency transients developed from thyristor excitation controls may also cause shaft voltages that can damage bearings."[49]

This method consists in the frequency spectrum analysis of the shaft voltage acquiring a signal from a filter also used for deleting the voltage spikes produced by the static exciter (the signal represents one of the supervision system inputs). The evaluation of this term could be useful to help evaluate shorted turns phenomenon gravity. As it will be clear in the paragraph 4.7, the shaft voltage is not a perfect alternate sinusoid; subsequently, there are some harmonics besides the fundamental (50 Hz).

"The effect of rotor winding shorted turns will result in local losses of magnetic force; sequentially, make magnetic force which has short circuit pole generate local flux losses. Therefore inter-turn short circuit may be regarded as magnetic force distribution of demagnetization". Neglecting saturation, the effect of the shorted field coil may be considered as the standard field with an additional one mainly due to a fictitious coil of the same number of turns as the shorted turns but with opposite current flow (Fourier series).[50]

There are several kinds of shaft voltages and consequently, several effects in function of the cause:

1. **Shaft voltage due to a stator magnetic asymmetry**: this is the main cause of shaft voltage. Possible asymmetries in the stator magnetic circuit (magnetic circuit reluctance) could cause shaft voltage; thus the phenomenon importance changes according to the manufacturers choices. High number poles generators in hydroelectric power plant are often built with a stator with two semi-cylinders (with a constant axial air gap and thus there is always a flux distortion); instead turbo-generators for thermal application are built with semi-circles sheets (staggered and laminated). This shrewdness involves lesser flux distortion than the first solution, consequently, lesser magnitude of shaft voltage.

[49] IEEE Std 1129-1992, Recommended practice for monitoring and instrumentation of turbine generators, p. 17.

[50] To compare Wang Xiao-hua, Li Yong-gang, Wu Yu-cai, Fan Jing, Method of fault diagnosis on inter turn-short-circuit in turbine generator rotor windings based on shaft voltage, North China Electric Power University, Baoding, China, IWISA 2009, p. 296.

2. **Shaft voltage due to axial rotor leakage fluxes**: these fluxes do not link together the stator windings because they are located at the end of the rotor, at the windings end. Consequently, these fluxes link together the solid rotor, inducing shaft voltages.

3. **Shaft voltage due to rotor eccentricity**: during on-load operation possible rotor eccentricity (static and dynamic) could cause shaft voltages because of unbalance of magnetic flux in the air gap (the magnetic circuit reluctance changes). Unfortunately, this may be due to building defects.

4. **Shaft voltage due to external voltage supply**: rotor winding was insulated by the driving shaft then there is a capacitive coupling between them. Power electronic inside the static excitation system (e.g. S.C.R.) contains many high frequency components in its voltage output such as voltage spikes due to the switches commutations, thus a shaft voltage could be induced on the shaft; fortunately, a capacitive filter between the shaft and the ground may contain spikes magnitude from many dozens of Volts to few units of Volts or fewest (the harmonic order of shaft voltage due to this phenomenon is over dozens kHz).

5. **Shaft voltage due to electrical charges**: some electrical charges could be produced by the collision of the water drops in the steam with the turbine blades. These charges flow through the shaft to the ground. To limit shaft voltages due to electrical charges it is possible to install a shaft grounding brush on the driving shaft, e.g. between the generator and the steam turbines (this shrewdness protects the bearings).

During the normal operation the space distribution of the m.m.f. is close to the step-like distribution (the m.m.f. jumps at every slot); nevertheless when inter-turn short circuit occurs the effective coils number on the rotor winding reduce, leading to a decrease of the m.m.f. magnitude.
This means that the m.m.f. at the both sides of the winding becomes asymmetric, and this phenomenon leads to additional harmonic e.m.f. in the stator winding. [34] The harmonic analysis conventionally, is developed with the Fourier series, it is possible to make reference to [17-18-34] .
In a different way from other methods this one involves the deployment of a frequency spectrum, particularly of the shaft voltage, to detect inter-turns short circuit. The supervision system acquires the shaft voltage data and prints their trends on a graph (magnitude [V] - time); then a frequency factorization is carried out to gain a frequency spectrum. With reference to [17] on normal generator operation only odd order harmonics are content in the shaft voltage frequency spectrum; thus if an inter-turn short circuit occurs also even order harmonics are contained in the shaft voltage frequency spectrum as the 2^{nd}, the 4^{th} and the 6^{th} (Fourier). The magnitude of these even harmonics represents an index of the short circuit severity but unfortunately, it is not possible to know the exact location of this defect.
This method could be an effective alternative compared to the magnetic flux probe because the grounding device is just installed inside the generator shaft, as already analysed in the paragraph 3.4.2 (no further costs). Or this device may be integrated with the flux probe such as in the supervision system utilized in this work, increasing the system reliability.
The harmonics may cause many problems to rotating machines, such as vibrations and additional losses in the stator (copper and iron), rotor and in the damper windings due to the different speed of the harmonic rotating field.

4.4.3 Rotor dynamic impedance measure

This method consists of the measurement of the rotor winding impedance to detect possible shorted turns. Nevertheless it was utilized until some years ago before the introduction of the rotor flux analysis but it was characterized by a high error degree because it involves the combination of two direct measures (voltage and current) both of them are affected by errors. The measurement occurs through the voltage-current method at several rotational speeds always at 50 HZ A.C. on the collector rings (usually each 100 rpm). Nowadays, digital acquiring systems may reduce this uncertainty through a point-to-point process. This involves an increase of the results reliability. Unfortunately, the winding impedance does not change a lot when a short circuit on the rotor winding occurs.

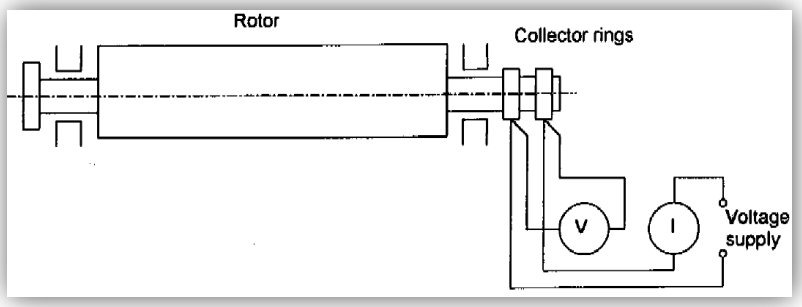

Figure.4.6: Voltage-current measurement to assess the rotor impedance.[51]

The single-phase rotor winding impedance (A.C) may be determined by:

$$\underline{Z_n} = \frac{\underline{V}}{\underline{I_n}} = R + jX$$

where "n" is the number of the measurement each 100 rpm . It is possible to calculate the maximum impedance percentage range:

$$\Delta Z_n\% = \frac{[(Z_n - Z_{n-1}) * 100]}{Z_{zero}}$$ [52]

Z_{zero} is the impedance value at the standard operation. Nevertheless under 30% of the rated speed it is not possible to gain a fixed value of the impedance because of the damper winding is not fully closed. For higher speeds must be $\Delta Z_n\% < 3\%$.[53]

[51] Ansaldo Energia, Dynamic impedance measurement on rotor windings, 11/04/2002, p. 2.
[52] Ansaldo Energia, Dynamic impedance measurement on rotor windings, 11/04/2002, p. 3.
[53] Ansaldo Energia, Dynamic impedance measurement on rotor windings, 11/04/2002, p. 3. To compare IEEE Std 56-1977. Nevertheless the value of the impedance range depends by the numbers of coils and turns.

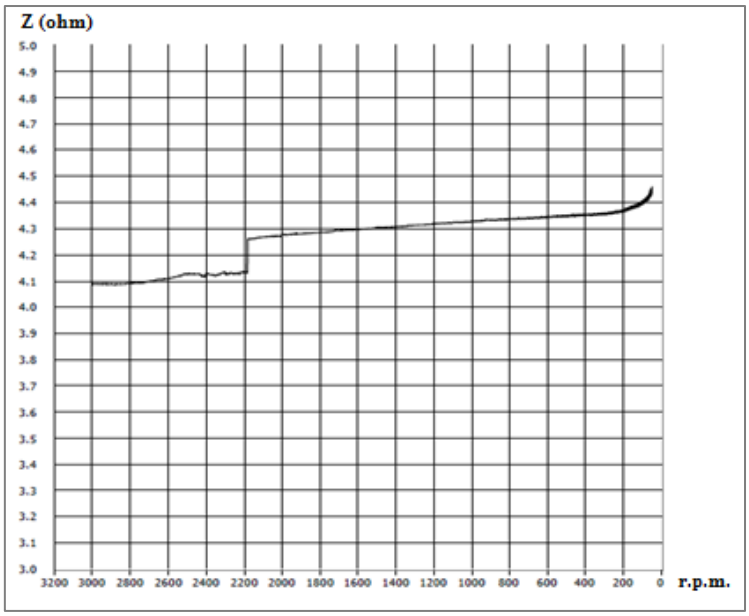

Figure.4.7: Dynamic impedance measure.[54]

4.4.4 Time domain reflectometry[55]

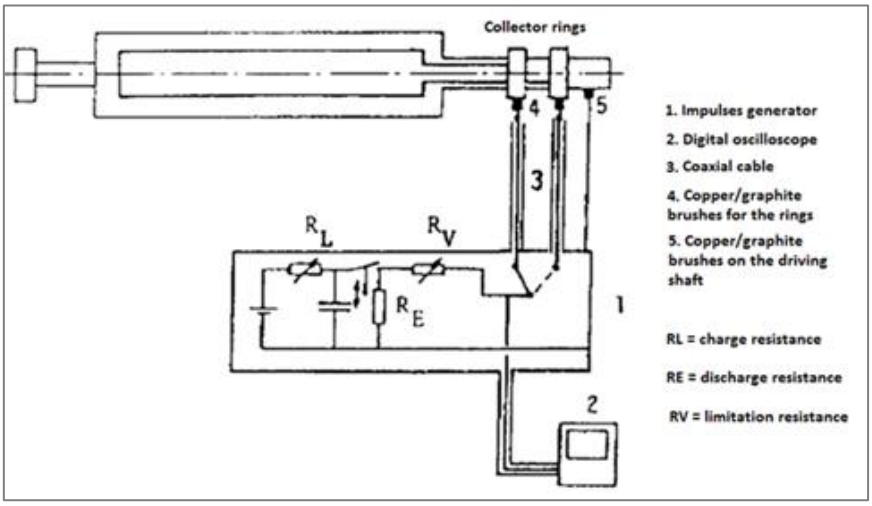

Figure.4.8: Measurement electrical circuit.[56]

The aim of this method is to locate of possible shorted turns on the rotor winding using a voltage wave reflection in the coils; the reflection times of a healthy turn and of a shorted one are different. Several voltage impulses (by an external supply) with steep slope (≈10 ns) are applied through R_V between a ring and the ground, the other link keeps free. It is possible to use a step wave generator.

[54]Data processing edited by the specialized assistance of Enel spa (Enel GEM/SAI/ASP-ELA). Step in figure represents a short circuit on the rotor winding; near to 0 rpm the damper windings effects are clears. Look IEEE Std 56-1977 about the method theory.

[55] This theme is well described by J. W. Wood, but the method was called Recurrent surge oscillograph (RSO), 1986.

[56] Dal Mut, Controllo dei corto circuiti tra spire di rotori di turboalternatori con il metodo dell'onda mobile a bassa tensione, Ansaldo Energia, 23/07/2007, p. 3.

The voltage trend between ring and ground may be displayed by an oscilloscope; at the impulse end the winding voltage may discharge through R_E. But the measure is not easy; the capacities to the ground may drain high-frequency components of the voltage signal, thus the time of measure changes along the winding. Consequently, it is possible to detect the shorted coil but not exactly the shorted turn.

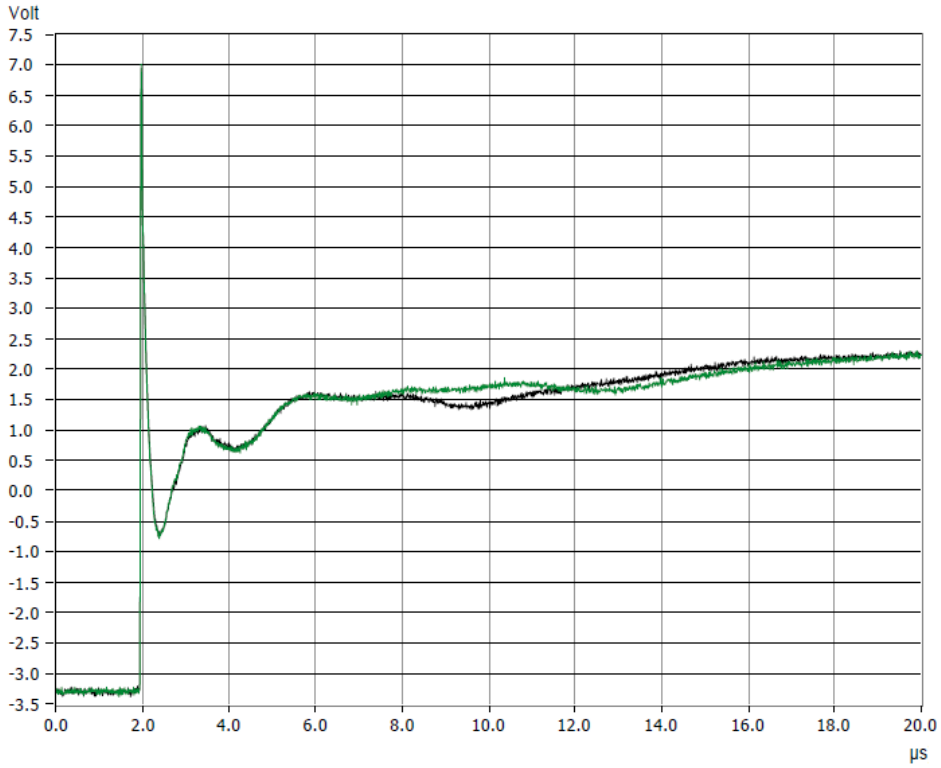

Figure.4.9: Example of ring-to-ring voltage comparison trend.[57]

The oscilloscope must be supplied by an insulation transformer and R_V must be near in value to the mean wave rotor resistance, to avoid a movable wave reflection at the head of the winding. This may be gotten altering the R_V value until the reflection signal is equal to the half impulse magnitude ($U_W \approx U/2$). Subsequently, the ground link of the ground rotor protection must be disconnected and the grounding brush must be raised (same operation about the rings brushes).
These operations will allow reaching the T time value. The measurements must be performed for each ring and consequently, from the two digital signals comparison, it will be possible to display the presence of possible shorted turns (look the figure 4.9). To detect the location of a winding flaw it is possible to deploy the ratio between the travelling time T_F of the movable wave until the flaw (signals division) over the travelling time T until the winding end through:

$$N_F = N * \frac{T_F}{T}$$

where N is the total number of winding turns and N_F is the shorted turn.
Another method could be the measurement of the shaft current, feasible only for generators with only one side of the shaft is grounded.
Nowadays the most utilized methods to detect inter-turn short circuits are the first and the second, suggested coupled with others sensors systems and data elaboration.

[57] Data processing edited by the specialized assistance of Enel spa (Enel GEM/SAI/ASP-ELA).

4.5 Materials

According to the paragraph 3.4.2 the supervision system represents a useful solution to supervise the rotor winding conditions, particularly about the *Marcinelle* power plant because of its complex driving shaft framework with an insulated joint to one of two turbines.
This system allows monitoring these possible problems:

1. Shorted turns on the rotor with the magnetic flux probe;
2. Shorted turns on the rotor with the shaft voltage harmonic analysis;
3. Correct operation of the grounding shaft system of the rotor;
4. Correct insulation of the supports to the ground and of the coupling flange.

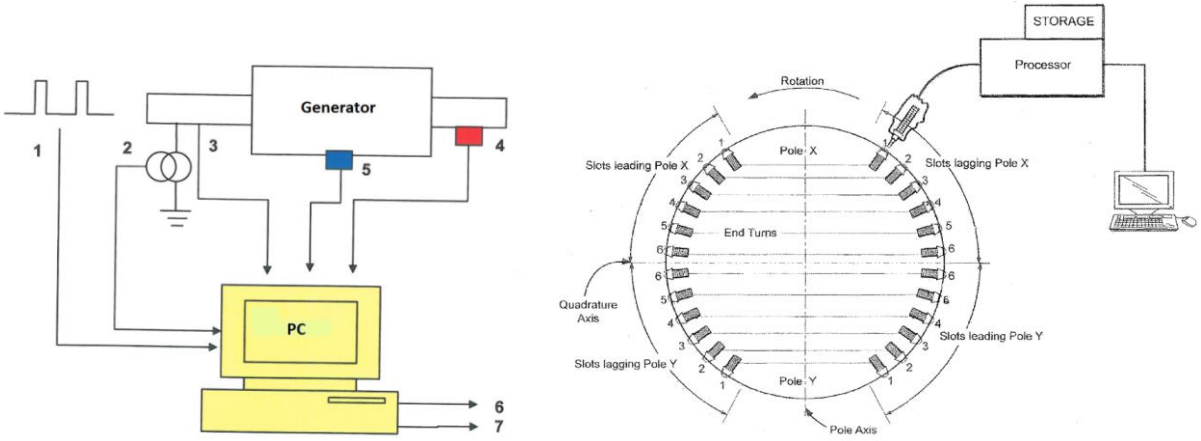

Figure.4.10: The supervision system connection outline.[58]

According to the figure 4.10 the schedule of the connections:

1. Tachometric reference 1 per rpm;
2. Shaft current to the ground through the C.T. ;
3. Grounding device voltage brush (M.A.T.);
4. Brush and filter for shaft voltage;
5. Flux probe;
6. No-energizing terminal (possible use about warning);
7. L.A.N. relay.

The supervisory PC consists of three main parts:[59]

- Industrial PC ASEM PR4040;
- Windows XP pro sp3;
- Data acquisition cards;
- Software Rotmon 4.4;
- K.V.M. module (keyboard, video, mouse).

[58] Keith Franklin Beatty, Online monitoring system and method to identify shorted turns in a field winding of a rotor, General Electric Company (U.S.), April 11,2011.
[59] Look A. Ballerini, Computer for generator rotor monitoring system "MORAL", Enel spa, 07/06/2010, p. 4.

The computer and K.V.M. module specifications were related in Appendix B. The acquisition data cards required instead is only one type, due to compatibility between software and hardware that are utilized in the monitoring system: Daqcard M series PCI 6233 (National Instruments).

4.6 Shorted turns detection

A well balanced machine should have in the rotor winding two poles with the same magnetic flux value. If an inter-turn short circuit occurs on a pole, the rotor magnetic flux of this one will be reduced (with reference to the shorted coil) and it should be easily detected.

In 2012 the generator was provided with a permanent flux probe (in 2013 a new installation was necessary after its breaking); the supervision system was installed in June 2012 and from the data acquired was possible to examine the rotor winding state. Beginning from the fluxes analysis in June 2012 two shorted turns on the rotor winding were detected, the first one is located on the 4th coil (pole A), the second on the 3rd coil (pole B). They may be displayed in the chart in figure 4.11. Data are taken at various loads for maximizing resolution of the analysis for each coil of the rotor field winding. The magnetic flux probe test was carried out with the following load profile:

- 0 MW, 0 Mvar (no load);
- 68.5 MW, -7.4 Mvar;
- 198.1 MW, 11.8 Mvar;
- 368.5 MW, 22.5 Mvar (full load).

These short circuits most probably are the cause of the new "thermal sensitivity" of the rotor; it means that the rotor vibrations change with the excitation current. The discontinuous operation could lead to a worsening of the rotor winding state. A first daily rotor winding monitoring was carried out on 13th June 2012 at several load conditions; it was reported in figure 4.11.

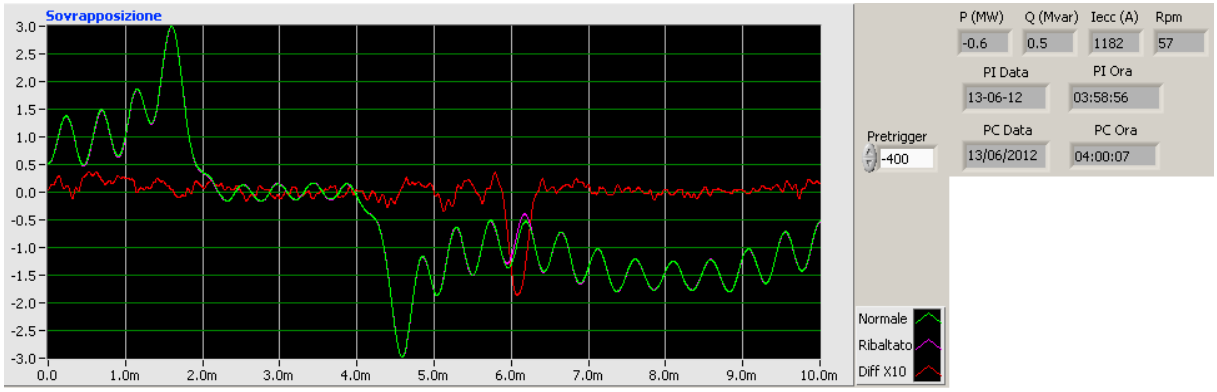

No-load test (shorted turns on the 4th coil are clear).

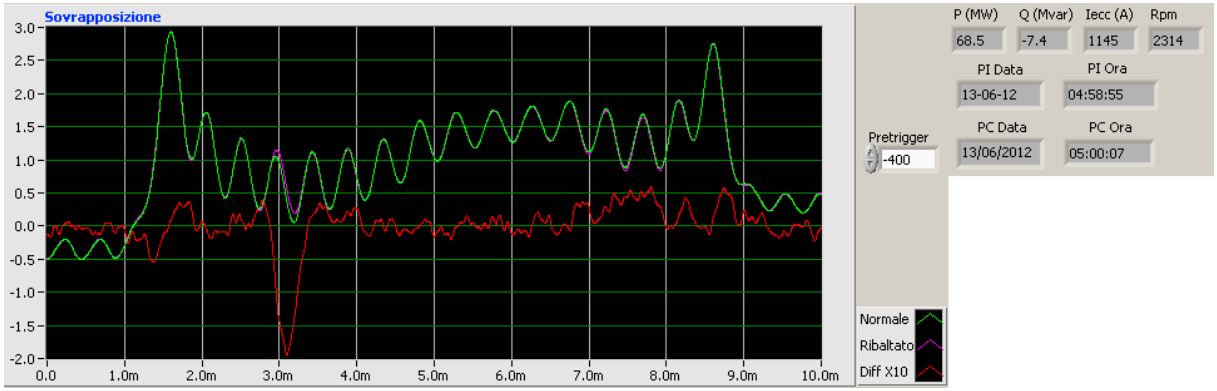

Low load test.

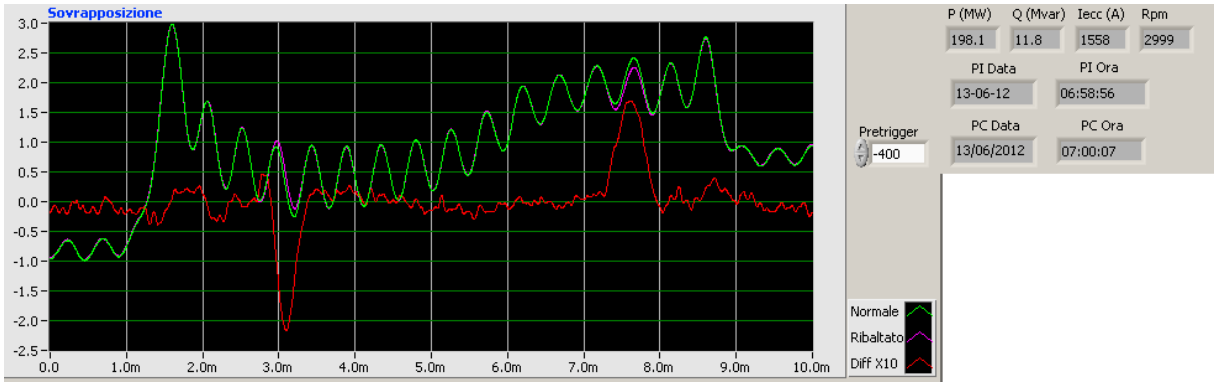

Middle load test.

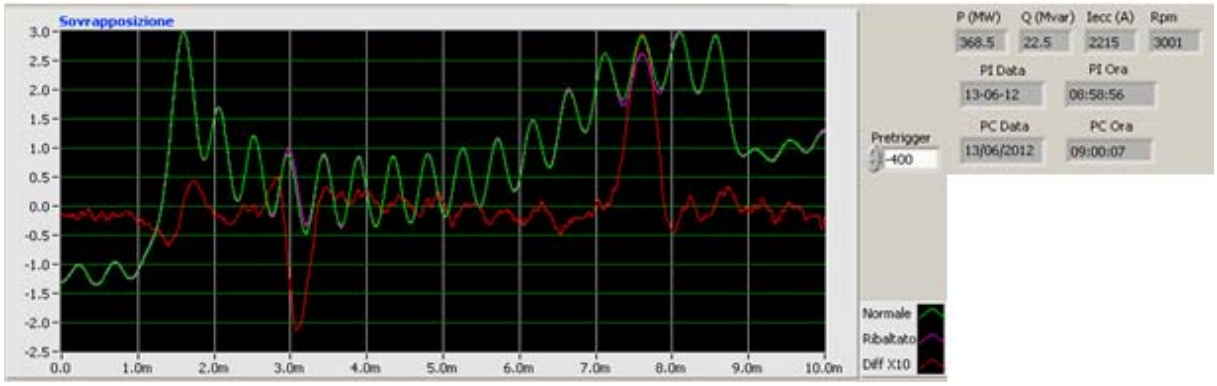

Full load test (clears the 4th and 3rd coils defects).

Figure.4.11: Flux probe signal trend, 13/06/2012.

The green and pink lines represent two poles flux trend, thus the red line is their magnitude difference (X10).
From the last chart two defects are clear: one on the 4th coil and another on the 3rd one. The defect on the 4th coil was detected in April 2012. The shaft voltage frequency spectrum was acquired on June 14th 2012 using a temporary grounding device installation (before the permanent installation). The chart in figure 4.12 represents it. The next paragraph will explain how to use the shaft voltage harmonic analysis to complete the rotor winding monitoring. It is of utmost importance a real-time monitoring of the rotor winding.

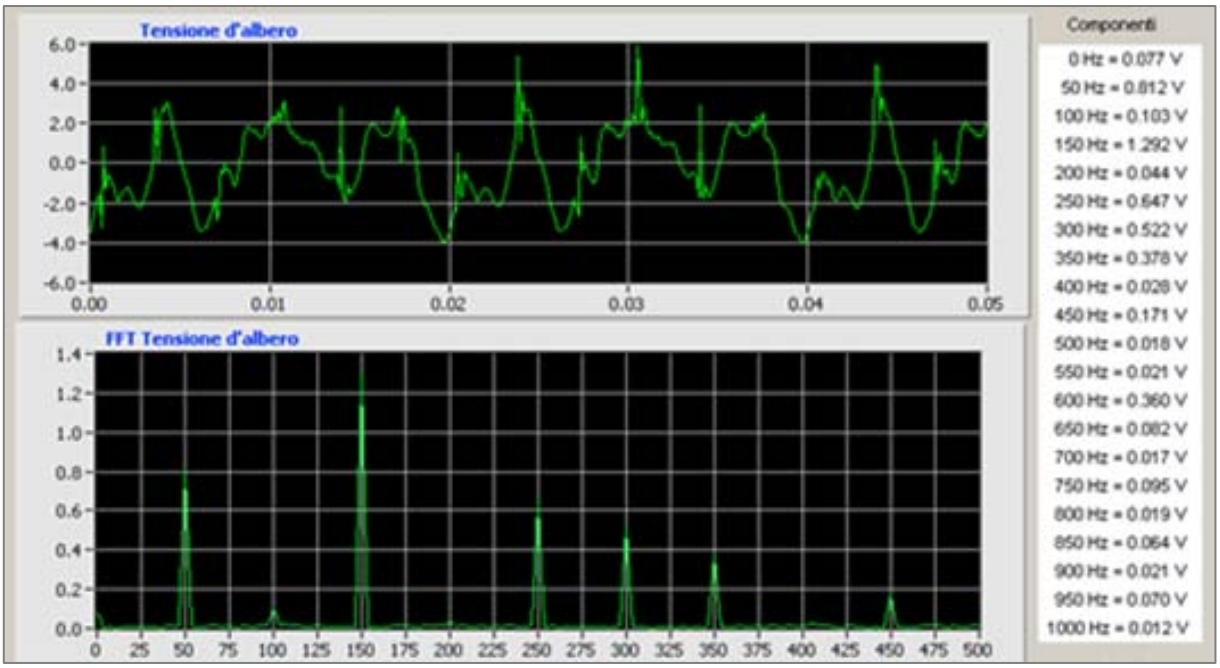

Figure.4.12: Shaft voltage frequency spectrum, 14/06/2012.

Figure.4.13: Shaft voltage frequency spectrum: 1) good operation, 2) fault operation (presence of even harmonics).

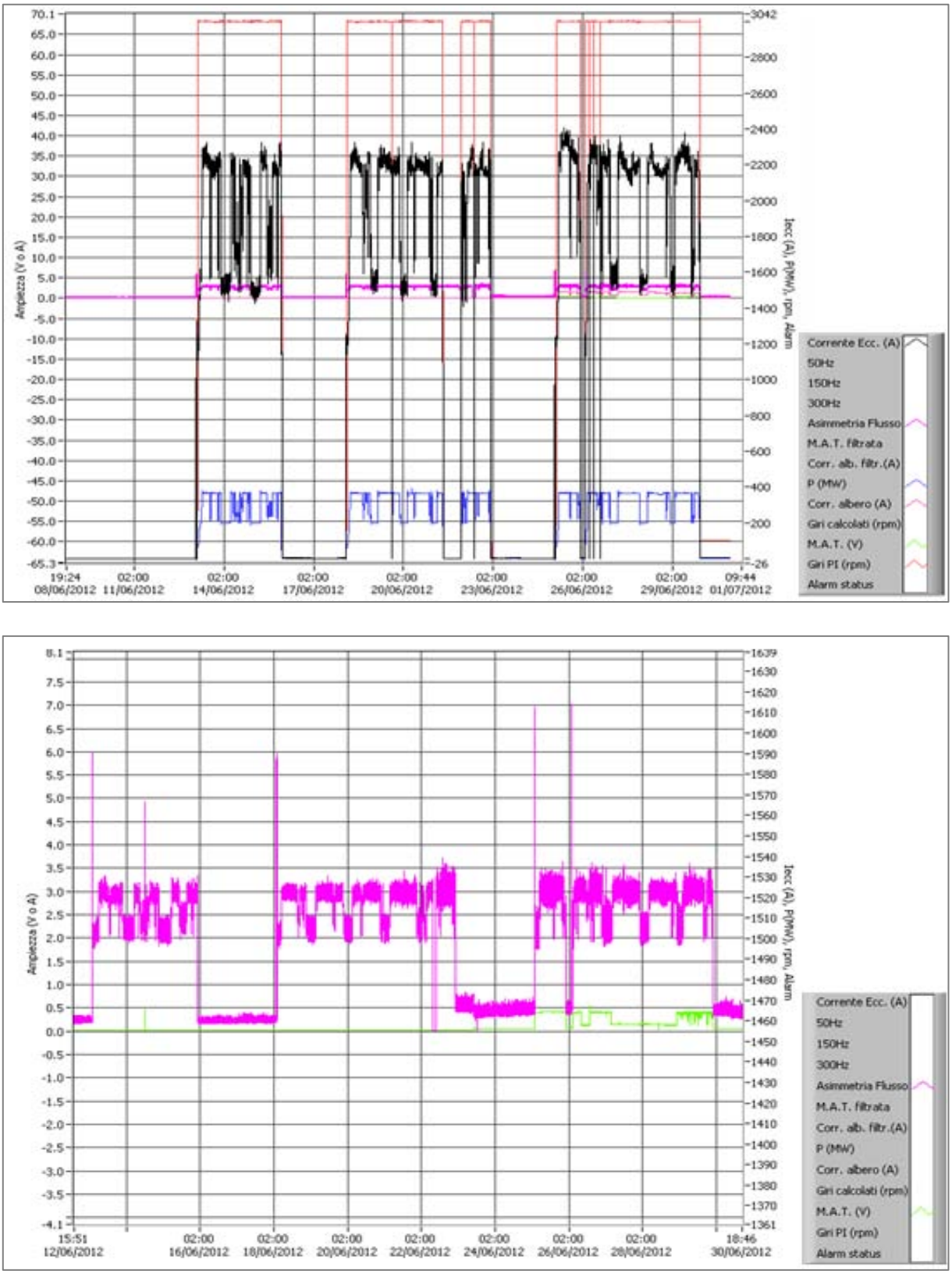

Figure.4.14: Shorted turns detection of June 2012 (main rotor flux magnitude = pink line).

The charts in figure 4.14 show the flux asymmetry amplitude with reference to the excitation current (black line), power output (blue line) and speed (red line); this asymmetry is not equal to zero thus shorted turns phenomenon occurs.

4.7 Rotor fault condition and monitoring

If the percentage of the shorted turns is small the generator may be able to run at the rated load; nevertheless a larger percentage of shorted turns could lead to severe problems, it involves a forced outage.

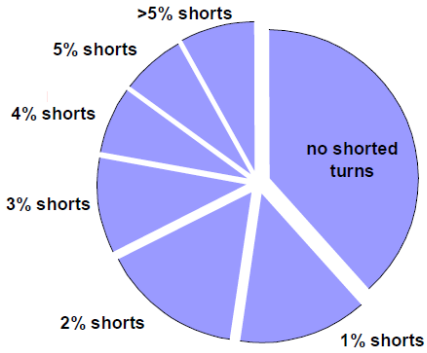

Figure.4.15: % of shorted turns for synchronous generators (by Generatortech, Inc.)[60].

"The problems experienced by these machines range from excessive vibration to reduced load capability to forced outage"[61]. The next data are related to 2013. On June 19th 2013, a starting trend was acquired.

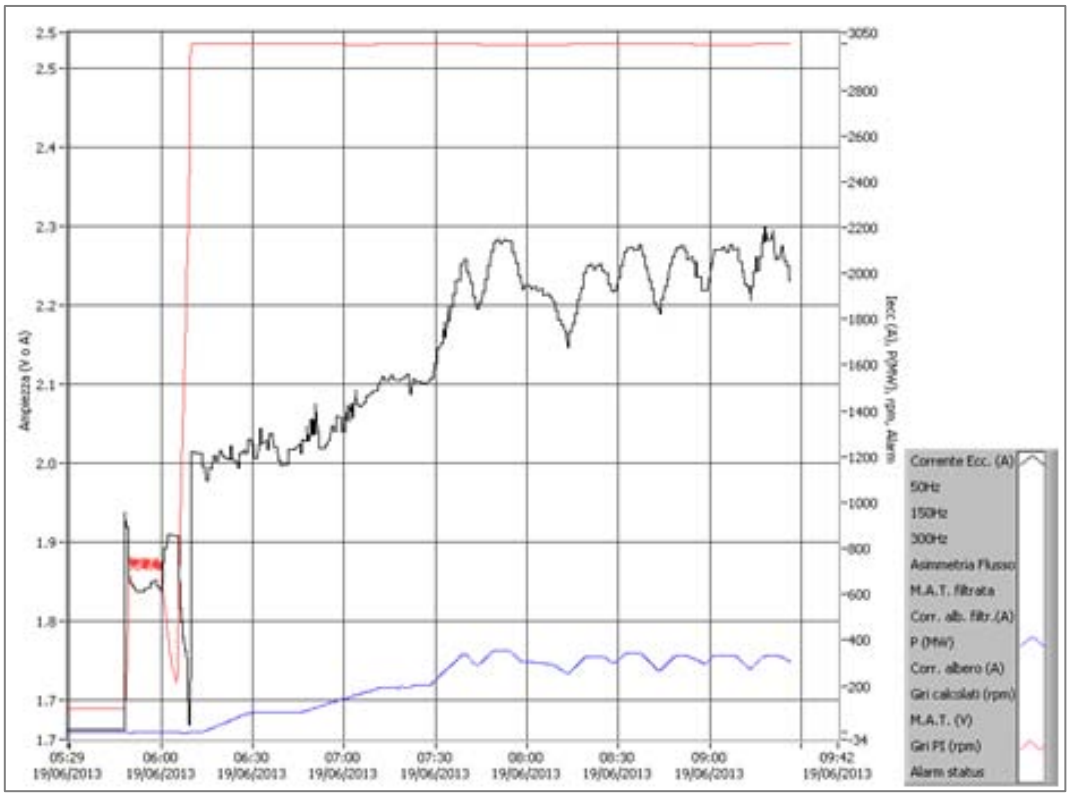

Figure.4.16: *Marcinelle* power plant starting trend, 19/06/2013.

[60] Donald R. Albright, David J. Albright, Generator field winding shorted turns: observed conditions and causes, Generatortech, Inc, 2007, p. 1. Make reference to the previous 13 years data collection.
[61] Donald R. Albright, David J. Albright, Generator field winding shorted turns: observed conditions and causes, Generatortech, Inc, 2007, p. 2.

Figure 4.16 caption:

- Active power output: blue line [MW];
- Excitation current: black line [A];
- Speed: red line [rpm].

The chart in figure 4.17 displays the wide variability of the flux amplitude during a plant starting. Δ+ = + 6.1 V, Δ- = + 0.4 V.

The flux data must be separated from others in figure 4.17 because of the different amplitude scale.

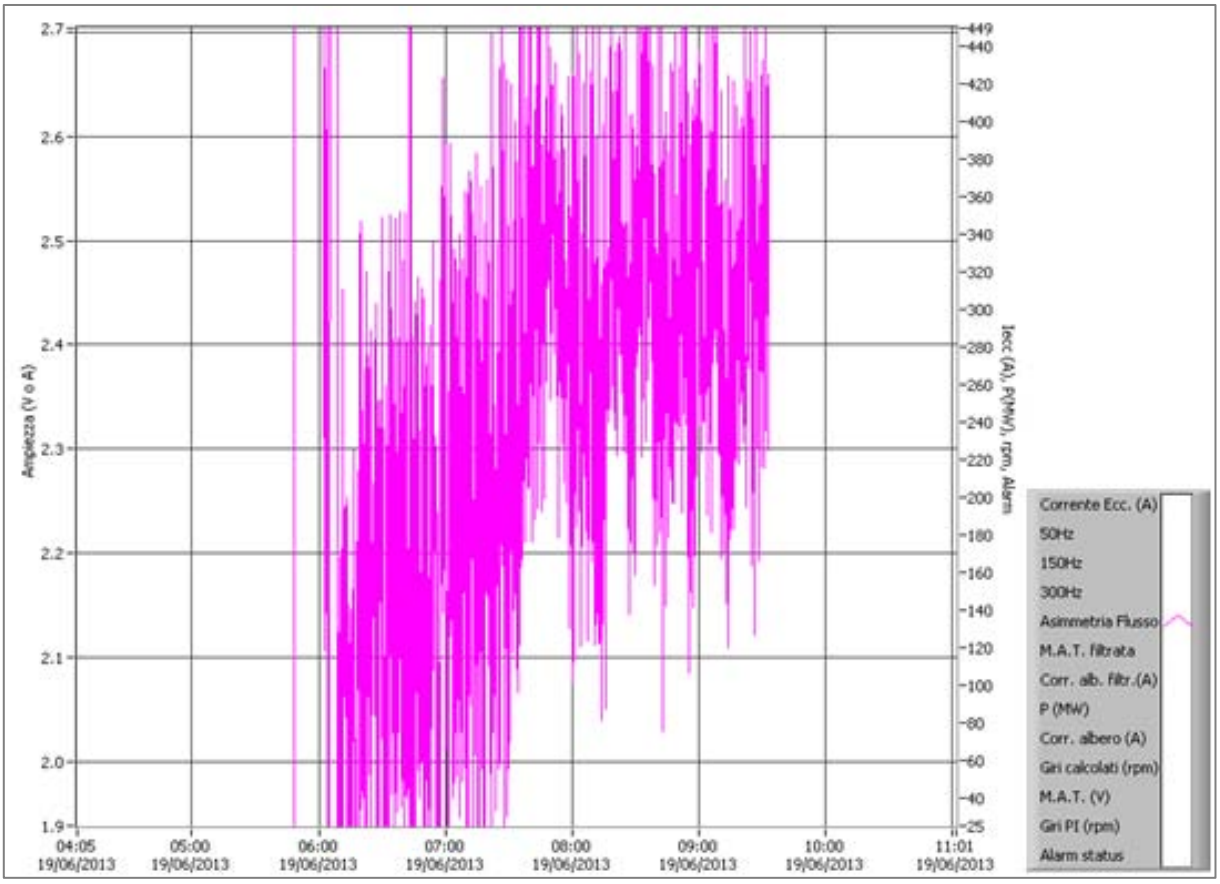

Figure.4.17: Main rotor magnetic flux magnitude trend, 19/06/2013.

On June 18th 2013, 12:07:41 pm, the next data were acquired:
P = 364.3 MW, Q = 28.7 Mvar, Iexc = 2259 A, n = 3000 rpm.

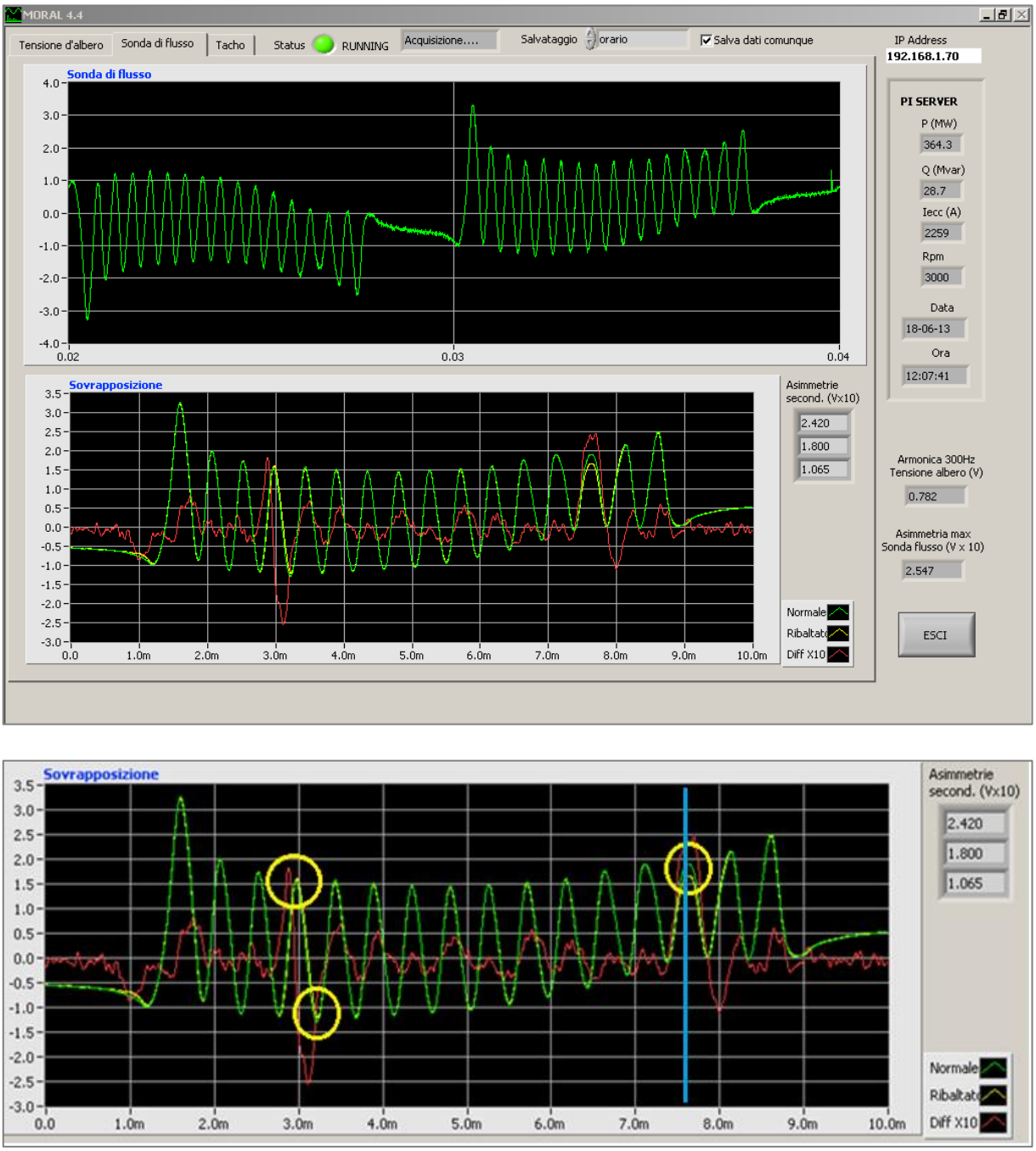

Figure.4.18: Magnetic flux probe output and focus on the slots flux of the rotor winding, full load test.

As already analysed in the paragraph 4.6 a full load test may reveal two shorted turns. The yellow circles in the chart in the figure 4.18 show these ones. The measure is reliable because the F.D.Z.C. point at full load tests is near the pole axis (cyan line).
The current state of the generator could be due to frequent starts and stops of the power plant.

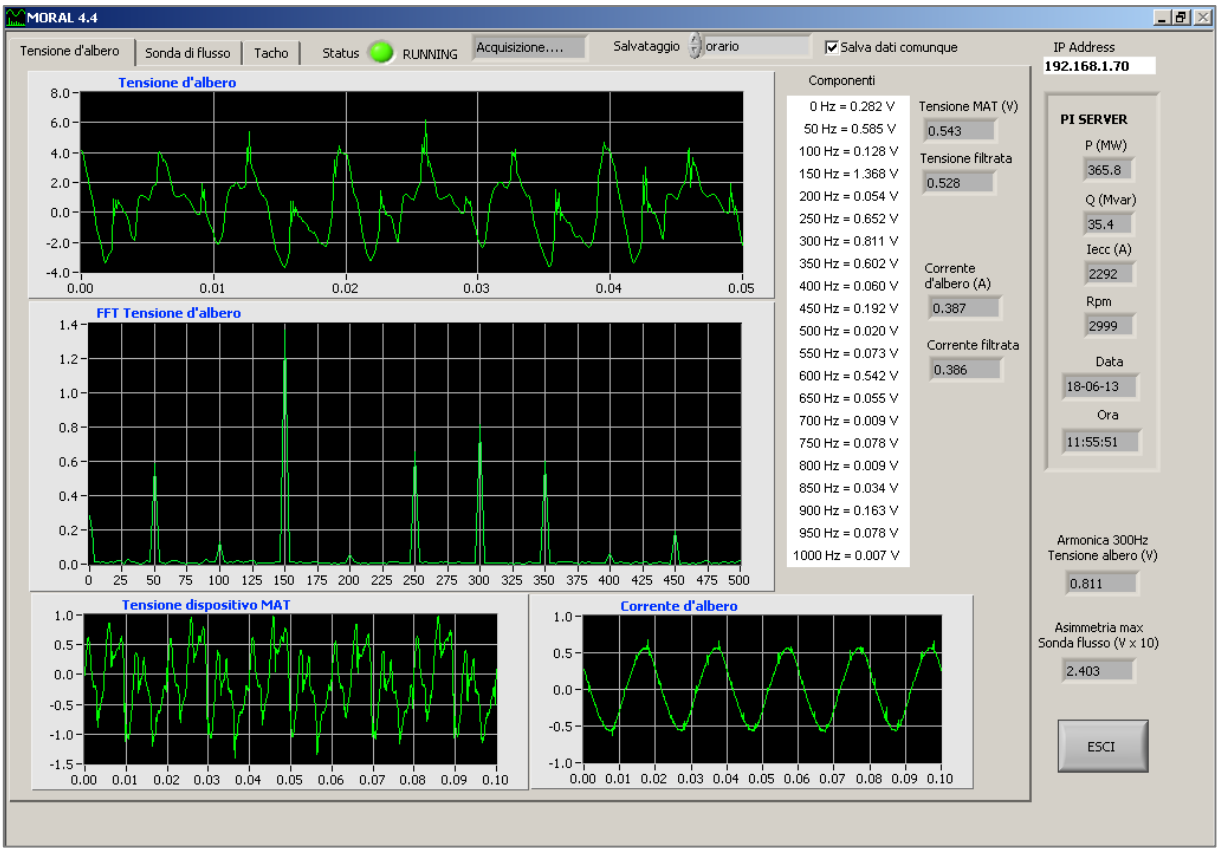

Figure.4.19: Shaft voltage and current waveforms, 18/06/2013.

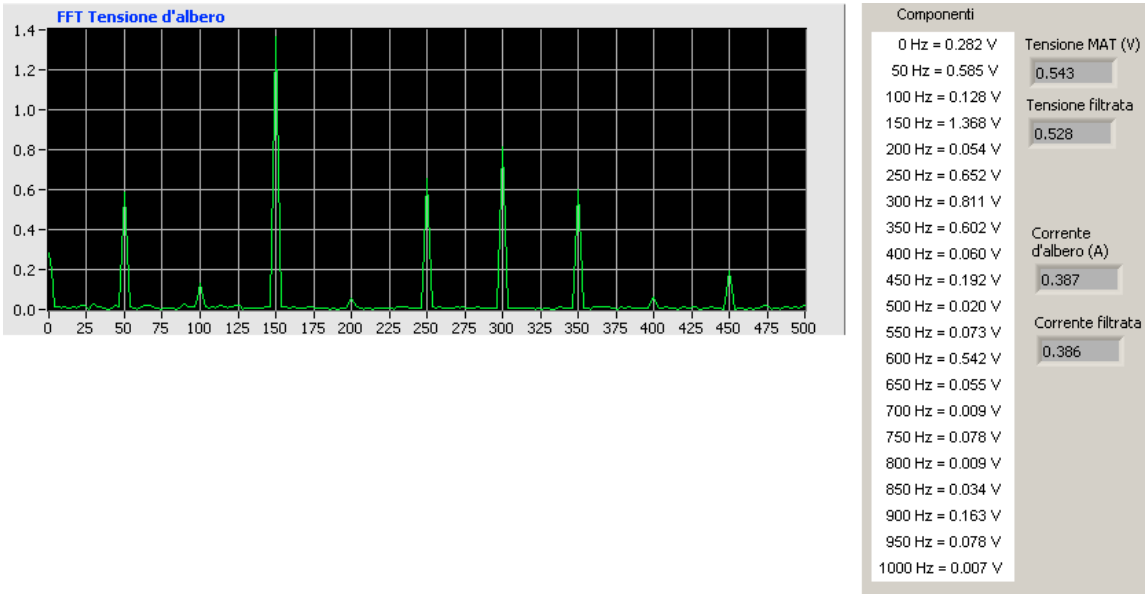

Figure.4.20: Frequency spectrum of shaft voltage, 18/06/13.

"On normal condition important frequency components in shaft potentials are the fundamental and the third. When an inter-turn short circuit defect occurs, the 2nd, the 4th and the 6th harmonics increase noticeably with the short circuit."[62]

[62] Wang Xiao-hua, Li Yong-gang, Wu Yu-cai, Fan Jing, Method of fault diagnosis on inter turn-short-circuit in turbine generator rotor windings based on shaft voltage, North China Electric Power University, Baoding, China, IWISA 2009, p. 297.

Rotor winding monitoring on June 18th 2013 from power plant start time to normal operation one:

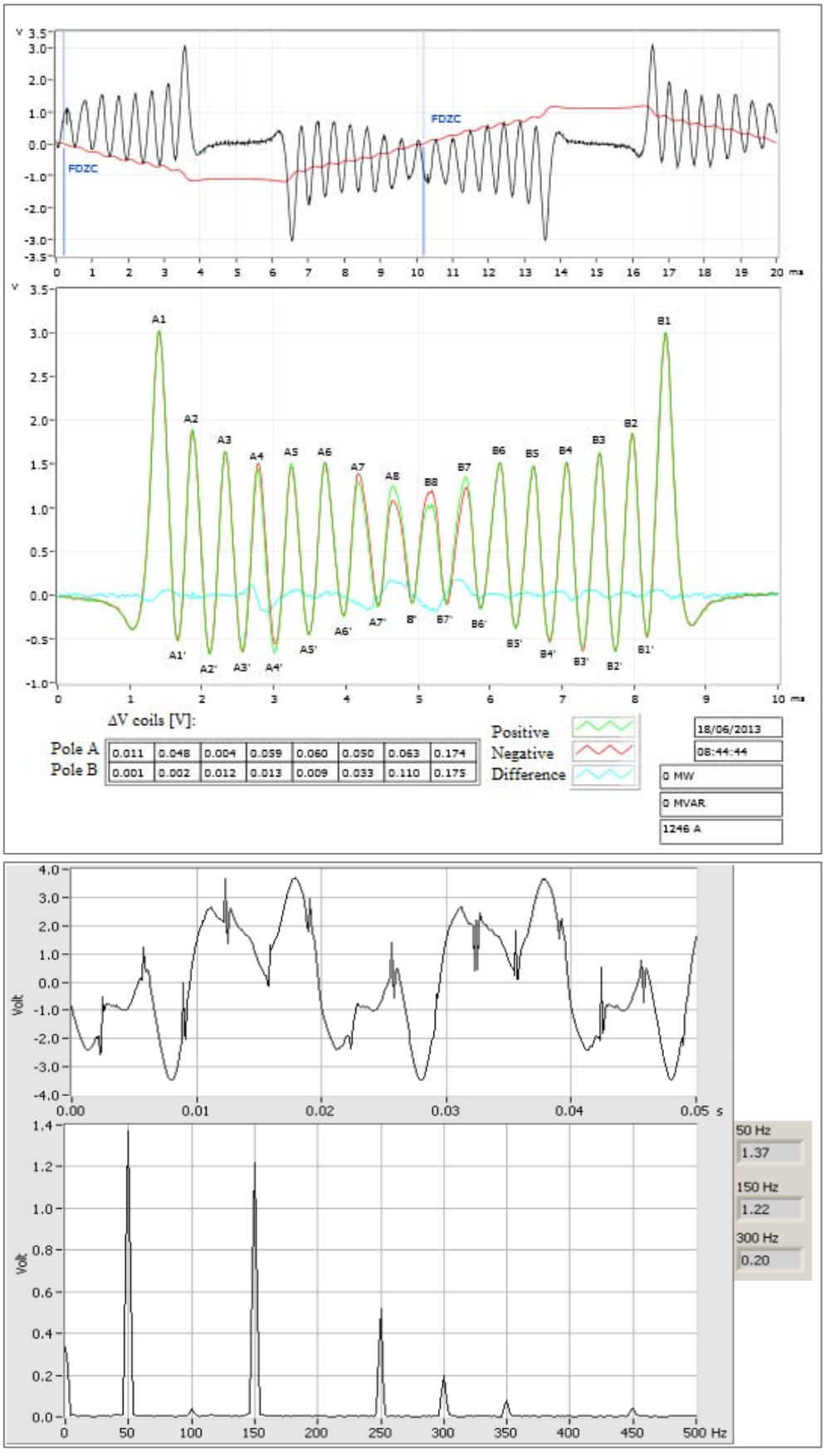

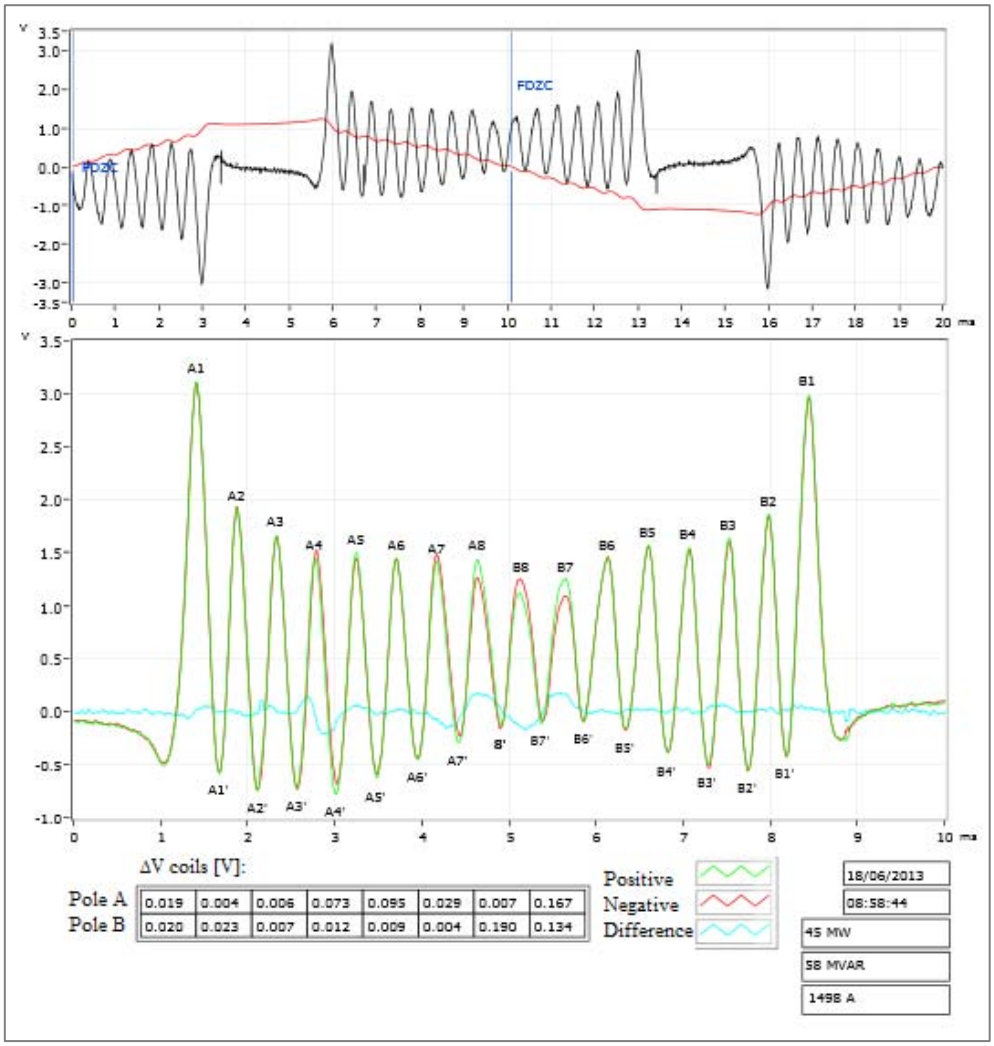
FDZC
FDZC
A1
A2
A3
A4
A5
A6
A7
A8
B8
B7
B6
B5
B4
B3
B2
B1
A1'
A2'
A3'
A4'
A5'
A6'
A7'
8'
B7'
B6'
B5'
B4'
B3'
B2'
B1'
ΔV coils [V]:
Pole A
Pole B
0.019 0.004 0.006 0.073 0.095 0.029 0.007 0.167
0.020 0.023 0.007 0.012 0.009 0.004 0.190 0.134
Positive
Negative
Difference
18/06/2013
08:58:44
45 MW
58 MVAR
1498 A

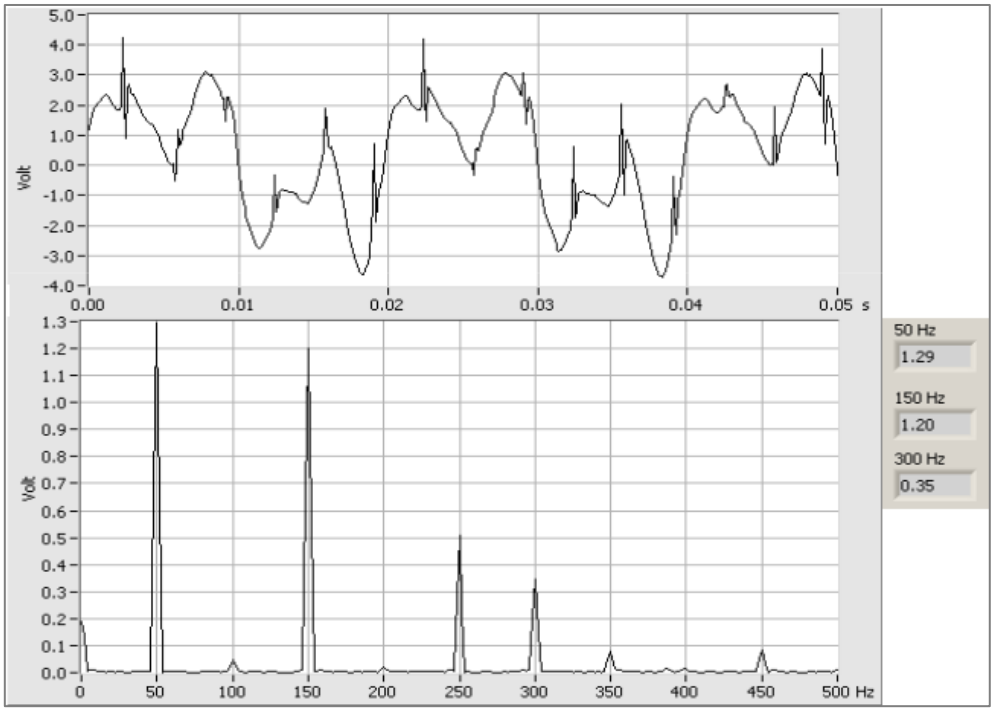
Volt
s
Volt
Hz
50 Hz
1.29
150 Hz
1.20
300 Hz
0.35

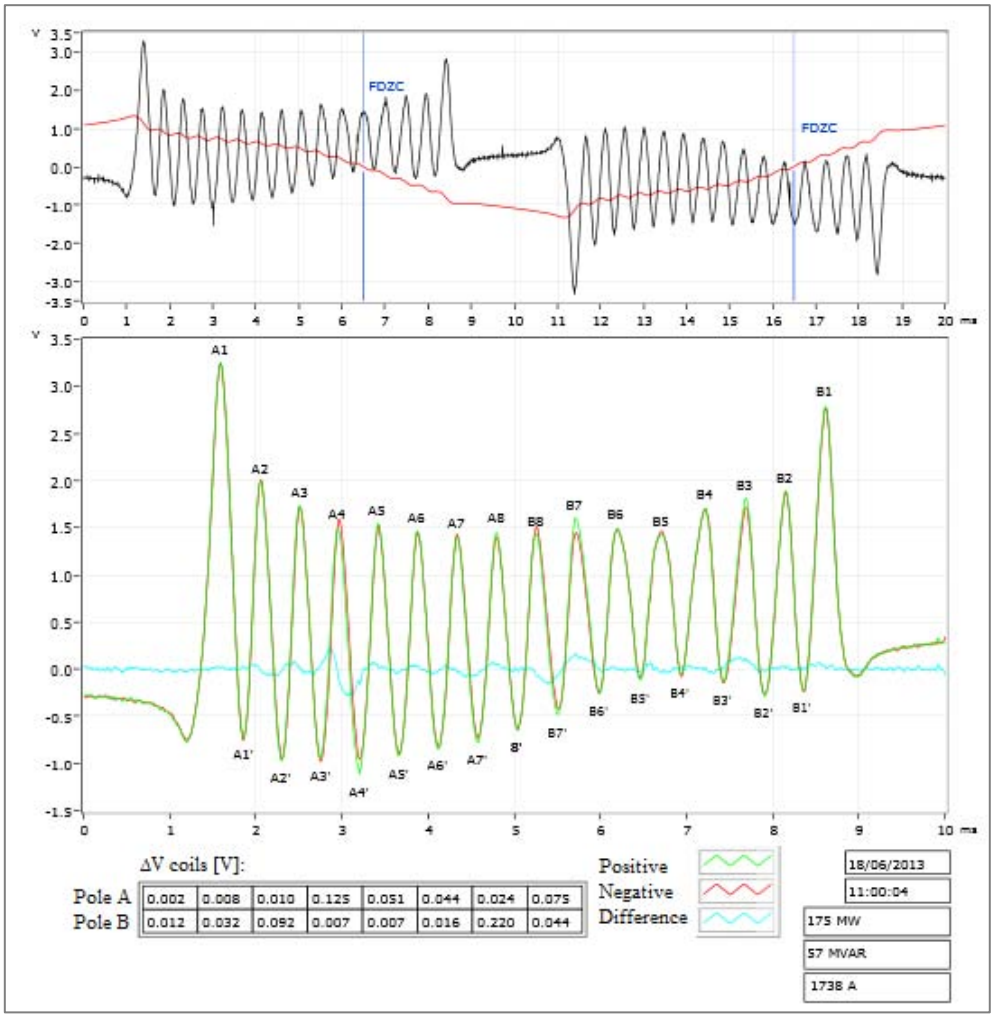
FDZC
FDZC
A1
A2
A3
A4
A5
A6
A7
A8
B8
B7
B6
B5
B4
B3
B2
B1
A1'
A2'
A3'
A4'
A5'
A6'
A7'
8'
B7'
B6'
B5'
B4'
B3'
B2'
B1'
ΔV coils [V]:
Pole A 0.002 0.008 0.010 0.125 0.051 0.044 0.024 0.075
Pole B 0.012 0.032 0.092 0.007 0.007 0.016 0.220 0.044
Positive
Negative
Difference
18/06/2013
11:00:04
175 MW
57 MVAR
1738 A

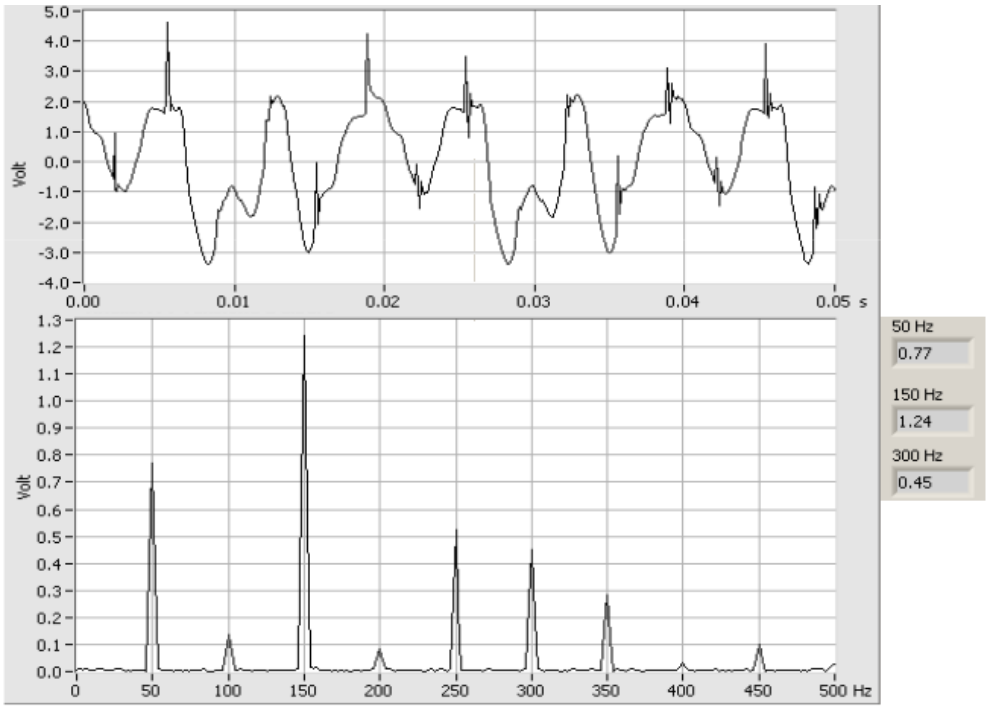
Volt
s
Volt
Hz
50 Hz
0.77
150 Hz
1.24
300 Hz
0.45

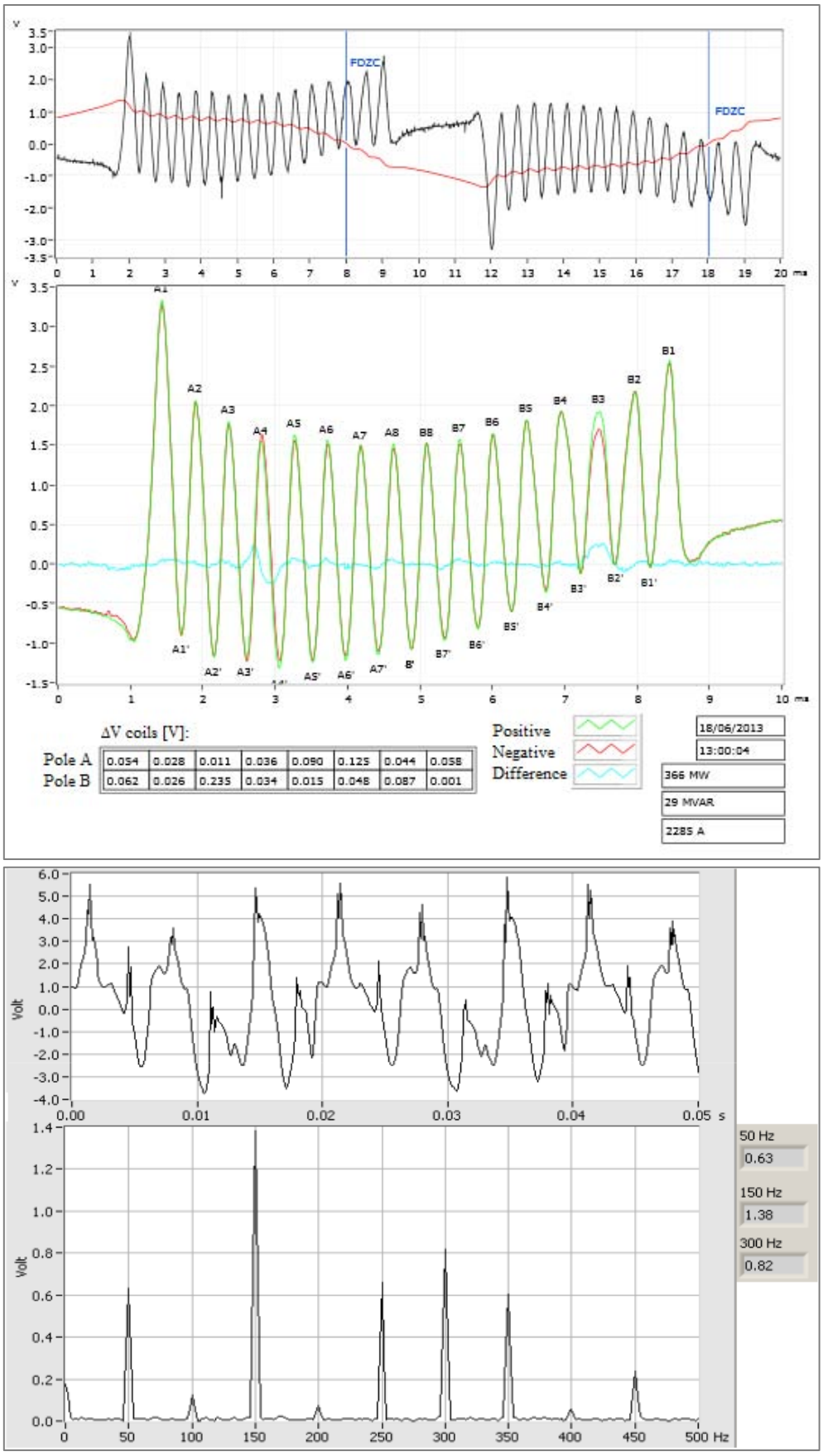

Figure.4.21: Rotor slots flux and shaft voltage monitoring of 18/06/2013.[63]

[63] Data processing edited by the specialized assistance of Enel spa (Enel GEM/SAI/ASP-ELA).

With reference to the data acquired in June 2012, now at no-load and at low-load operations it is possible to display new shorted turns, particularly on 7th and 8th coils. At no-load operation the F.D.Z.C. point is near the quadrature axis. In July 3rd 2013, a new start trend was acquired; the task of this reading is the detection of the 300 Hz harmonic component of shaft voltage and of the flux asymmetry.

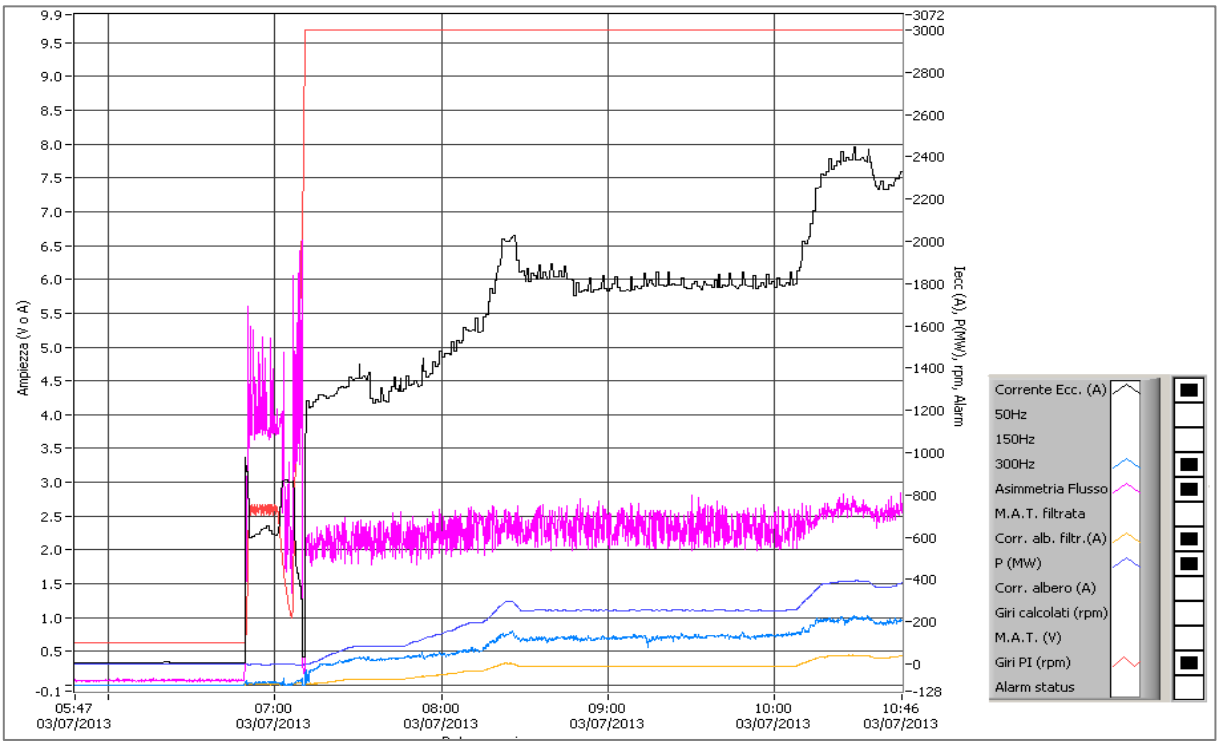

Figure.4.22: Start trend of the *Marcinelle* power plant, 03/07/2013.

From the chart in figure 4.22 it is clear the strong connection between the power output (dark blue line), or better the excitation current (black line), and the 300 Hz harmonic component of the shaft voltage (blue line). Moreover after the first phase of the start also the asymmetry flux follows the power output because of the constant value of the speed (red line).

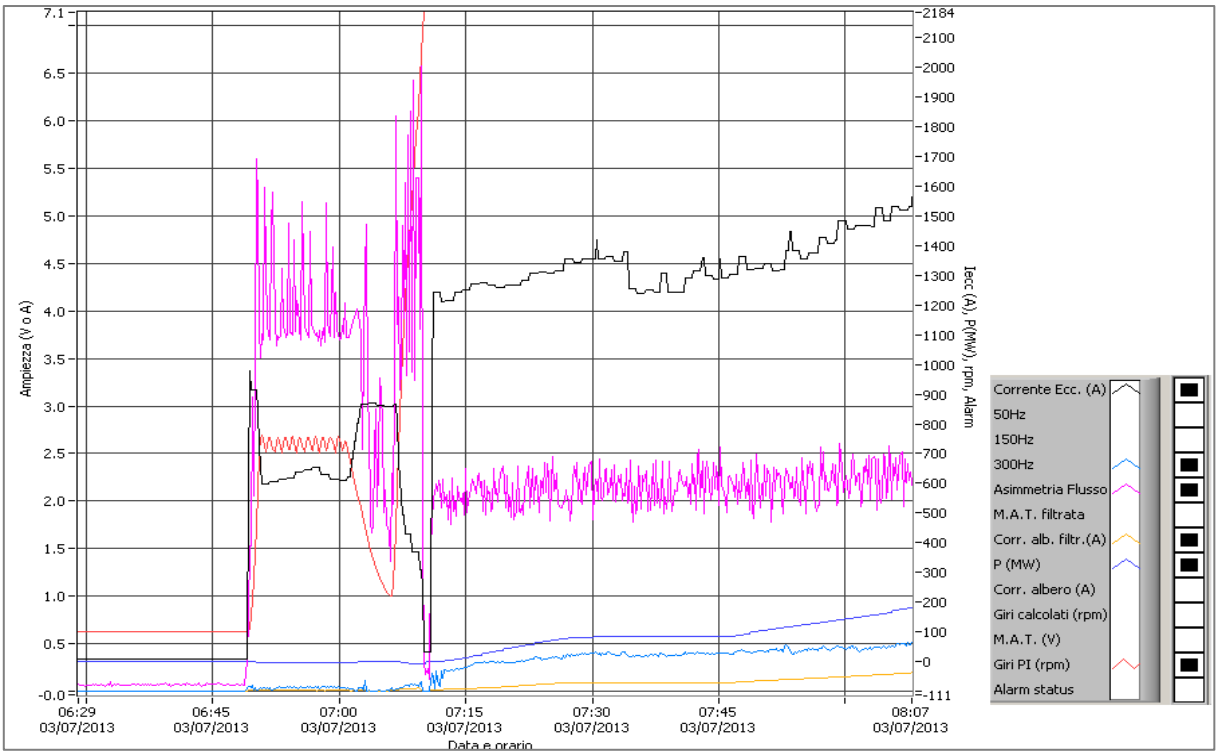

Figure.4.23: Focus of figure 4.22.

It is possible to note a wide fluctuation of the asymmetry rotor flux value in the first instants of the machine start, due to the high value of the speed gradient. This is clear in figure 4.24.

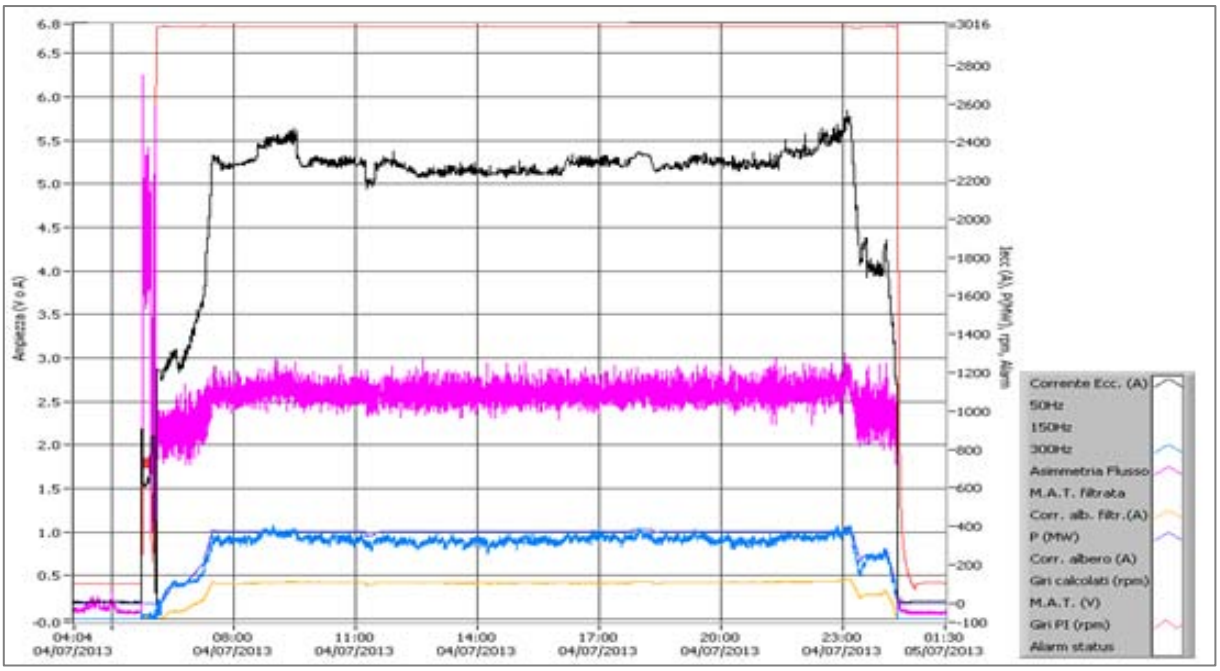

Figure.4.24: Trend of 04/07/2013.

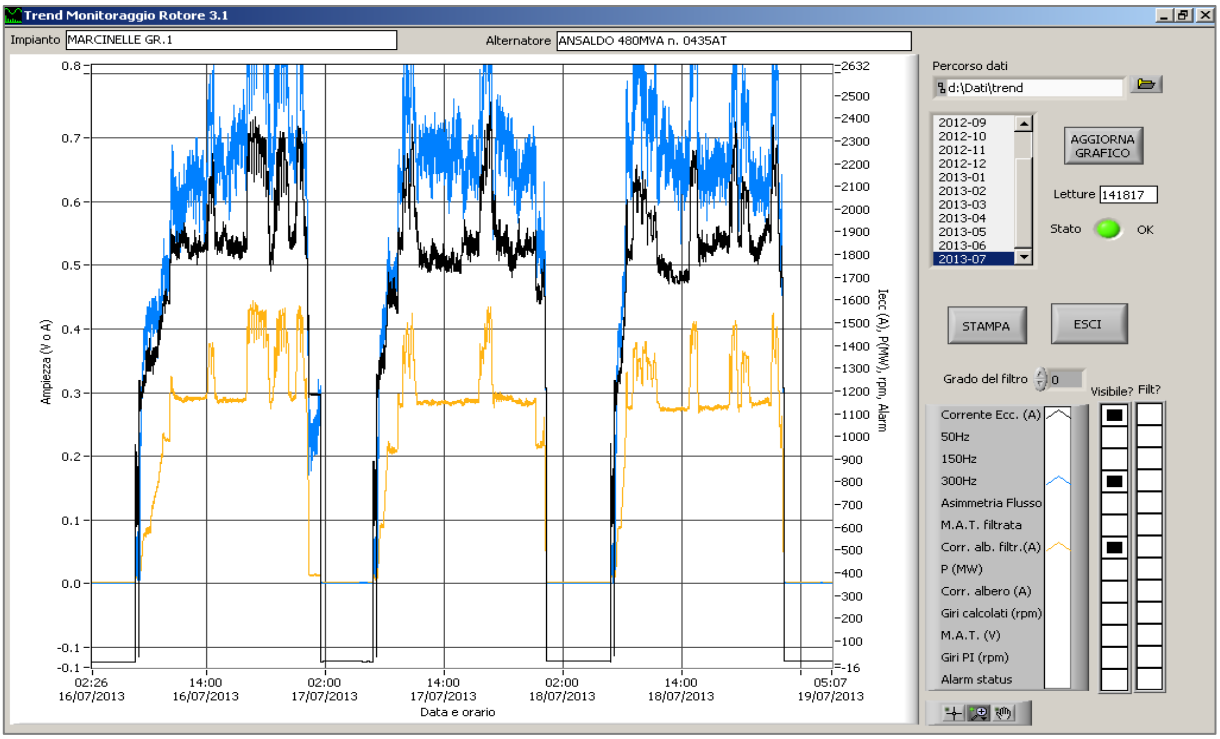

Figure.4.25: Trend of 07/2013.

Figure 4.25 shows the July 2013 trend of the *Marcinelle* power plant. It is very interesting to note that there is a strong connection between 300 Hz harmonic component of shaft voltage (blue line) and shaft current (yellow line) with reference to the excitation current (black line).

4.8 Conclusions

This project has deployed several methods to detect possible shorted turns on the rotor winding. The flux probe represents a very accurate method to detect the exact location of a possible shorted turn with reference to the amplitude difference of the flux between the two poles. But a strong limitation of this method is its connection with the F.D.Z.C. point and thus with the load; this particularity could lead to several reliabilities of the results and then it may involve erroneous conclusions about the entity of the defect. Because of this uncertainty, the monitoring system uses another method too: the shaft voltage F.F.T. analysis. The last method may help understand the real nature of a short circuit on the rotor winding, with reference to the entity of shaft current and possible even harmonics in the frequency spectrum of the shaft voltage. Unfortunately, the distribution of the voltage harmonics inside the spectrum may change with reference to the construction specifications of the generator. But there are few particularities in common to all of turbo-generators, even harmonics are always present if there are shorted turns (the 300 Hz is the greatest); its magnitude constitutes an indicator of the gravity of a fault, independently of the F.D.Z.C. point.

CHAPTER 5

Results

In the previous chapter a method to analyze and detect possible inter-turn short circuits on the rotor was developed, employing a magnetic flux probe and a shaft voltage frequency analysis. Now the results will be introduced and discussed.

5.1 Shaft configuration

Beginning from the data acquired in this project, it has been possible understand how to detect shorted turns on the rotor winding. Figure 5.1 shows a simple outline of the power plant shaft. The shaft has been equipped with a RC filter and a grounding brush.

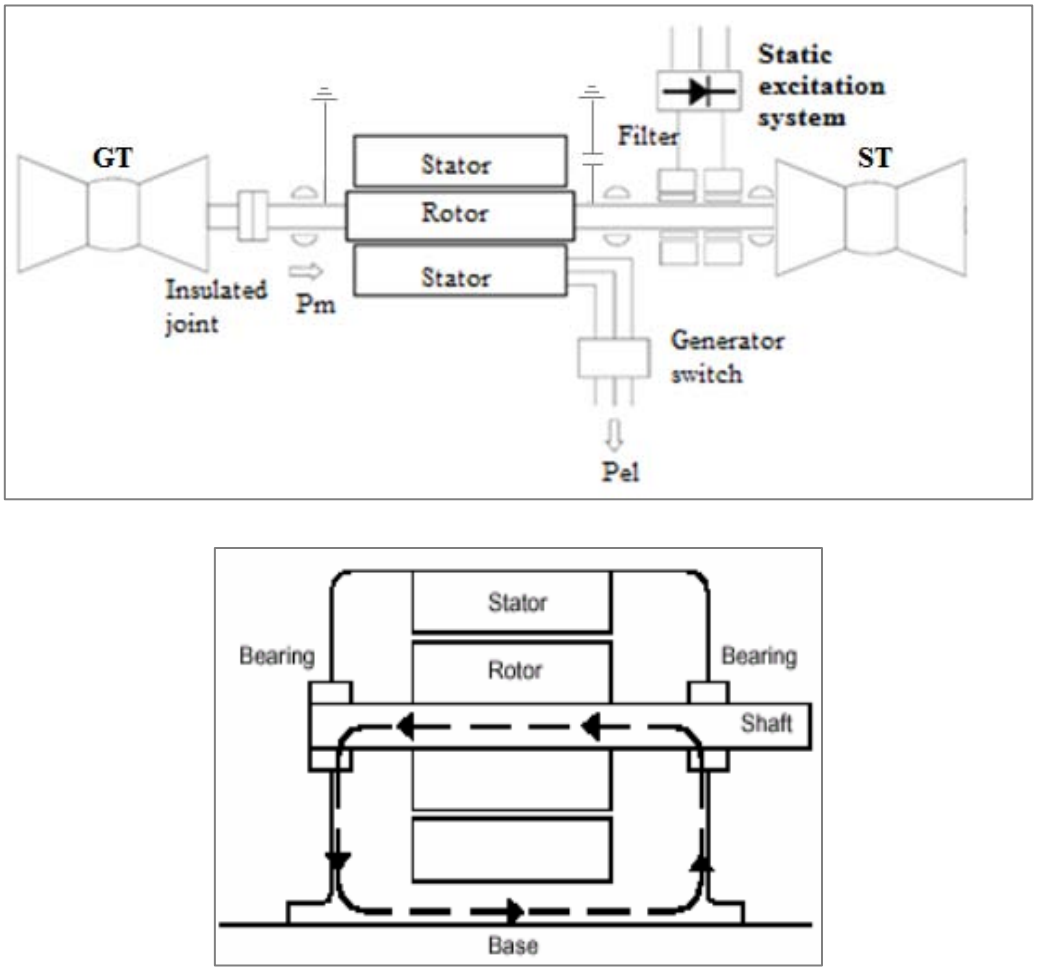

Figure.5.1: Coupling turbines and generator, grounding brush and capacitive filter. Shaft current on bearings.[64]

[64] To compare http://www.tundrasolutions.ca/files/Applying%20SCIM%20on%20LVASDs%20Rev1.pdf

5.2 Analysis

Beginning from 2012 - 2013 data store, it has been possible to locate new short circuits on the rotor winding. By means of the flux probe difference signal trend between the two poles, several anomalous situations have been detected; but another method was utilized, the F.F.T. analysis of the shaft voltage. Now an analysis of data gathered will be proposed.

It is clear that a low load (the first charts in figure 4.21) involves a high distortion of the slot fluxes, but the F.D.Z.C. point is near the quadrature axis (maximum sensitivity on the near coils) [28]. Thus, from the first charts in figure 4.21, two new short circuits on the 7th and the 8th coils may be seen.
From the analysis of the charts in figure 4.21, it is possible to evaluate the strong connection between the excitation current and the rotor slot fluxes; the green and pink lines are the trends of the poles flux, the red line represents the amplitude difference.
The frequency spectrum of shaft voltage has changed in time (from 2012 to 2013). In April 2012 there were even harmonics such as 100 Hz and 200 Hz, but with small amplitude. In June 2013 also a 300 Hz component has been detected; its magnitude is higher than other even harmonics. Moreover, the shaft voltage frequency spectrum provides for a 300 Hz component wider and wider according to the excitation current.

"When rotor windings inter turn short-circuit occurs, the m.m.f. includes a series of odd order harmonics, but also contains even harmonics. These harmonics produce a corresponding rotating magnetic field then it induces shaft voltage."[65] Positive sequence harmonics (fundamental, 4, 7, 10, 13, etc.) produce magnetic fields rotating in the same direction as the fundamental frequency harmonic. Negative sequence harmonics (2, 5, 8, 11, 14, etc.) develop magnetic fields that rotate in a direction opposite to the positive frequency harmonics. Zero sequence harmonics (3, 9, 15, 21, etc.) do not develop usable torque, but produce additional losses in the generator.
Consequently, if inside the frequency spectrum of the shaft voltage there are only odd harmonics, it is possible to conclude that there are not shorted turns or faults on the rotor winding because, when a shorted turn occurs, the step distribution of the rotor flux undergo a distortion and the order of harmonics changes because also even harmonics are present inside the frequency spectrum.

At full load the amplitude of the 300 Hz component is fully comparable to the 50 Hz one (fundamental). During the monitoring the range values has changed between 600 mV and 1 V. To sum up several defects were detected beginning from April 2012:

- 4^{th} coil, detected in April 2012 (full load test);
- 3^{rd} coil, detected in June 2012 (full load test);
- 7^{th} and 8^{th} coils, detected in June 2013 (open circuit and low load test).

Instead the 300 Hz harmonic component of the shaft voltage has been detected as:

- It is no present in April 2012;
- It appears in June 2012 at the same time with the 3^{rd} coil defect forming;
- Already present with the 7^{th} and 8^{th} coils defects.

[65] Look D. R. Rankin and I. Wilson, "The use of shaft voltage to detect air gap eccentricity and shorted turns in salient pole alternators", IEE Conference on Electrical Machines and Drivers, 11 – 13/09/1995, No. 412, pp. 194 - 197.

Conditions being equal (active power, excitation current, rpm, etc…) its magnitude has increased but not much with reference to June 2012 and to July 2013 in figure 5.2; this result corroborates the statement that possible shorted turns near the quadrature axis (7^{th} and 8^{th} coils) do not have wide effects towards the magnetic asymmetry of the rotor and consequently, towards the frequency spectrum of the shaft voltage, as seen in paragraph 4.1.2. Also the data acquired during the rest of 2012 lead to the same conclusion.

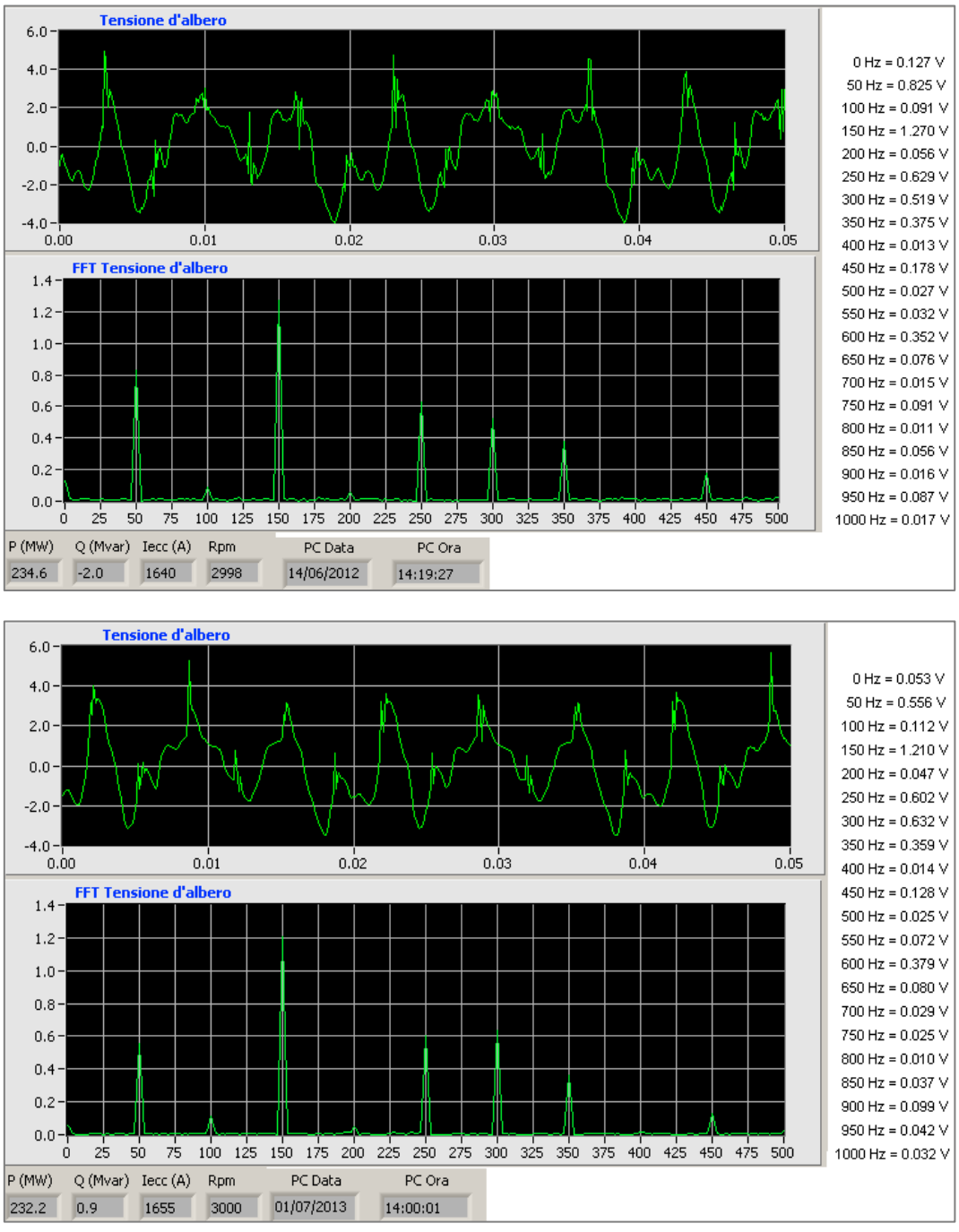

Figure.5.2: June 2012 and July 2013 shaft voltage frequency spectrum comparison (examples).

Consequently, the 300 Hz harmonic component of shaft voltage may be used as an index of possible shorted turns on the rotor winding. Several days were monitored with the generator supervision system; some trends of the main parameters measured during the monitoring have been reported below. The full data store has been reported in Appendix C.

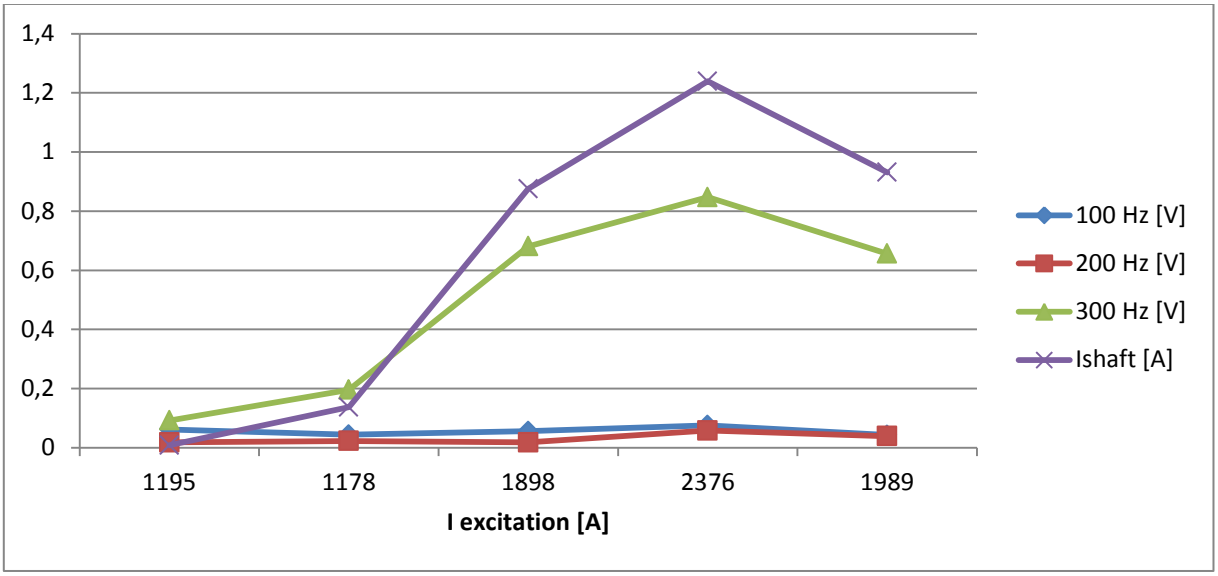

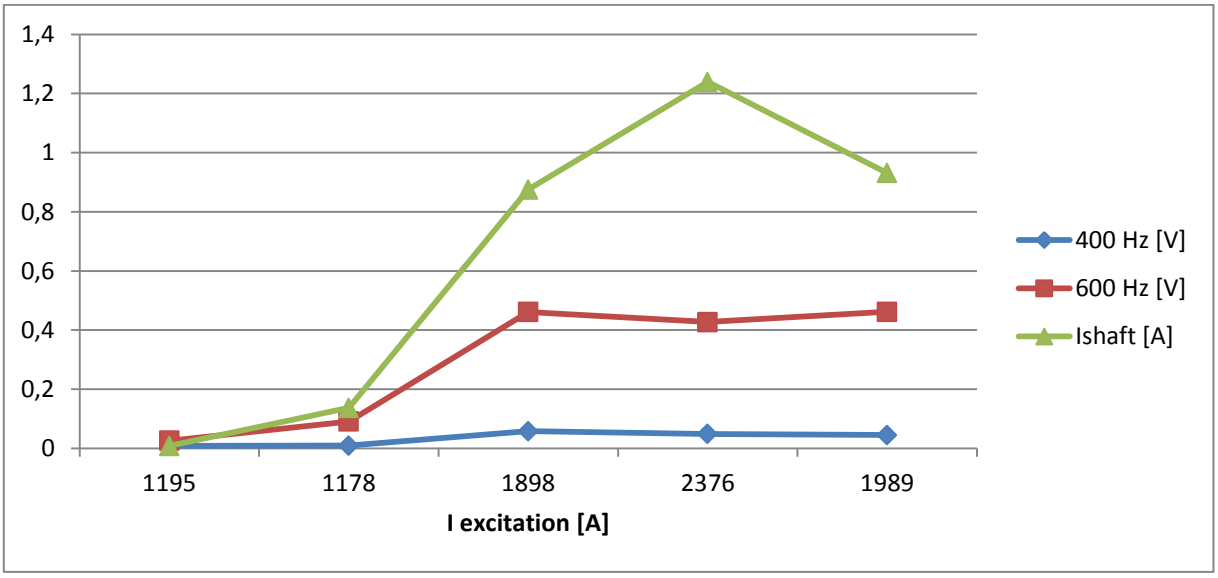

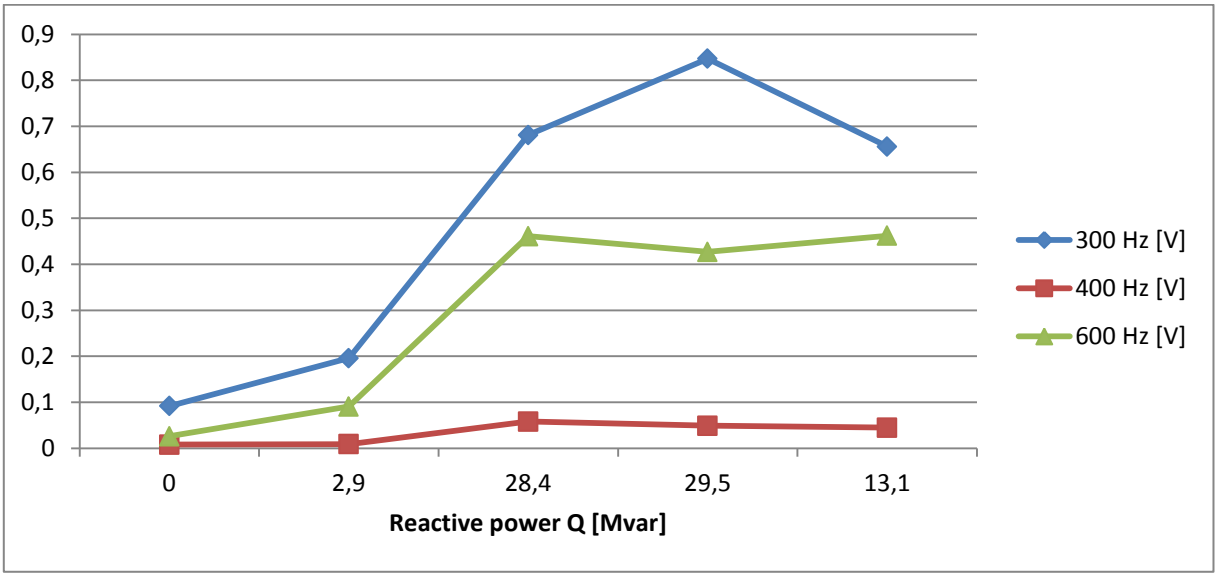

Figure.5.3: Monitoring of 16/07/2012.

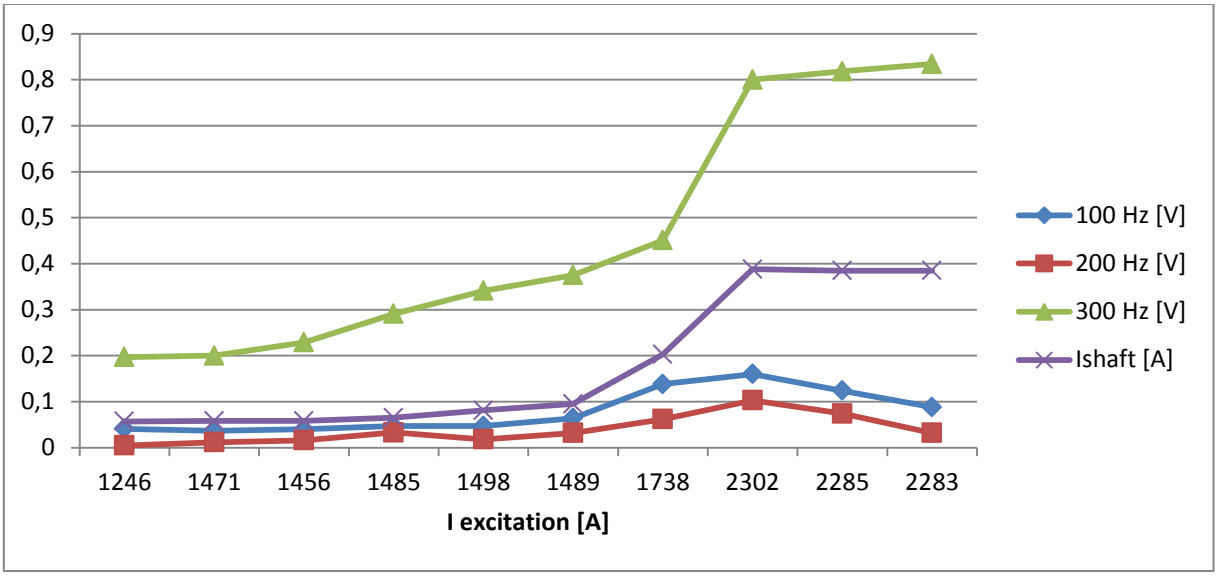

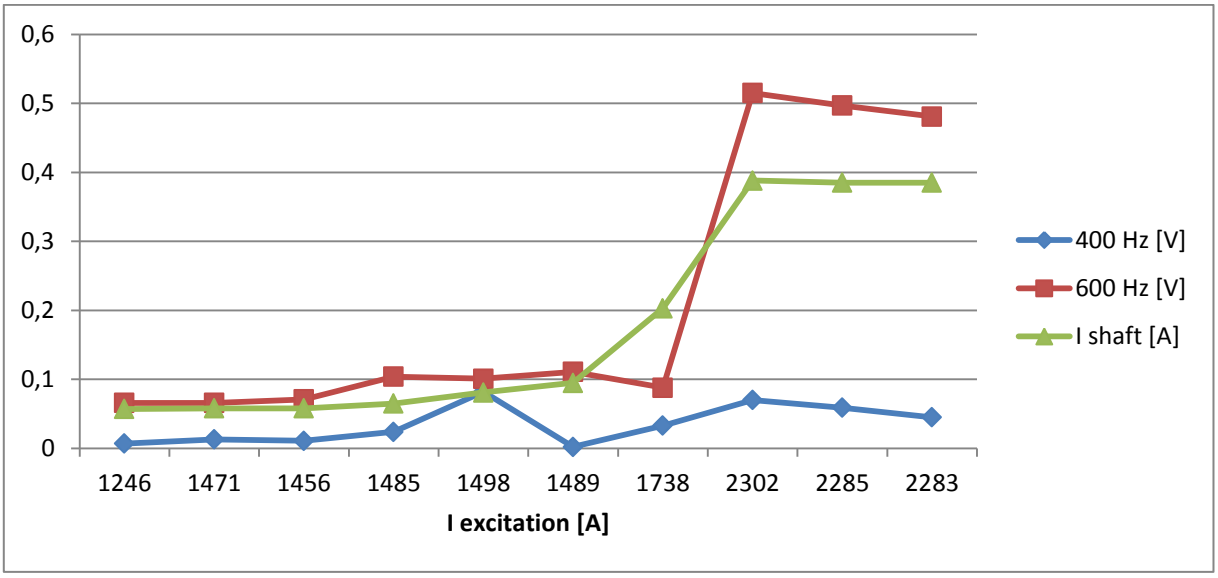

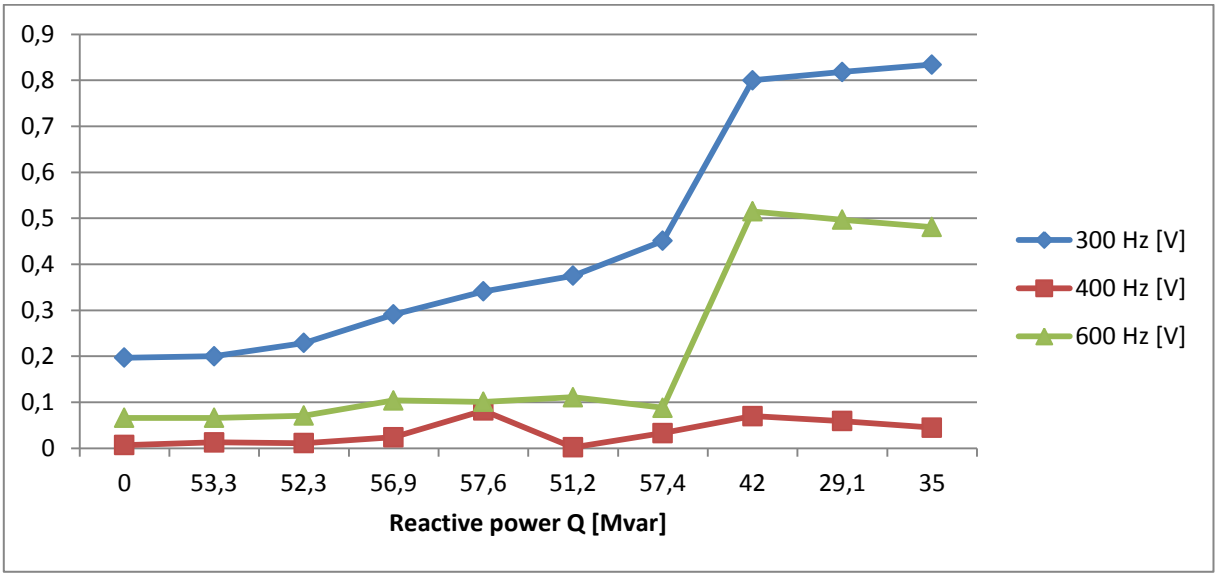

Figure.5.4: Monitoring of 18/06/2013.

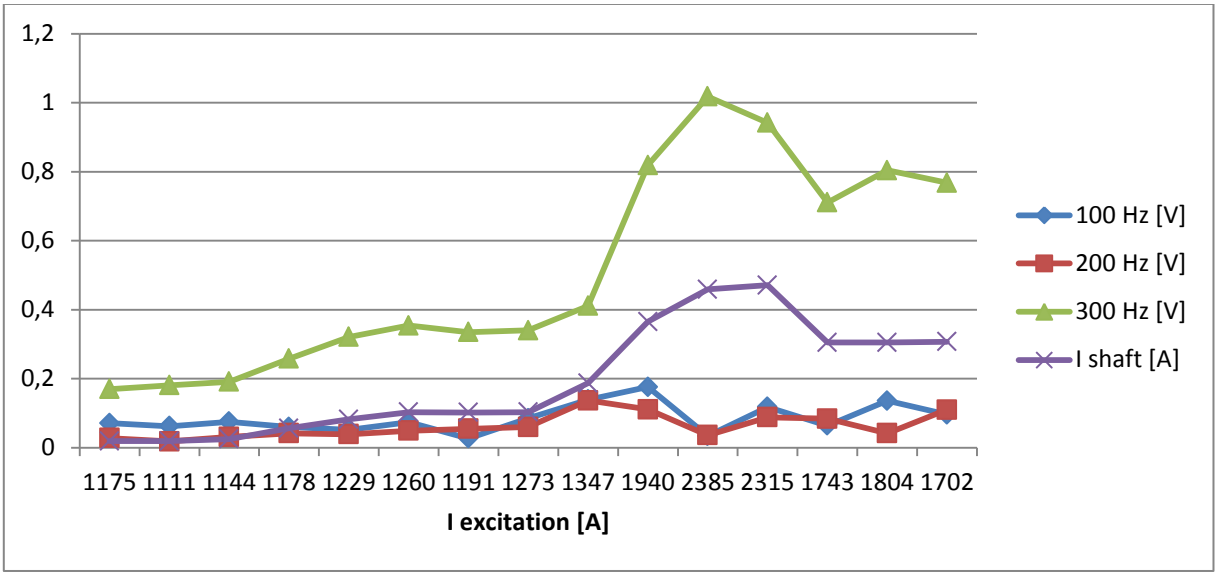

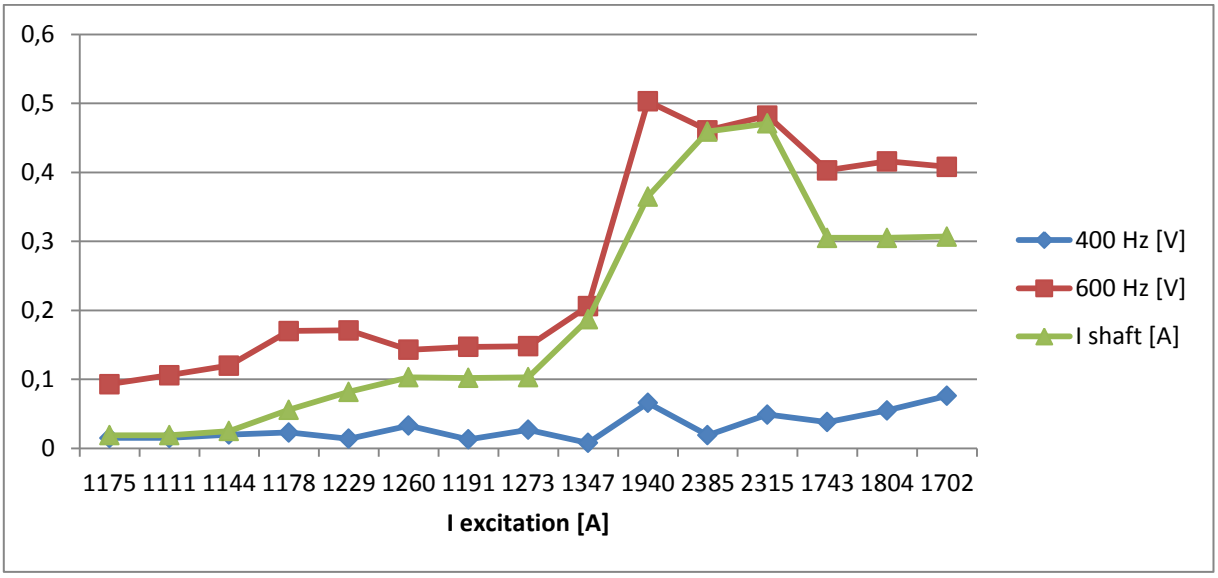

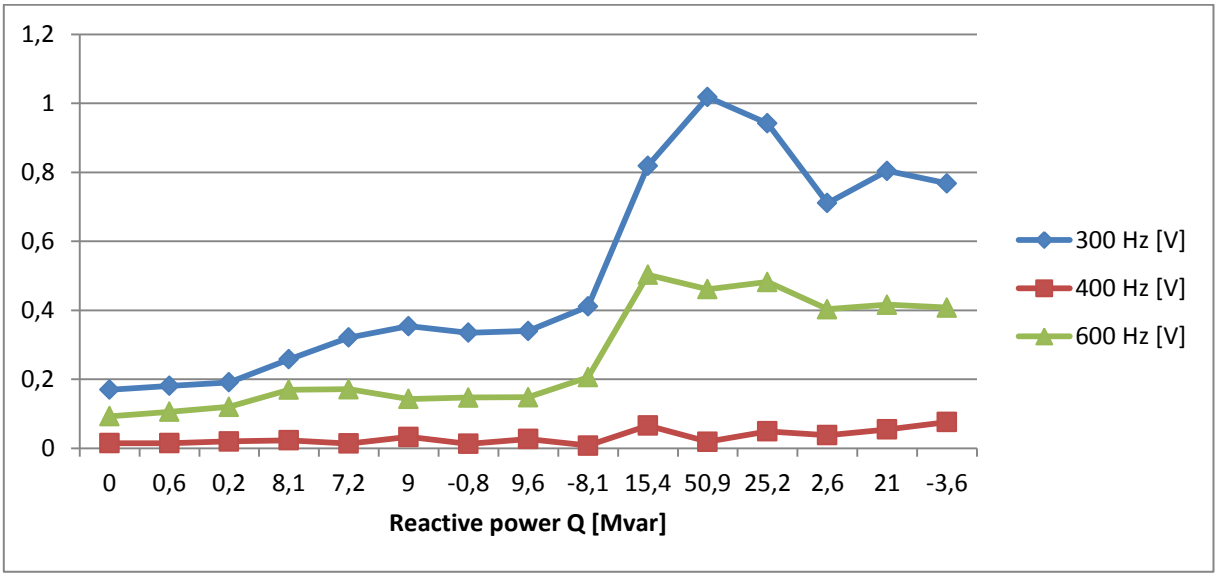

Figure.5.5: Monitoring of 21/06/2013.

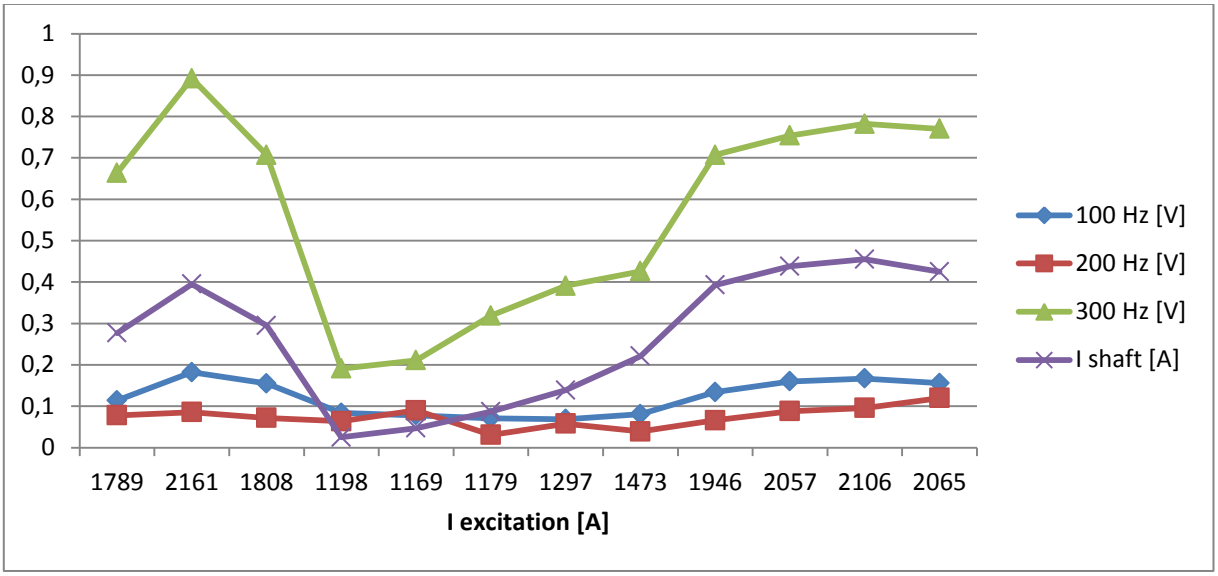

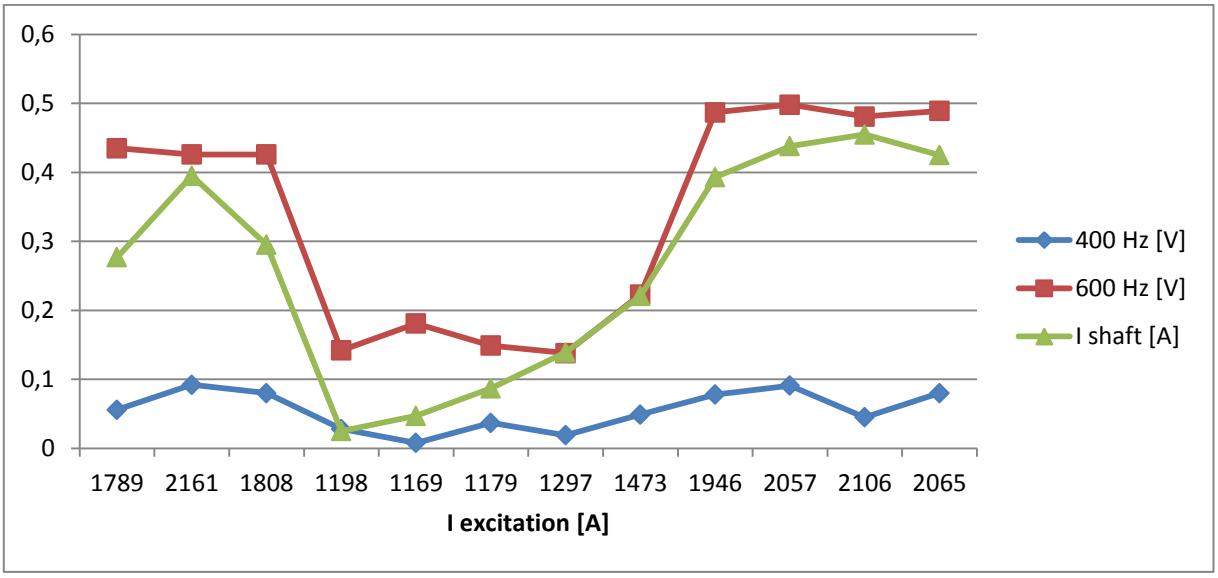

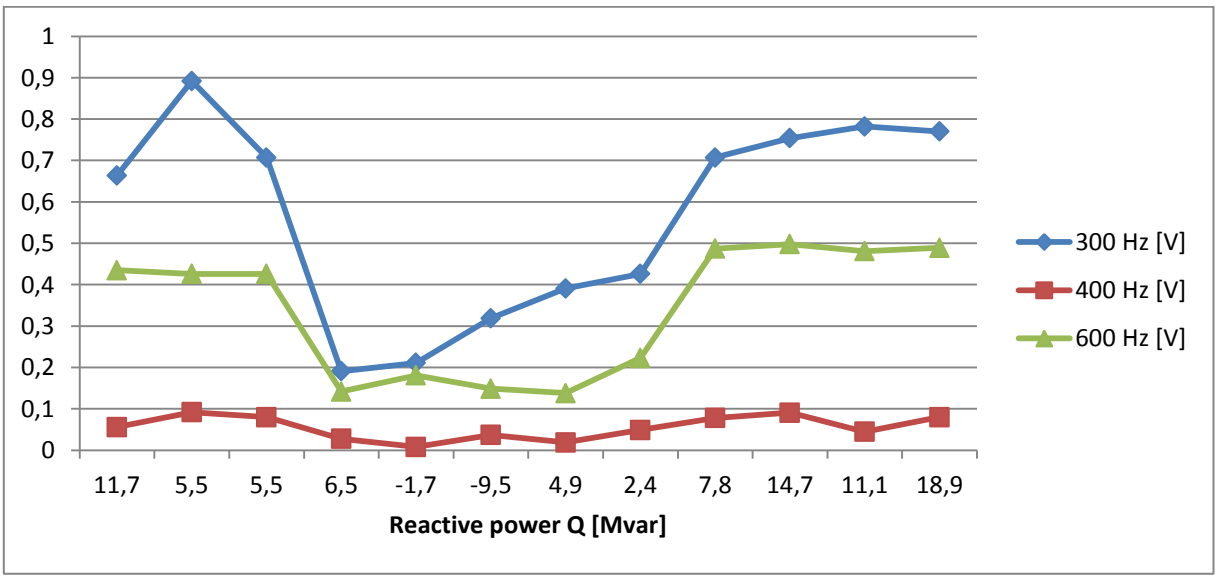

Figure.5.6: Monitoring of 23/07/2013.

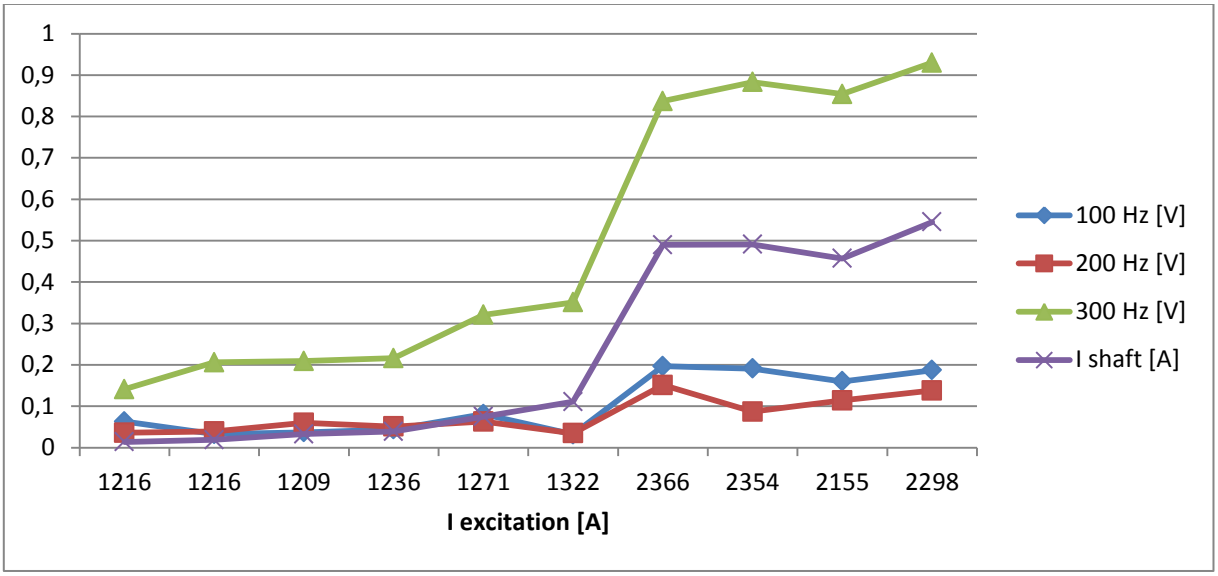

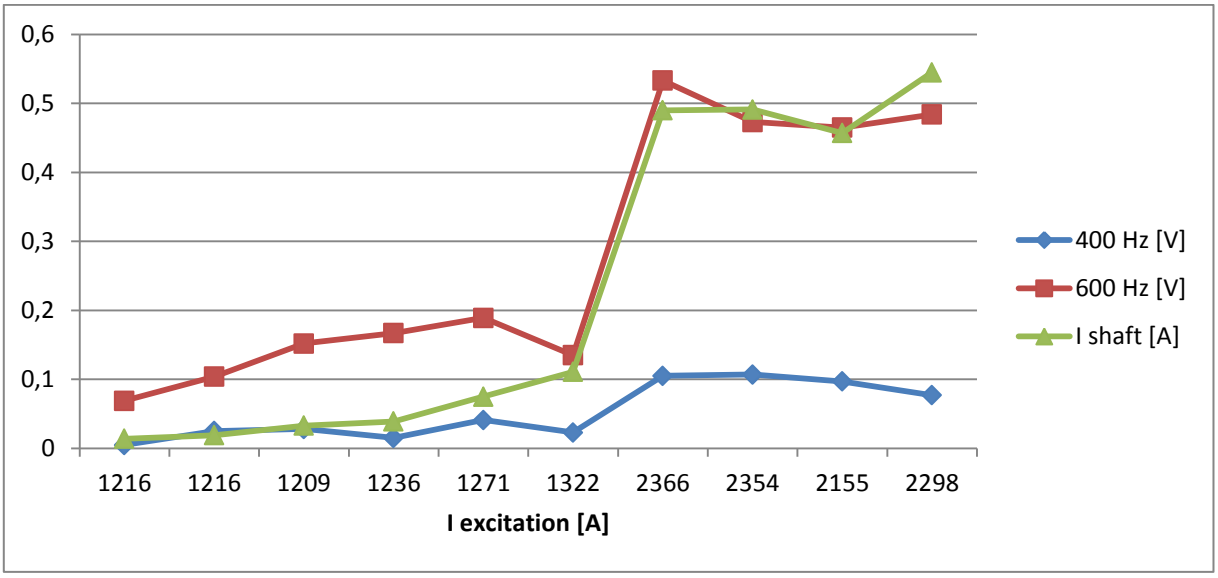

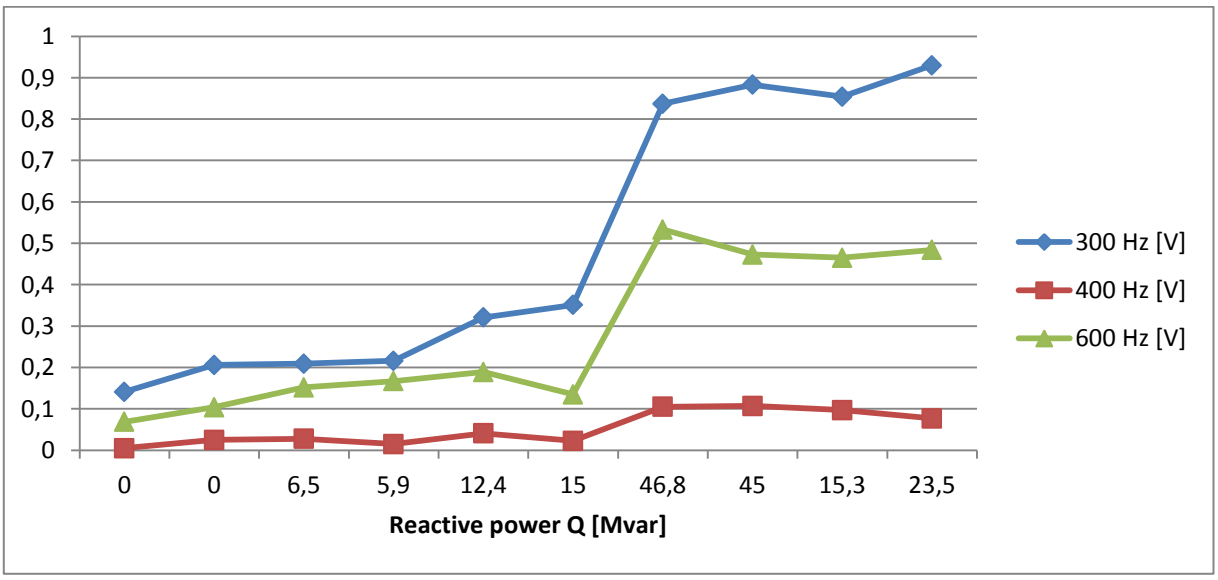

Figure.5.7: Monitoring of 25/07/2013.

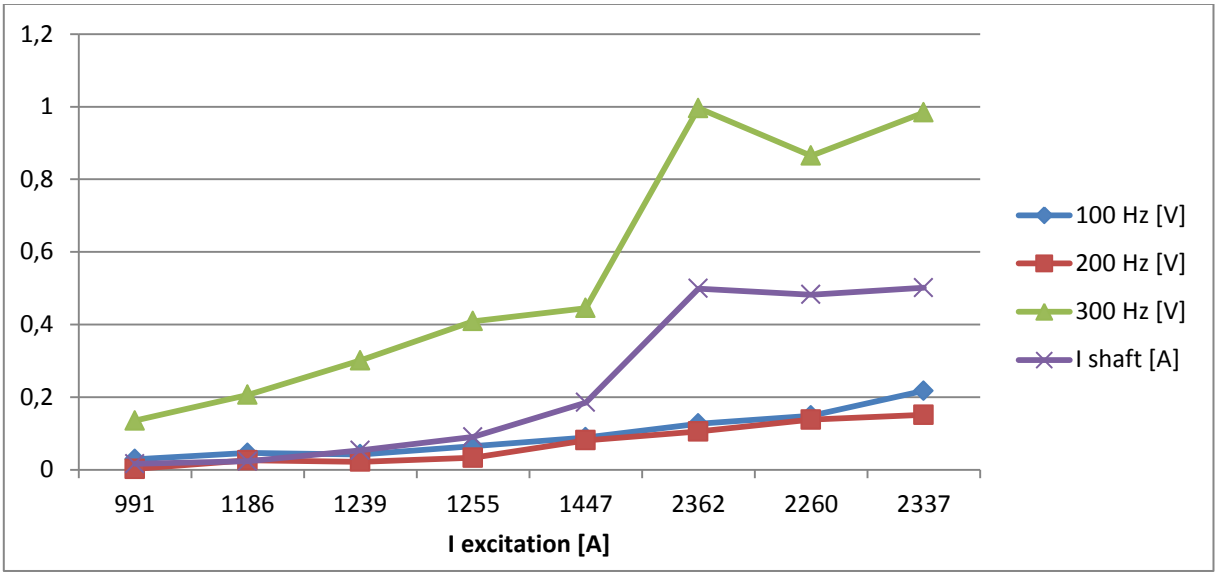

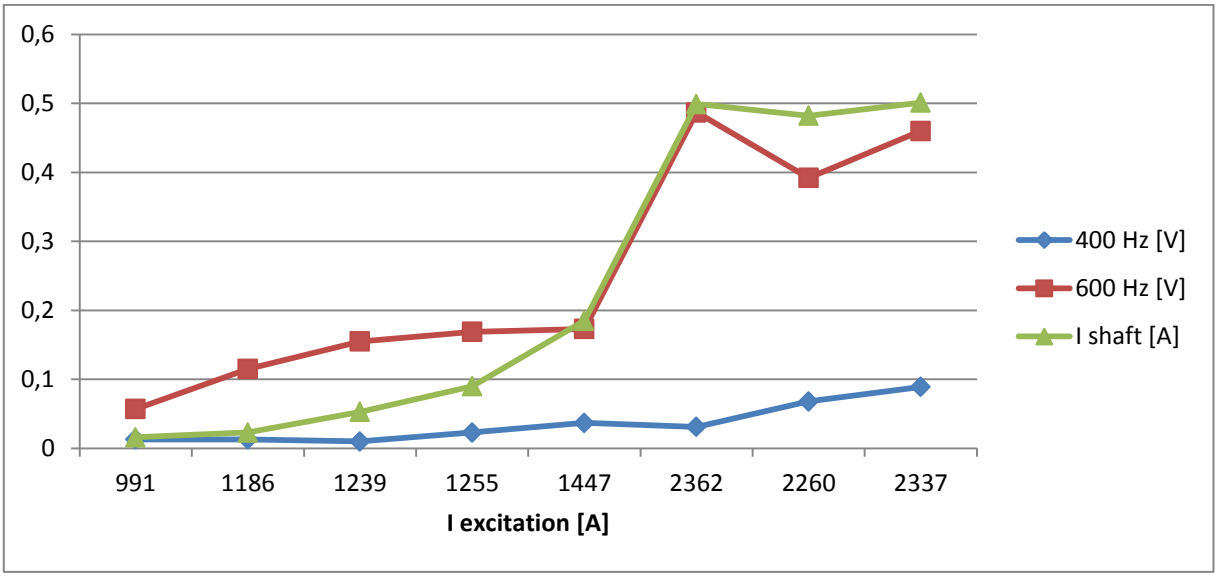

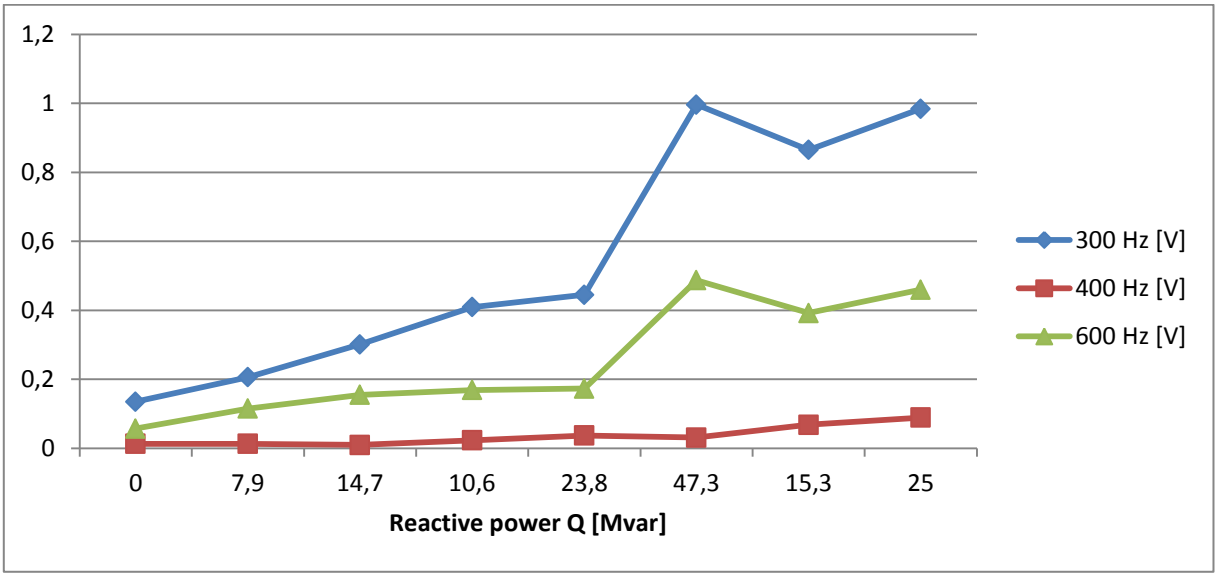

Figure.5.8: Monitoring of 29/07/2013.

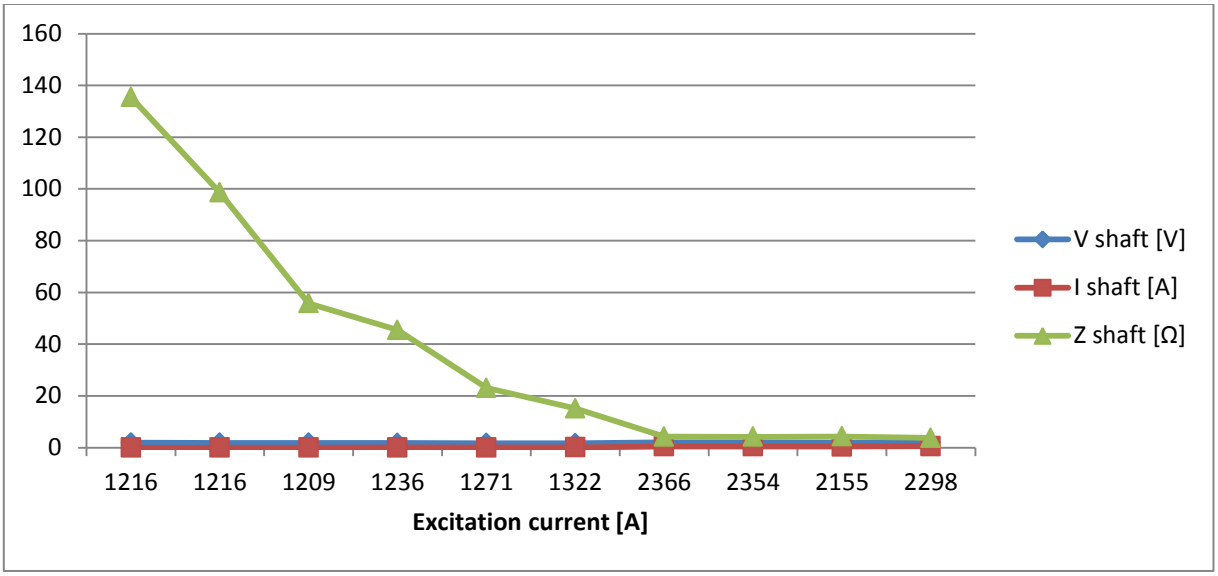

Figure.5.9: Trend of shaft impedance, 25/07/2013.

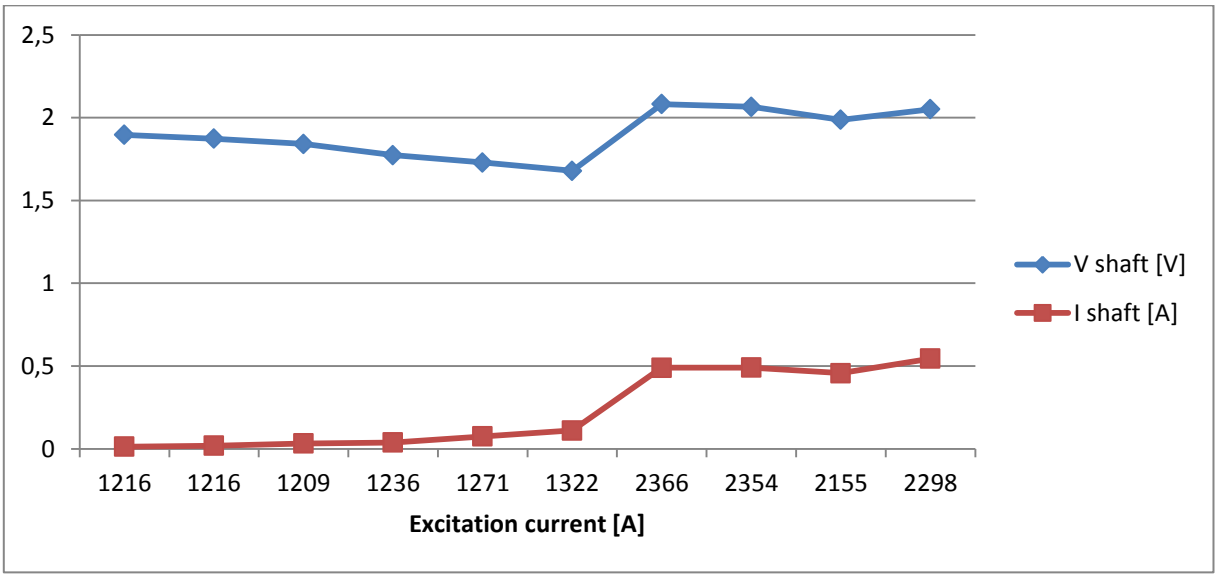

Figure.5.10: Focus of figure 5.9, shaft voltage and shaft current.

The shaft voltage has a wide frequency spectrum but the monitoring system supervises the harmonics components from 0 Hz until 1000 Hz. The trend of the R.M.S. value of shaft voltage was reported in the chart in figure 5.10. The shaft impedance during the operation becomes lower and lower because the shaft current increases its value. This is due to the behaviour of the shaft, as a Ω-L circuit.

5.3 Discussions

Several tests were carried out on the generator by the manufacturer (according to C.E.I. standards). One of these tests is the F.F.T. analysis of the stator phase voltage at no-load operation: an example was proposed in figure 5.11 with reference to a 170 MVA and 15 kV no-salient poles synchronous generator.

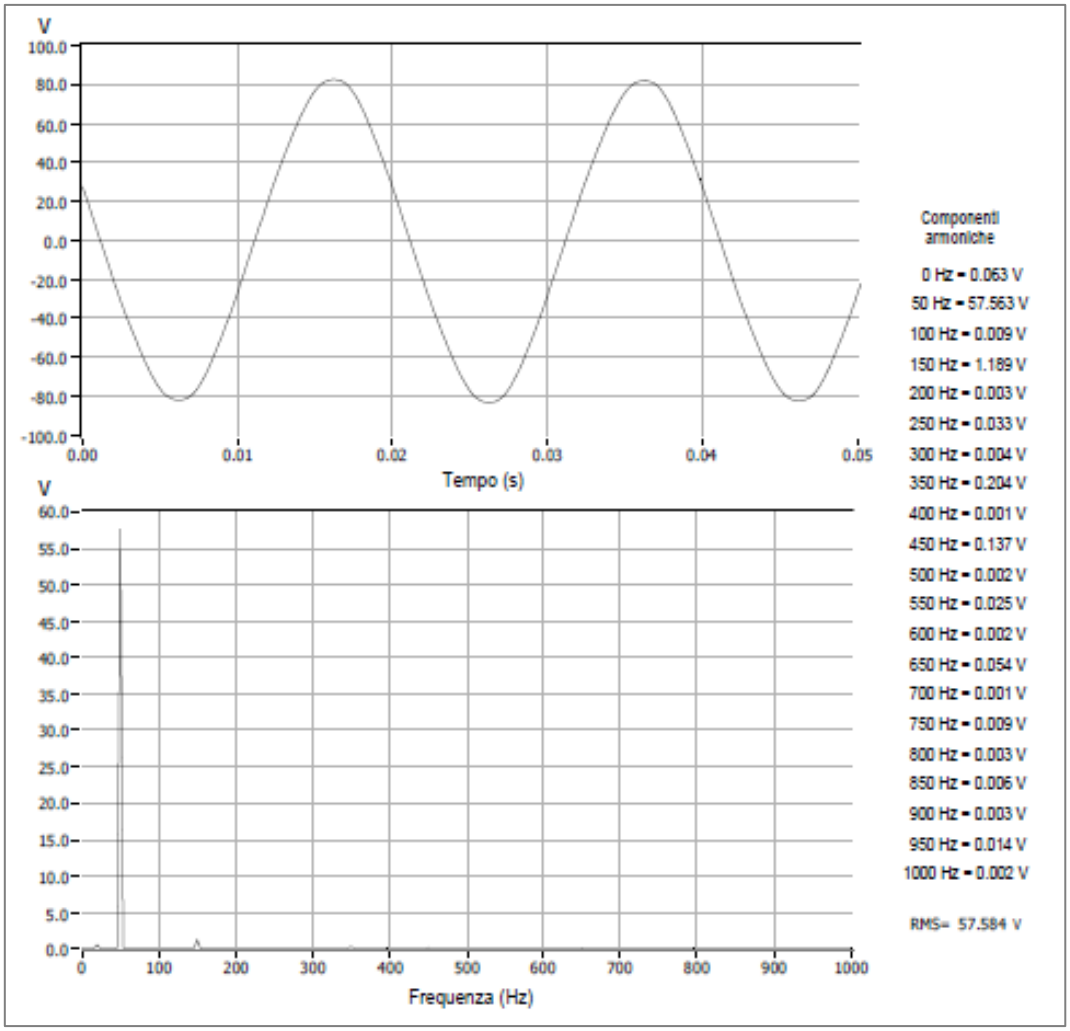

Figure.5.11: Time domain stator phase voltage and F.F.T. . [66]

It is obvious that a correct operation of the generator results from a clear F.F.T. . In it, only 50 Hz harmonic component of phase voltage should be present. Actually, there are acceptable ranges for other harmonics.

[66] Data processing edited by the specialized assistance of Enel spa (Enel GEM/SAI/ASP-ELA).

Contrary to what you could think, shorted turns do not produce an increase of the winding temperature because the Joule's losses $R*I^2$ are lower than nominal operation (without shorted turns). The excitation current, imposed by the static excitation system, crosses a coil with "fewer" turns, then the total coil resistance will be lower, if the cooling conditions are the same (no-load operation).
However, the temperature gradient due to shorted turns depends on the value of the excitation current and on the operative conditions of the generator. Nevertheless, the main effect of shorted turns is local magnetic field loss of a pole (Amp-turns).
In this analysis several short circuits were detected: some are visible at no-load or low load conditions (as on the 4th, the 7th and 8th coils), some at full load (as on the 3rd and 4th coils). This is due to the F.D.Z.C. point position with reference to the power output.
If the rotor winding state is compromised, a total re-winding of the rotor winding could be necessary, through the extraction of the shaft. As seen in the previous paragraphs, the shorted turn phenomenon is widespread but usually its magnitude is limited to a few percent units of total winding turns. On the contrary, this case represents an exception; the quick aging of the rotor winding is mainly due to many start and stop cycles to which the machine has been exposed (thermal and electric shocks).

When a shorted turn occurs, the operator may follow two ways: continue the operation of the generator (and thus of the power plant) or remove the shaft and perform a total re-winding of the rotor winding. Nevertheless, if the power plant is furnished with a real-time rotor winding supervision system, the operator may decide carefully what to do, avoiding unnecessary costs.
The shaft voltage increases with the severity of the rotor winding inter-turn short circuit fault, on-load and at no-load. "Half times harmonic appears after rotor inter-turn short circuit, which can be used as the criterion of rotor inter-turn short circuit". [33] Unfortunately, F.F.T. analysis of the shaft voltage does not allow to locate shorted turns in the rotor winding. Thus the deployment of both methods represents a smart choice.
The first charts in figures 5.3, 5.4, 5.5, 5.6, 5.7 and 5.8 show a strong connection between the shaft current (I shaft) and the 300 Hz harmonic component of shaft voltage with reference to the excitation current. The same conclusion may be obtained with reference to the 600 Hz and 900 Hz harmonics components of shaft voltage and the shaft current (second charts in figures 5.3, 5.4, 5.5, 5.6, 5.7 and 5.8), particularly when there is the transition from low to full load.
On the contrary, the 100 Hz, 200 Hz and 400 Hz components of shaft voltage are always very contained in magnitude with reference to the excitation current (and thus to the load). The increase of some harmonics components of shaft voltage leads to an increase of the R.M.S. value of shaft voltage and thus to the shaft current. The 300 Hz harmonic component of shaft voltage increases with severity of faults on the rotor winding (the same for 600 Hz and 900 Hz).
Nevertheless, the 300 Hz harmonic component of shaft voltage did not appear in April 2012 when a defect of the 4th coil has been detected, but it appeared in June 2012 with the defect on the 3rd coil. This could be due to a small entity of the fault.
The F.F.T. analysis of the shaft voltage could represent a more reliable method than the rotor slots flux leakage, because with the last method the sensitivity depends on the percentage of shorted turns and on the position of the F.D.Z.C. point; if shorted turns exceed 15% of the total turns, the reliability of the method is acceptable. [34]
To sum up:

- 100 Hz (2nd) and 200 Hz (4th) harmonics components of shaft voltage are mainly due to mechanical shaft vibrations (air gap variation) but their amplitude is always very contained;

- 250 Hz (5^{th}) harmonic component increases with rotor static eccentricity and its relative orientation.[67] Its amplitude has increased in time because of shaft bending due to a thermal difference between two poles (effect of shorted turns);[68]

- 300 Hz (6^{th}) harmonic component has an anomalous behaviour during an inter-turn short circuit in the rotor winding. If a shorted turn or more occurs, its amplitude increases noticeably in a different way from all others even harmonics. This phenomenon could be due to a mechanical resonance in the shaft between shaft vibrations (due to thermal effects of shorted turns such as shaft bending) and the excitation system that supplies the rotor winding through a six-pulse rectifier bridge. In this case the harmonic order of the currents on the three-phase A.C. side is h = 6n±1 (n = 1, 2 …) and the voltage ripple on the D.C. side is six times that one of the line frequency (h = 6*50 Hz).
  Some harmonics currents in the stator winding may produce magnetic fields that link together the shaft and they produce shaft currents; e.g. the 5^{th} (negative sequence) and 7^{th} (positive sequence) harmonics may combine to produce a torsional stimulus on the shaft at the 6^{th} harmonic frequency and they may induce mechanical oscillations that increase shaft vibrations. These orders of harmonics will induce harmonics currents in the rotor (6 x line frequency). This involves a mechanical resonance and thus, the 300 Hz harmonic component of shaft voltage increases its amplitude (as 600 Hz, 900 Hz, etc…). In this case the mechanical resonance frequency is close to the electrical stimulus from the static exciter and this leads to an electrical resonance at the same frequency of the shaft voltage with the shaft current, with reference to the excitation current.

- 600 Hz (12^{th}) harmonic component has the same trend of 300 Hz;[69]

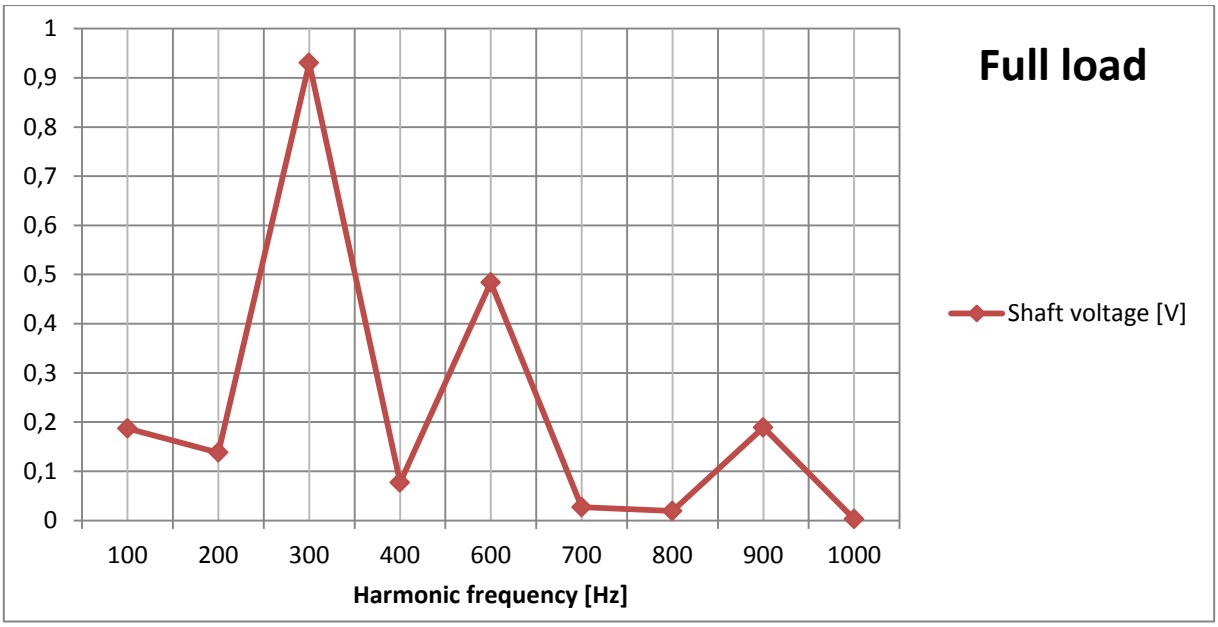

Figure.5.12: The F.F.T. spectrum of the shaft voltage, 25/07/2013 (11.00 pm).

[67] To compare Daniel de Canha, The analysis of shaft voltages in a synchronous generator with various induced faults, School of Electrical and Information Engineering, University of the Witwatersrand, Johannesburg, 2008, p. 58.
[68] Appendix D.
[69] Figures 5.3 to 5.8.

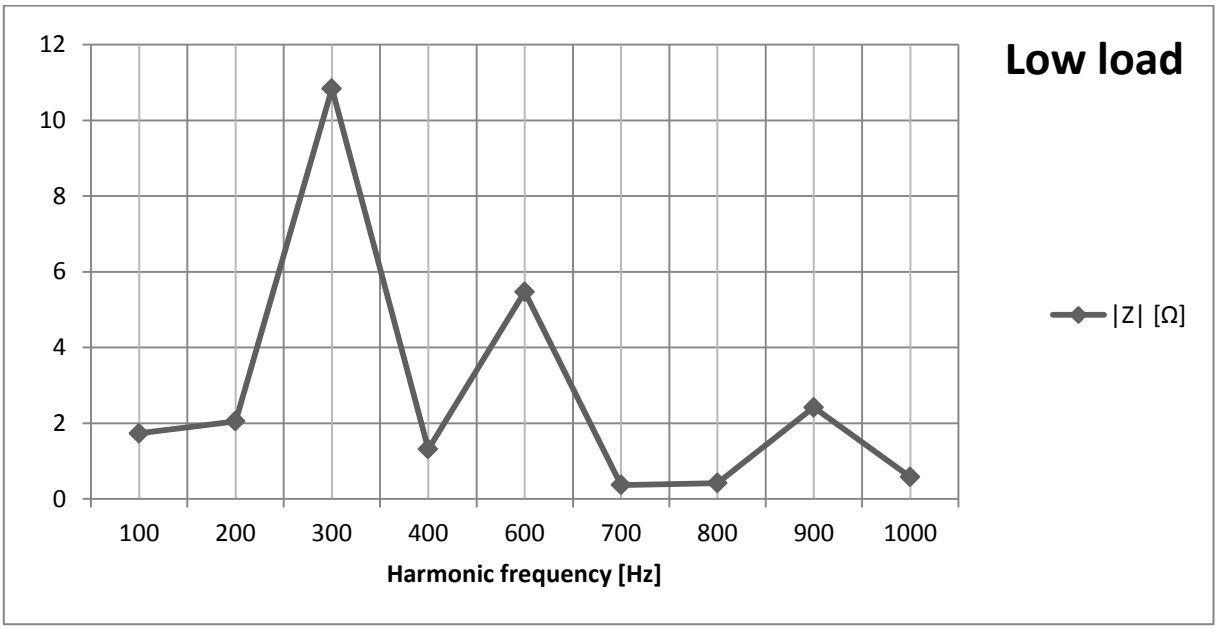

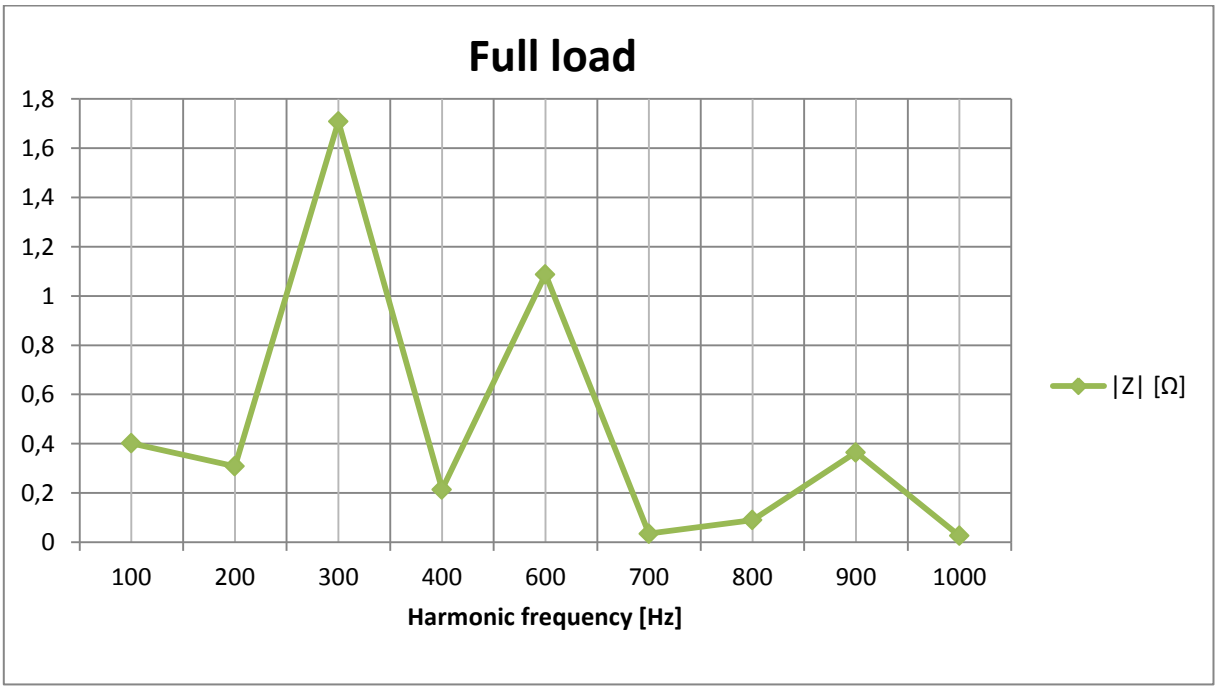

Figure.5.13: Harmonics spectrums of the shaft voltage and shaft impedance, low (7 am) and full load (9 am) (25/07/2013).[70]

In the charts in figure 5.13 are clear the resonance peaks at 300 Hz, 600 Hz, 900 Hz, etc… Shorted turns increase shaft vibrations at these frequencies, particularly for 300 Hz (6^{th}); this corroborates the statements that the main causes of shaft voltage (and its variability) are the stator configuration and stator harmonics currents.

[70] Appendix F.

5.4 Neutral grounding

Perhaps the generator is the most delicate and expensive part of a power plant, consequently, its protection from faults, anomalies and non-availability is of the utmost importance.

Figure.5.14: Neutral grounding of the synchronous generator.

Conventionally, the neutral grounding of the stator winding is connected to the ground through a high value resistance or impedance, mainly due to the need to decrease the single-phase short circuit current (phase-ground fault of a phase or a M.V. bar). The neutral grounding of the generator is provided for a stator earth fault 95% - residual overvoltage protection (64S – 95%). The stator winding instead is provided for a stator earth fault 100% protection through a low frequency current injection. In the Marcinelle power plant is provided for a neutral grounding cubicle:

Manufacturer: Alfa Standard spa;
Operating voltage: 20 kV;
Rated voltage: 24 kV
Rated insulation level: 50/125 kV.

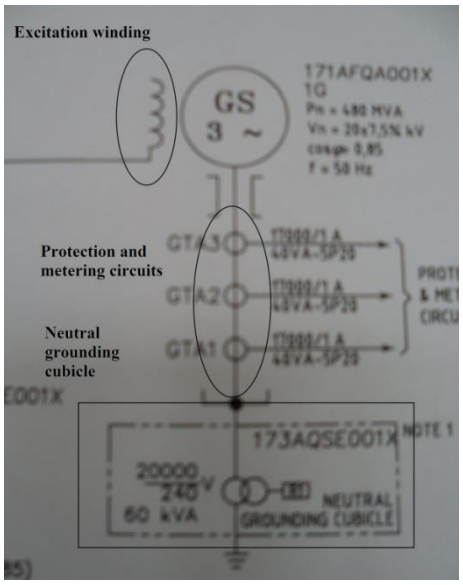

Figure.5.15: The neutral grounding cubicle.

Figure.5.16: Step-up transformer neutral grounding reactor.

As seen in figure 5.16, the neutral grounding of the power transformer has been linked to the ground through an inductive reactor.

5.5 Conclusions

The results of the rotor winding monitoring have been exposed in this chapter. This supervision system represents an efficient integration of hardware and software, because it allows comparing several signals coming from several instruments. Unfortunately, shorted turns phenomenon is frequent in power generation sector but in most cases this does not represent operational difficulties. Shorted turns detection by magnetic flux probe use provides good chances to locate shorted turns in a rotor winding, although the sensitivity of the measure changes with reference to the F.D.Z.C. point. A useful stratagem could be the contemporaneous utilization of a magnetic flux probe and a shaft voltage analysis; the combination of both methods could increase the results reliability. The knowledge of the number and location of these turns may help the operators during the operation and the maintenance. The magnetic flux probe may be also used to check turns conditions if a new rotor balance is required.

CHAPTER 6

Future developments and Conclusions

6.1 Future developments of the rotor monitoring

As already examined in this work, the rotor flux analysis (with other parameters) has allowed to detect shorted turns on the rotor winding, and to supervise this anomalous operation to avoid furthers damages. The generator is the most delicate machine of a power plant and a real-time supervision is necessary to ensure its correct operation. Future developments could be a more extensive use of sensors and detectors for all of generator parameters and a digital analysis of their signals.
It is possible to expect an improvement about the data acquisition system, software analysis and in particular an integration of the parameters as air gap flux, generator output, shaft vibrations (thermals and magnetics), etc… through only one system, the Air gap monitoring system (A.G.M.S. ®).
Another important step of overcomes would be to avoid the more expensive CO2 → H2 (and conversely) transition about the probe insertion, as it requires much time.

Remote supervision system by company operator, and data accessed via company intranet. The staff could not travel to the power station under testing (this is very important for remote hydropower plants, where there is not permanent on-site staff). Ethernet communication is possible through any number of third-party terminal servers to convert either one or more monitors to T.C.P./I.P. Ethernet. At that point, additional communications options as WiFi are possible. The data collected by the supervision system could be used to estimate the expected remaining life of the main generator components and parts. Consequently, an existing failure rates may be applied to the future. These failure rates may be estimated as:[71]

- The replacements with "in kind" parts do not justify changes in the power plant-specific failure rates. The average random failure rate of a plant component remains the same over the whole normal operating life under the same maintenance and operating conditions;

- The re-winding of a rotor winding is normally justified in order to correct identified generic design or assembly problems. The reconditioned or new components, such as a re-insulated rotor winding, are deemed to incorporate the available design improvements and technological enhancements.

- The power plant-specific future failure rate of such components would be expected to improve and perform in the range of industry average failure rate for the ones;

- A decision to re-wind or replace a rotor with a new one will depend on the assessment of the condition of the rotor forging. Low or high cycle fatigue crack

[71] Look EPRI, Life Cycle Management Planning Sourcebooks, Volume 5 Main Generator, pp. 8.1 – 8.2.

initiations in stress concentrated regions and their propagation in-service are the main risks to the integrity of the forging.

- The purchase of a new rotor instead of a rewind may also be justified in instances where the re-winding may not be completed within the planned outages, thus causing unit outage extensions and loss of production. The cost of a fully machined forging is on the order of 20% of the final rotor cost. The cost of a new rotor vs. rotor rewind can thus be justified a few days of unit production loss. The excitation system controls and voltage regulators may contain significant number of such redundant circuits. The new digital microprocessors, multiple channel redundancy, self-checking circuits, and self-diagnostic fault features provide a strong incentive for modernizing the control and protection devices. Such optimization requires detailed calculations of synchronous generator parameters.

To reduce the shaft voltage phenomenon, it is necessary to improve the bearing insulation (to decrease currents due to shaft voltage) and the grounding connection on the sides of turbines.
As already said, one of the main causes of shaft voltage are stator asymmetries. In the specific instance, a non-uniformity of the magnetic circuit of the stator may lead to shaft voltage and thus shaft currents. This may be reduced through an accurate phase displacement of the stator magnetic sheets. Another cause are the axial fluxes; these leakage fluxes come out from the rotor ends and link together the same rotor (solid iron) and not the stator winding, because the armature windings have already ended. This involves shaft voltages and currents.
The 300 Hz harmonic component of shaft voltage is the widest one in the frequency spectrum; it is mainly due to the stator effect under shorted turn phenomenon.
Another important improvement is a better design of the magnetic pack at the end of the stator to limit axial fluxes at the end of the rotor winding. This could be obtained through a gradual drift of the last sheets of the magnetic pack at the end of the stator winding.
This shrewdness increases the air gap reluctance and reduces axial fluxes and shaft voltages. A wider and wider step structure at the end of the stator magnetic core may lead to few volts of shaft voltages; conversely, a short step structure of these sheets leads to high shaft voltages due to axial fluxes (some dozen of volts) and thus shaft currents near few hundred Amperes. Consequently, with this shrewdness it is possible to reduce the shaft voltage from 7 – 12 V to 0.5 V (average values).

Figure.6.1: Step-frame of the stator core at the end of the stator winding (first 750 MVA, second 370 MVA, 2 poles generators)[72].

[72] Courtesy of Enel spa (ASP_GEM).

A decrease of the shaft voltage R.M.S. value leads to a decrease of all harmonics in its spectrum. Also the damper winding may be insulated more and more to avoid eddy currents due to leakage fluxes. Besides a better design of the RC filter and of the grounding brush may reduce the amplitude of 300 Hz component because this one could be drained to the ground without dangerous effects.

6.2 Conclusions

The monitoring system utilized in this project may help to understand and to avoid anomalous conditions for the synchronous generator. The power generation sector is always changing and, to offer a good power quality to the costumers, it is necessary to ensure a correct operation of power plants wherever they may be. A real-time supervision of the generator parameters may prevent dangerous unavailability of a power plant and it may lead to a strong connection among many plants avoiding blackout and a grid collapse. The main effects of shorted turns lead to shaft vibrations (thermal effect); they are due to some harmonics in stator currents, in turn due to a distortion of the main rotor flux. Shaft voltage is always present in the driving shaft, but normally its amplitude is not dangerous for bearings and for insulations. High harmonics components in shaft voltage may lead to amplify these shaft vibrations, speeding the aging of the rotor. Shorted turns are the most frequent fault in synchronous generators, but this project has proved that it is possible to prevent damages and long outages using a flux probe and a shaft voltage F.F.T. analysis.

APPENDICES

Appendix A:

Capability curves of the synchronous generator:

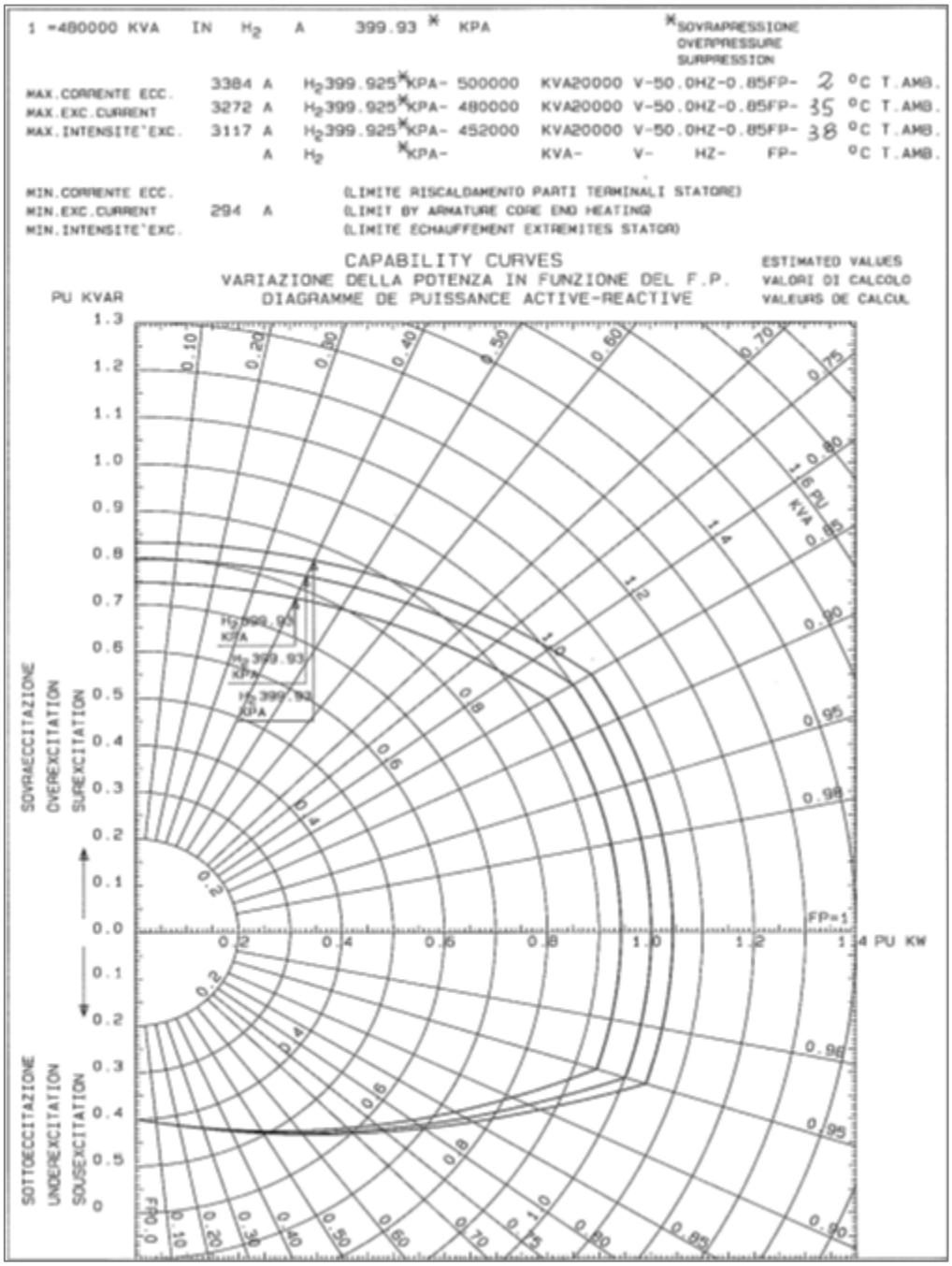

Appendix B:

Technical specifications of the supervision system computer (Tab. A) and of the data acquisition card (Tab. B) :

Item	Description
Form	Rackmount 19” industrial chassis
Dimension	W=19”, H=4U, Lmax<=520mm (front handle excluded)
Mother board	ATX with at least 4 free PCI slot
Socket	LGA775
CPU	Intel Core 2 duo
RAM	2GB
Hardisk	160GB SATA or above
Storage	DVD+/-RW SATA or IDE on front panel
LAN	2 x 10/100 on board (no cards)
Video	VGA on board (Favourite), or PCI Express card, connector DB-15
I/O Ports on front panel	1xUSB2.0, or more.
I/O Ports on rear	2xRS232, 4xUSB2.0, mouse PS/2, keyboard PS/2, or more.
Audio	On board
Power supply	100/240VAC auto MTBF>=100000 hours, or redundant type
Operating system	Windows XP Professional
Software antivirus	Symantec Antivirus10 c.e. (or other ENDESA standard); not required for Enel Produzione
ON-Site installation	Not required

Tab. A.

Item	Description
Form	Rackmount 19” KVM
Dimensions	W=19”, H=1U
Video	15” TFT Color LCD display, resolution 1024x768, AC power input, DB-15
Keyboard	88÷105 keys, English layout, PS/2
Pointing device	Touchpad or trackball, PS/2
Audio	Not required
Switch kvm	Not required

Tab. B.

Appendix C:

Monitoring of 16/07/2012:

100 Hz [V]	200 Hz [V]	300 Hz [V]	400 Hz [V]	600 Hz [V]	I shaft [A]	V MAT [V]	Iexc [A]	P [MW]	Q [Mvar]
0,062	0,018	0,092	0,008	0,026	0,008	0,33	1195	0	0
0,044	0,023	0,196	0,009	0,091	0,137	0,29	1178	51,6	2,9
0,056	0,018	0,681	0,058	0,461	0,875	0,41	1898	286,2	28,4
0,076	0,058	0,847	0,049	0,427	1,239	0,46	2376	402	29,5
0,043	0,039	0,656	0,045	0,462	0,931	0,43	1989	320	13,1

Monitoring of 18/06/2013:

100 Hz [V]	200 Hz [V]	300 Hz [V]	400 Hz [V]	600 Hz [V]	I shaft [A]	V MAT [V]	Iexc [A]	P [MW]	Q [Mvar]
0,041	0,005	0,197	0,007	0,066	0,057	0,62	1246	0	0
0,037	0,012	0,2	0,013	0,066	0,058	0,62	1471	5,1	53,3
0,04	0,016	0,229	0,011	0,071	0,058	0,62	1456	9,5	52,3
0,047	0,033	0,291	0,024	0,104	0,065	0,61	1485	24,1	56,9
0,047	0,018	0,341	0,082	0,101	0,081	0,57	1498	45	57,6
0,064	0,032	0,375	0,002	0,111	0,095	0,54	1489	68,7	51,2
0,138	0,062	0,451	0,033	0,088	0,203	0,47	1738	175,3	57,4
0,16	0,103	0,8	0,07	0,515	0,388	0,56	2302	365,4	42
0,124	0,074	0,818	0,059	0,497	0,385	0,55	2285	366,4	29,1
0,088	0,032	0,834	0,045	0,481	0,385	0,53	2283	362,6	35

Monitoring of 21/06/2013:

100 Hz [V]	200 Hz [V]	300 Hz [V]	400 Hz [V]	600 Hz [V]	900 Hz [V]	I shaft [A]	V MAT [V]	Iexc [A]	P [MW]
0,071	0,028	0,17	0,015	0,093	0,072	0,019	0,5	1175	0
0,062	0,018	0,181	0,015	0,106	0,085	0,019	0,5	1111	5,5
0,075	0,031	0,191	0,02	0,12	0,075	0,025	0,48	1144	13,8
0,06	0,042	0,258	0,023	0,17	0,099	0,056	0,44	1178	44,8
0,052	0,039	0,321	0,014	0,171	0,091	0,082	0,43	1229	60,2
0,074	0,049	0,354	0,033	0,143	0,096	0,103	0,4	1260	85,8
0,027	0,055	0,335	0,013	0,147	0,089	0,102	0,4	1191	86,6
0,085	0,06	0,34	0,027	0,148	0,098	0,103	0,41	1273	86,3
0,139	0,137	0,411	0,008	0,206	0,081	0,187	0,38	1347	153,3
0,176	0,111	0,819	0,066	0,503	0,189	0,365	0,45	1940	297,7
0,034	0,036	1,018	0,019	0,461	0,225	0,459	0,43	2385	372
0,118	0,088	0,942	0,049	0,482	0,266	0,471	0,43	2315	380,6
0,064	0,084	0,711	0,038	0,403	0,16	0,305	0,31	1743	254,6
0,136	0,042	0,804	0,055	0,416	0,172	0,305	0,31	1804	255
0,096	0,11	0,768	0,076	0,408	0,199	0,307	0,31	1702	253,5

Monitoring of 03/07/2013:

100 Hz [V]	200 Hz [V]	300 Hz [V]	400 Hz [V]	600 Hz [V]	I shaft [A]	V MAT [V]	Iexc [A]	P [MW]	Q [Mvar]
0,044	0,039	0,228	0,013	0,098	0,028	0,55	1212	0	0
0,039	0,022	0,246	0,018	0,115	0,027	0,54	1249	12,4	18,8
0,034	0,039	0,306	0,02	0,112	0,051	0,5	1267	43,2	16,5
0,015	0,037	0,336	0,025	0,122	0,069	0,46	1306	58,6	18,1
0,063	0,017	0,388	0,012	0,153	0,092	0,41	1342	82,2	24,8
0,11	0,093	0,436	0,018	0,176	0,156	0,34	1483	146,5	12,4
0,104	0,049	0,698	0,032	0,39	0,276	0,32	1765	254,1	14,9
0,223	0,087	0,924	0,055	0,451	0,414	0,37	2287	372,5	26,4
0,115	0,05	1,009	0,074	0,423	0,427	0,37	2350	380	33,3
0,157	0,104	0,647	0,067	0,409	0,274	0,35	1733	254,7	-1,2
0,136	0,043	0,752	0,059	0,475	0,337	0,4	1972	306,4	12,9
0,138	0,064	0,741	0,044	0,425	0,31	0,38	1864	271	14,2

Monitoring of 04/07/2013:

100 Hz [V]	200 Hz [V]	300 Hz [V]	400 Hz [V]	600 Hz [V]	I shaft [A]	V MAT [V]	Iexc [A]	P [MW]	Q [Mvar]
0,025	0,013	0,206	0,014	0,101	0,016	0,51	1162	0	0
0,011	0,035	0,251	0,006	0,126	0,026	0,57	1181	8,9	5,4
0,034	0,02	0,287	0,022	0,137	0,031	0,51	1211	23,8	5,1
0,034	0,02	0,318	0,027	0,17	0,043	0,47	1232	34	11,9
0,047	0,021	0,348	0,021	0,164	0,061	0,46	1259	54,5	10
0,101	0,063	0,372	0,02	0,172	0,086	0,41	1311	74,9	15,3
0,104	0,027	0,433	0,023	0,188	0,16	0,38	1435	146,3	9,1
0,108	0,007	0,874	0,057	0,399	0,423	0,53	2271	373,4	19,4
0,182	0,1	0,919	0,1	0,446	0,416	0,52	2282	373,4	24,2
0,206	0,105	1,003	0,069	0,421	0,432	0,51	2342	385,6	20,8
0,253	0,169	0,971	0,126	0,494	0,444	0,53	2442	381,1	53,6
0,084	0,052	0,732	0,046	0,424	0,313	0,42	1834	267,2	3,6

Monitoring of 16/07/2013:

100 Hz [V]	200 Hz [V]	300 Hz [V]	400 Hz [V]	600 Hz [V]	I shaft [A]	V MAT [V]	Iexc [A]	P [MW]	Q [Mvar]
0,04	0,011	0,108	0,013	0,049	0,019	1,33	465	0	0
0,048	0,006	0,075	0,01	0,054	0,015	0,47	1152	0	0
0,065	0,038	0,211	0,026	0,094	0,021	0,57	1173	10,8	6,6
0,084	0,066	0,24	0,026	0,129	0,028	0,54	1150	20	-5,4
0,099	0,067	0,245	0,026	0,132	0,028	0,55	1150	20	-5,4
0,08	0,057	0,23	0,026	0,126	0,03	0,53	1150	20	0
0,07	0,045	0,35	0,041	0,187	0,069	0,45	1194	59,3	4,8
0,11	0,092	0,461	0,032	0,24	0,228	0,36	1596	193,8	18,5
0,19	0,116	0,818	0,08	0,462	0,392	0,4	2150	339,1	27,3
0,221	0,185	0,771	0,089	0,455	0,369	0,43	2065	316	19,1

Monitoring of 17/07/2013:

100 Hz [V]	200 Hz [V]	300 Hz [V]	400 Hz [V]	600 Hz [V]	I shaft [A]	V MAT [V]	Iexc [A]	P [MW]	Q [Mvar]
0,094	0,071	0,146	0,017	0,093	0,02	0,5	1180	4,6	0
0,124	0,082	0,226	0,027	0,16	0,036	0,48	1269	20,7	17,2
0,122	0,047	0,197	0,039	0,142	0,039	0,44	1210	31	8,3
0,136	0,049	0,224	0,047	0,157	0,04	0,45	1210	31	8,3
0,095	0,046	0,381	0,027	0,132	0,091	0,43	1346	82	13,3
0,134	0,067	0,714	0,088	0,492	0,342	0,36	2048	303,3	28,6
0,213	0,132	0,81	0,057	0,474	0,366	0,37	2172	311,2	54,1
0,166	0,102	0,668	0,087	0,406	0,284	0,37	1824	254,2	25,6

Monitoring of 18/07/2013:

100 Hz [V]	200 Hz [V]	300 Hz [V]	400 Hz [V]	600 Hz [V]	I shaft [A]	V MAT [V]	Iexc [A]	P [MW]	Q [Mvar]
0,036	0,008	0,133	0,006	0,065	0,015	1,32	375	0	0
0,039	0,009	0,03	0,01	0,057	0,016	0,54	1126	0	0
0,05	0,014	0,143	0,004	0,065	0,015	0,64	1126	0	0
0,053	0,021	0,147	0,017	0,069	0,018	0,55	1126	0	0
0,091	0,054	0,223	0,02	0,147	0,031	0,5	1161	24,7	-2,6
0,113	0,073	0,376	0,027	0,153	0,089	0,44	1287	84	7,1
0,209	0,083	0,768	0,098	0,505	0,329	0,35	1977	290,1	32,2
0,134	0,13	0,67	0,096	0,467	0,318	0,36	1896	286,9	14,1
0,129	0,095	0,666	0,058	0,424	0,302	0,37	1893	263,8	36,4

Monitoring of 22/07/2013:

100 Hz [V]	200 Hz [V]	300 Hz [V]	400 Hz [V]	600 Hz [V]	I shaft [A]	V MAT [V]	Iexc [A]	P [MW]	Q [Mvar]
0,057	0,021	0,178	0,01	0,041	0,014	0,52	1249	0	0
0,101	0,061	0,187	0,023	0,098	0,02	0,55	1128	12,1	-2,9
0,1	0,051	0,237	0,017	0,135	0,028	0,52	1136	21,9	-1,1
0,11	0,067	0,323	0,014	0,166	0,047	0,51	1204	39,4	8
0,101	0,069	0,35	0,028	0,157	0,075	0,48	1277	66	14,9
0,096	0,084	0,335	0,025	0,175	0,075	0,45	1178	69,2	-3,4
0,057	0,049	0,434	0,028	0,152	0,143	0,39	1372	126,9	12,4
0,119	0,079	0,523	0,068	0,293	0,215	0,34	1574	193,8	16

Monitoring of 23/07/2013:

100 Hz [V]	200 Hz [V]	300 Hz [V]	400 Hz [V]	600 Hz [V]	I shaft [A]	V MAT [V]	Iexc [A]	P [MW]	Q [Mvar]
0,114	0,078	0,664	0,056	0,435	0,277	0,32	1789	254,6	11,7
0,182	0,086	0,892	0,092	0,426	0,395	0,36	2161	353,1	5,5
0,155	0,072	0,707	0,08	0,426	0,295	0,33	1808	263,4	5,5
0,084	0,064	0,191	0,028	0,142	0,025	0,47	1198	9,6	6,5
0,078	0,09	0,211	0,008	0,181	0,047	0,43	1169	34,1	-1,7
0,071	0,031	0,319	0,037	0,149	0,087	0,37	1179	64,9	-9,5
0,069	0,058	0,391	0,019	0,138	0,139	0,36	1297	103,5	4,9
0,081	0,039	0,426	0,049	0,223	0,221	0,32	1473	170,4	2,4
0,134	0,066	0,707	0,078	0,487	0,393	0,37	1946	298,4	7,8
0,16	0,088	0,754	0,091	0,498	0,438	0,38	2057	327,8	14,7
0,167	0,096	0,782	0,045	0,481	0,455	0,4	2106	339,3	11,1
0,156	0,12	0,77	0,08	0,489	0,425	0,38	2065	320,7	18,9

Monitoring of 24/07/2013:

100 Hz [V]	200 Hz [V]	300 Hz [V]	400 Hz [V]	600 Hz [V]	I shaft [A]	V MAT [V]	Iexc [A]	P [MW]	Q [Mvar]
0,122	0,067	0,442	0,076	0,217	0,247	0,37	1586	195,5	14,8
0,104	0,073	0,514	0,069	0,264	0,248	0,33	1589	195,1	16,7
0,169	0,109	0,848	0,097	0,521	0,452	0,36	2206	343,9	37,3
0,202	0,166	0,896	0,113	0,507	0,485	0,4	2298	373,3	27,3
0,218	0,142	0,86	0,073	0,485	0,48	0,39	2293	372,6	22,5
0,2	0,116	0,956	0,073	0,48	0,49	0,4	2338	373,3	32,2

Monitoring of 25/07/2013:

100 Hz [V]	200 Hz [V]	300 Hz [V]	400 Hz [V]	600 Hz [V]	I shaft [A]	V MAT [V]	Iexc [A]	P [MW]	Q [Mvar]
0,063	0,036	0,141	0,005	0,069	0,014	0,58	1216	0	0
0,033	0,039	0,206	0,025	0,104	0,019	0,48	1216	0	0
0,037	0,06	0,209	0,028	0,152	0,033	0,47	1209	20	6,5
0,044	0,051	0,216	0,015	0,167	0,039	0,46	1236	30,2	5,9
0,081	0,063	0,321	0,041	0,189	0,075	0,42	1271	61,1	12,4
0,032	0,035	0,351	0,023	0,135	0,111	0,41	1322	84	15
0,197	0,151	0,837	0,105	0,533	0,49	0,41	2366	375,4	46,8
0,191	0,087	0,883	0,107	0,473	0,491	0,48	2354	327,7	45
0,16	0,114	0,854	0,097	0,465	0,457	0,52	2155	344,1	15,3
0,187	0,138	0,93	0,077	0,484	0,545	0,48	2298	373,3	23,5

V shaft [V]	I shaft [A]	Z shaft [Ω]	Iecc [A]
1,795	0,016	112,187	991
1,942	0,023	84,435	1186
1,942	0,053	36,642	1239
1,693	0,09	18,811	1255
1,53	0,185	8,27	1447
2,015	0,499	4,038	2362
1,86	0,482	3,859	2260
1,978	0,501	3,948	2337

Monitoring of 29/07/2013:

100 Hz [V]	200 Hz [V]	300 Hz [V]	400 Hz [V]	600 Hz [V]	I shaft [A]	V MAT [V]	Iexc [A]	P [MW]	Q [Mvar]
0,029	0,002	0,135	0,013	0,057	0,016	0,41	991	0	0
0,046	0,026	0,206	0,013	0,115	0,023	0,54	1186	14,6	7,9
0,042	0,022	0,301	0,01	0,155	0,053	0,54	1239	43	14,7
0,065	0,033	0,409	0,023	0,169	0,09	0,45	1255	68,6	10,6
0,089	0,081	0,445	0,037	0,173	0,185	0,36	1447	132,9	23,8
0,127	0,105	0,996	0,031	0,487	0,499	0,37	2362	374,1	47,3
0,149	0,138	0,865	0,068	0,392	0,482	0,36	2260	370,1	15,3
0,217	0,151	0,984	0,089	0,46	0,501	0,4	2337	373,2	25

shaft [V]	I shaft [A]	Z shaft [Ω]	Iexc [A]
1,795	0,016	112,187	991
1,942	0,023	84,435	1186
1,942	0,053	36,642	1239
1,693	0,09	18,811	1255
1,53	0,185	8,27	1447
2,015	0,499	4,038	2362
1,86	0,482	3,859	2260
1,978	0,501	3,948	2337

Appendix D:

250 Hz harmonic component of shaft voltage:

P [MW]	16/07/2012	19/06/2013	03/07/2013	18/07/2013
0	0,532	0,532	0,521	0,238
50	0,541	0,519	0,486	0,496
280	0,553	0,673	0,583	0,689
300	0,563	0,652	0,677	0,611

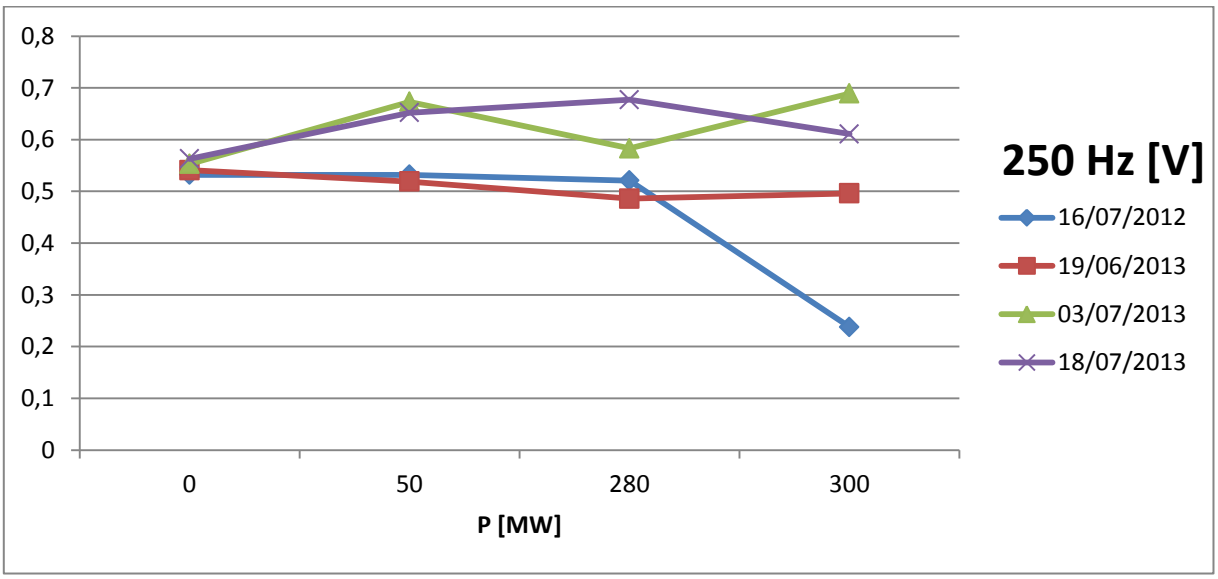

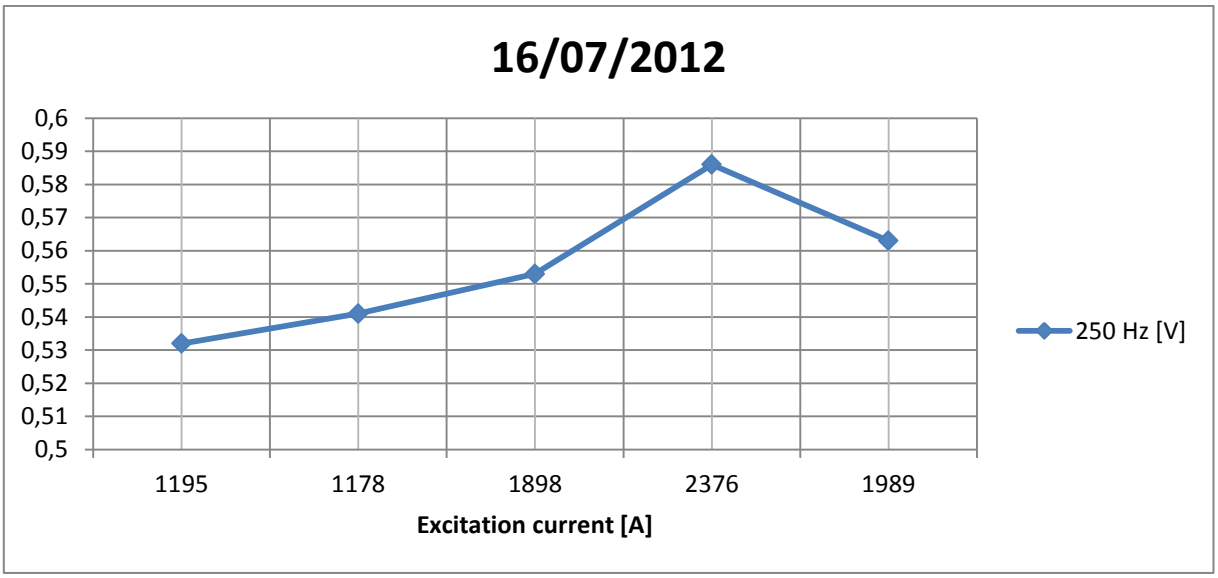

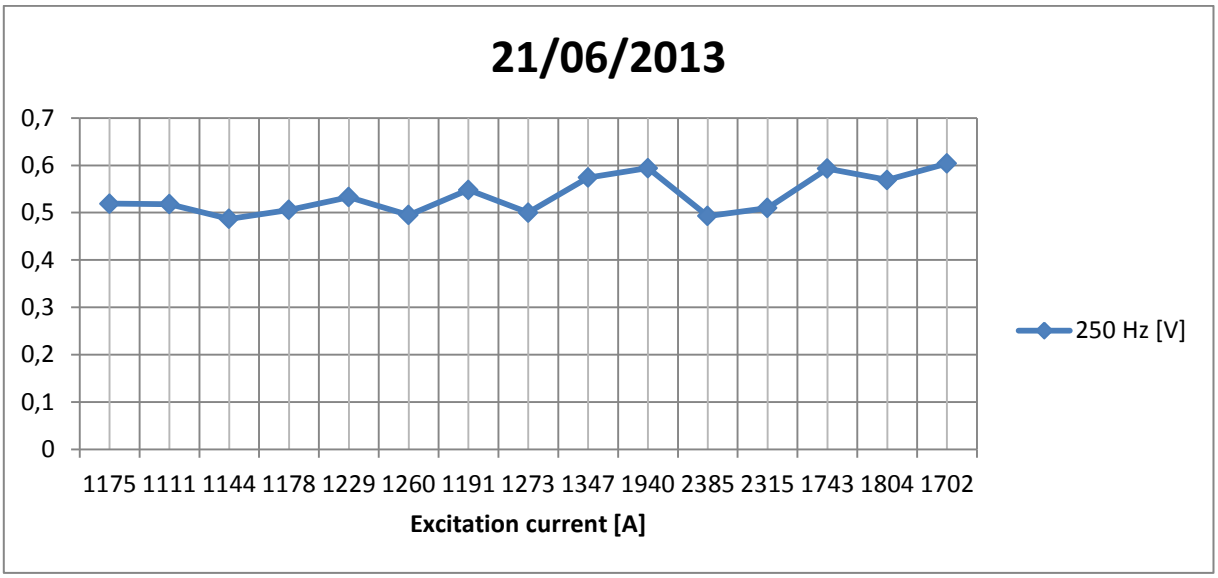
21/06/2013
0,7
0,6
0,5
0,4
0,3
0,2
0,1
0
1175 1111 1144 1178 1229 1260 1191 1273 1347 1940 2385 2315 1743 1804 1702
Excitation current [A]
250 Hz [V]

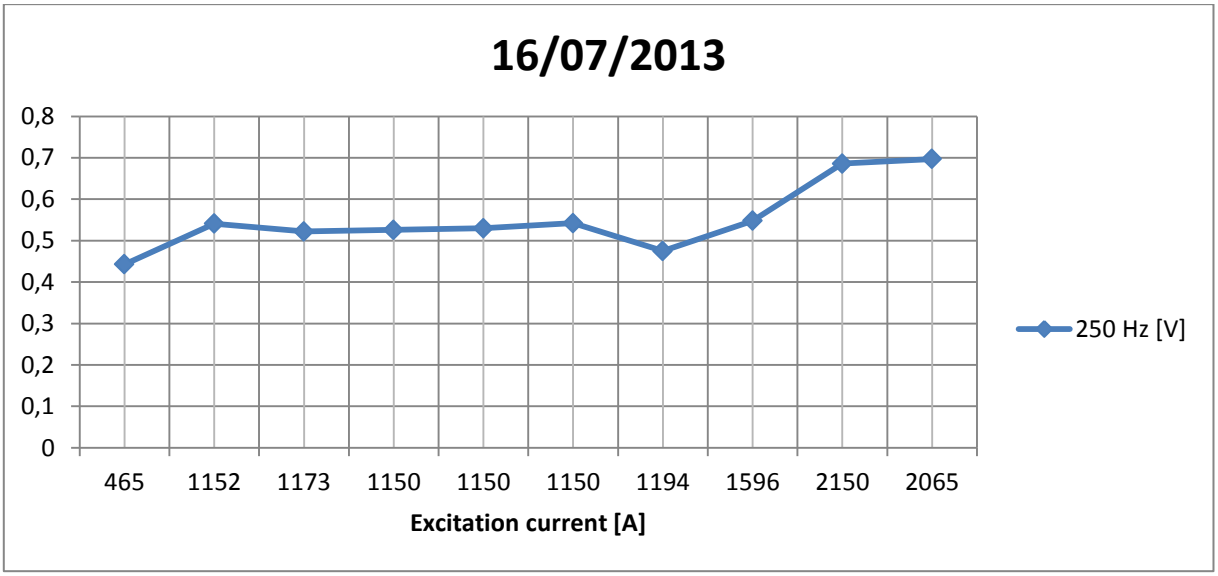
16/07/2013
0,8
0,7
0,6
0,5
0,4
0,3
0,2
0,1
0
465 1152 1173 1150 1150 1150 1194 1596 2150 2065
Excitation current [A]
250 Hz [V]

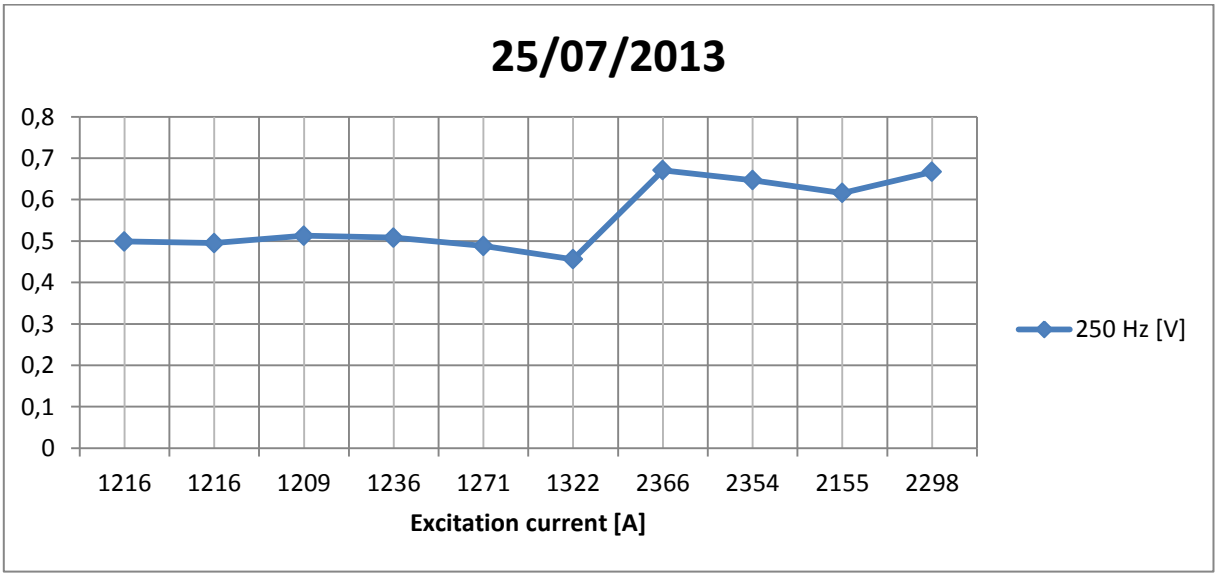
25/07/2013
0,8
0,7
0,6
0,5
0,4
0,3
0,2
0,1
0
1216 1216 1209 1236 1271 1322 2366 2354 2155 2298
Excitation current [A]
250 Hz [V]

Appendix E:

300 Hz harmonic component of shaft voltage:

I exc	16/07/2012	18/06/2013	21/06/2013	03/07/2013	23/07/2013	25/07/2013
1200	0,092	0,197	0,321	0,228	0,191	0,206
1400		0,229	0,411	0,436	0,426	0,351
1600		0,35	0,768	0,647	0,63	0,57
1800	0,681	0,451	0,804	0,741	0,707	0,7
2000	0,656	0,742	0,819	0,752	0,77	0,854
2200		0,834	0,942	0,924	0,892	0,93
2400	0,847	0,8	1,018	1,009	0,98	0,837

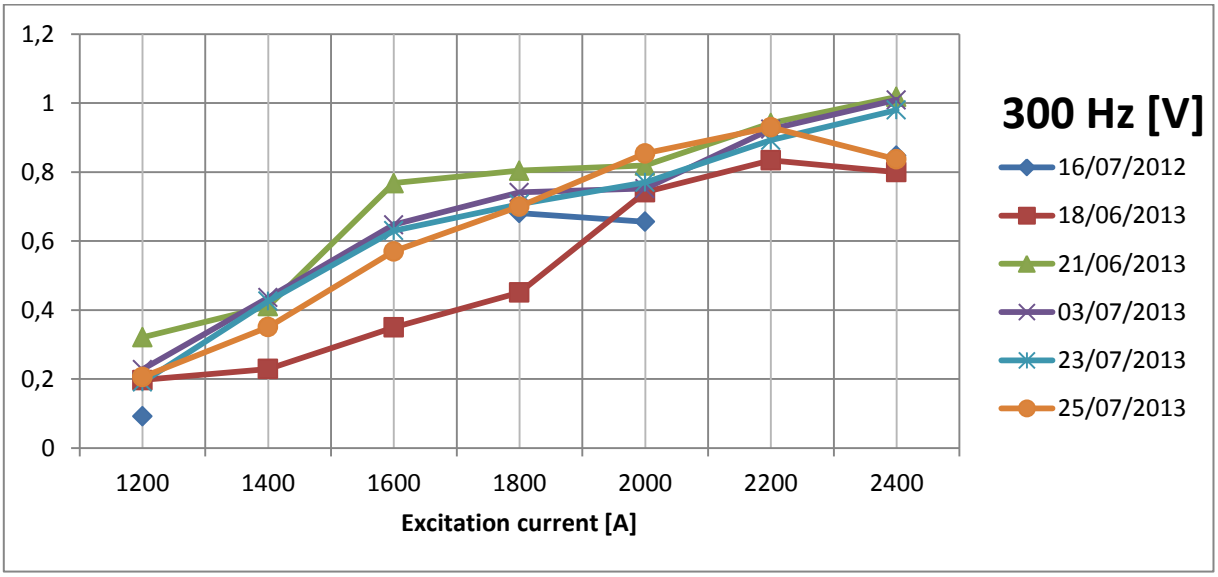

Appendix F:

From "IEEE 519-1992, Recommended Practice and Requirements for Harmonic Control in Electrical Power Systems":

Harmonic Order	Frequency (Hz)	Sequence Network	Stator Harmonic	Harmonic Rotation	Rotor Harmonic
1	60	Positive	1	Forward	-
5	300	Negative	5	Backward	6
7	420	Positive	7	Forward	6
11	660	Negative	11	Backward	12
13	780	Positive	13	Forward	12
17	1020	Negative	17	Backward	18
19	1140	Positive	19	Forward	18
23	1380	Negative	23	Backward	24
25	1500	Positive	25	Forward	24

Shaft impedance with reference to the frequency order of harmonics (25/07/2013), shaft voltage harmonics in Volts:

100 Hz	200 Hz	300 Hz	400 Hz	600 Hz	700 Hz	800 Hz	900 Hz	1000 Hz	I shaft [A]	I exc [A]
0,063	0,036	0,141	0,005	0,069	0,006	0,009	0,085	0,004	0,014	1216
0,033	0,039	0,206	0,025	0,104	0,007	0,008	0,046	0,011	0,019	1216
0,037	0,06	0,209	0,028	0,152	0,017	0,015	0,086	0,011	0,033	1209
0,044	0,051	0,216	0,015	0,167	0,019	0,013	0,084	0,017	0,039	1236
0,081	0,063	0,321	0,041	0,189	0,021	0,031	0,104	0,014	0,075	1271
0,032	0,035	0,351	0,023	0,135	0,031	0,02	0,086	0,014	0,111	1322
0,197	0,151	0,837	0,105	0,533	0,017	0,044	0,179	0,013	0,49	2366
0,191	0,087	0,883	0,107	0,473	0,021	0,009	0,215	0,026	0,491	2354
0,16	0,114	0,854	0,097	0,465	0,016	0,008	0,204	0,031	0,457	2155
0,187	0,138	0,93	0,077	0,484	0,027	0,019	0,189	0,003	0,545	2298

Z 100 [Ω]	Z 200 [Ω]	Z 300 [Ω]	Z 400 [Ω]	Z 600 [Ω]	Z 700 [Ω]	Z 800 [Ω]	Z 900 [Ω]	Z 1000 [Ω]	f [Hz]
4,5	2,5714	10,07	0,3571	4,9286	0,429	0,643	6,0714	0,2857	100
1,7368	2,0526	10,84	1,3158	5,4737	0,368	0,421	2,4211	0,5789	200
1,1212	1,8182	6,333	0,8485	4,6061	0,515	0,455	2,6061	0,3333	300
1,1282	1,3077	5,538	0,3846	4,2821	0,487	0,333	2,1538	0,4359	400
1,08	0,84	4,28	0,5467	2,52	0,28	0,413	1,3867	0,1867	600
0,2883	0,3153	3,162	0,2072	1,2162	0,279	0,18	0,7748	0,1261	700
0,402	0,3082	1,708	0,2143	1,0878	0,035	0,09	0,3653	0,0265	800
0,389	0,1772	1,798	0,2179	0,9633	0,043	0,018	0,4379	0,053	900
0,3501	0,2495	1,869	0,2123	1,0175	0,035	0,018	0,4464	0,0678	1000
0,3431	0,2532	1,706	0,1413	0,8881	0,05	0,035	0,3468	0,0055	

REFERENCES

Bibliography:

[1] Barbieri C., MARCINELLE_LG_2000 DESCRIZIONE GENERALE IMPIANTO.DOC, Enel University, Operations learning center, 20/10/2009.

[2] Barbieri C., MARCINELLE_LG_1041 aspetti costruttivi GVR.doc, Enel University, Operations Learning center, 20/10/2009.

[3] Roberto Caldon, Impianti di produzione dell'energia elettrica, Università degli studi Padova, Libreria Progetto Padova, 2011.

[4] Anna Stoppato, Turbine a gas, note corso di Impianti Energetici, Università di Padova, A.A. 2010-2011.

[5] Barbieri C., LG_4790.1_2 Principe fonctionnemnt turbines à gaz_FR.doc – Rev 0, Enel University, Operations learning center, 20/10/2009.

[6] Barbieri C., MARCINELLE_LG 4671.1_Aspetti costruttivi della turbine a gas SIEMENS V94.3A-FR.doc, Enel University, Operations learning center, 20/10/2009.

[7] Barbieri C., MARCINELLE_LG_1014 PRINCIPIO FUNZIONAMENTO ALTERNATORE.DOC, Enel University, Operations learning center, 20/10/2009.

[8] Giovanni Martinelli, Macchine Elettriche rotanti, Capitolo II macchine sincrone.

[9] M. Scagliotti, GENERATOR PERFORMANCE CURVES, Marcinelle CCGT power plant, Enel spa,10/10/2008.

[10] Barbieri C., MARCINELLE_LG_2005_CARATTERISTICHE COSTRUTTIVE E AUSILIARI ALTERNATORE.DOC, Enel University, Operations learning center, 20/10/2009.

[11] The McGraw-Hill Companies, Power generation handbook, Digital Engineering Library.

[12] Barbieri C., MARCINELLE_LG_4790_ECCITAZIONE E AVVIATORE STATICO.DOC, Enel University, Operations learning center, 20/10/2009.

[13] Ansaldo Energia, Sonda di flusso, certificato di taratura e collaudo, 13/9/2013.

[14] P.Bruzzone, Sistema Cortrot, Sonda di flusso, manuale operativo, Enel spa, 11/07/2005.

[15] A. Ballerini, P. Tattini, A. Rossi, Nota tecnica, installazione del sistema di monitoraggio rotore alternatore "MORAL", Enel spa, 20/08/2010.

[16] Donald R. Albright, David J. Albright, Generator field winding shorted turns: observed conditions and causes, Generatortech, Inc, 2007.

[17] Wang Xiao-hua, Li Yong-gang, Wu Yu-cai, Fan Jing, Method of fault diagnosis on intern turnshort-circuit in turbine generator rotor windings based on shaft voltage, North China Electric Power University, Baoding, China, IWISA 2009.

[18] Arthur L. Schoenstadt, An introduction to Fourier analysis, Department of Applied Mathematics, Naval postgraduate school, Monterey, California, February 23, 2006.

[19] S.R. Campbell, J.Kapler, M. Sasic, G.C. Stone, Detection of rotor winding shorted turns in turbine generators and hydrogenerators, IRIS Power LP, Canada, 2010 CIGRE.

[20] Dipl.-Ing. Hans Peter Hess, Prof. Dr.-Ing Klaus Weigelt, Dipl.-Ing. Michel Cochard, Operating experience with a generator stator end-winding vibration monitoring system.

[21] D. R. Albright, Internturn short circuit detector for turbine-generator rotor windings, IEEE transactions on power apparatus and systems, Volume PAS-90 Number 2, March/April 1971.

[22] M. Manarini, Metodo per l'esecuzione della misura dei flussi disperse con generatore sotto carico, Enel spa, 18/01/2012.

[23] Donald R. Albright, David J. Albright and James D. Albright, Flux probes provide on-line detection of generator shorted turns, Generatortech, Inc, 1999.

[24] Ansaldo Energia, Dynamic impedance measurement on rotor windings, Ansaldo Energia, 11/04/2002.

[25] Dal Mut, Controllo dei corto circuiti tra spire di rotori di turboalternatori con il metodo dell'onda mobile a bassa tensione, Ansaldo Energia, 23/07/2007.

[26] Keith Franklin Beatty, Online monitoring system and method to identify shorted turns in a field winding of a rotor, General Electric Company (U.S.), April 11,2011.

[27] A. Ballerini, Computer for generator rotor monitoring system "MORAL", Enel spa, 07/06/2010.

[28] Donald R. Albright, David J. Albright and James D. Albright, Generator fields winding shorted turn detection technology, IRMC, May 1999.

[29] D. R. Rankin and I. Wilson, "The use of shaft voltage to detect air gap eccentricity and shorted turns in salient pole alternators", IEE Conference on Electrical Machines and Drivers, 11 – 13/09/1995.

[30] Z. Eleschova, A. Belan, C. Gasparovsky, Rotor ground fault protection of generator with static excitation system, Slovak University of Technology in Bratislava, Slovak Republic, 2005.

[31] François Lalonde, Magnetic field measurement, I.R.E.Q. Institute de Recherche d'Hydro-Québec, Canada, 1992.

[32] EPRI, Life Cycle Management Planning Sourcebooks, Volume 5 Main Generator.

[33] Kyung-Tae Kim, Sang-Hoon Cha, Jin Hur, Jae-Sun Shim and Byeong-Woo Kim, Suppression of shaft voltage by rotor and magnet shape design of IPM-type high voltage motor, 2013.

[34] Wu Yucai, Li Yonggang, Wan Shuting, Li Heming, Investigation of turbine generator rotor winding intern-turn short circuit fault based on harmonic detection, Nanjing, China, April 2008.

[35] Daniel de Canha, The analysis of shaft voltages in a synchronous generator with various induced faults, School of Electrical and Information Engineering, University of the Witwatersrand, Johannesburg, 2008.

Sitography:

[1] http://info.ge-energy.com/contactrouting.html

[2] http://www.ge-energy.com/products_and_services/products/gas_turbines_heavy_duty/flexefficiency_50_combined_cycle_power_plant.jsp

[3] http://www.uotechnology.edu.iq/dep-eee/lectures/3rd/Electrical/Machines 2/II_SG.pdf

[4] http://www.tundrasolutions.ca/files/Applying SCIM on LVASDs Rev1.pdf